Fast Algorithms for Burst Detection

by

Xin Zhang

A dissertation submitted in partial fulfillment
of the requirements for the degree of
Doctor of Philosophy
Department of Computer Science
Courant Institute of Mathematical Sciences
New York University
September 2006

Dennis Shasha

© Xin Zhang

All Rights Reserved, 2006

To our lovely baby Marvin

Dedicated to my family who always support me

Acknowledgments

It has been a challenging process for me to finish this dissertation while working full time. Without the help of many individuals, this dissertation would never come into shape.

I warmly thank my advisor Professor Dennis Shasha. He always gives me kind encouragement and inspiring advice. Without his encouragement and help, I would not have been able to finish this work.

Many thanks to Professor Richard Cole, Professor Zvi M. Kedem, Professor Bhubaneswar Mishra for their inspiring comments and suggestions on this work.

I want to thank many friends in NYU: Xiaojian Zhao, Zhihua Wang, Congchun He and Yunyue Zhu. They have lent lots of help in sharing their resources in preparing this work.

I'd like to thank Anina Karmen, Professor Denis Zorin, Professor Margaret Wright, Rosemary Amico. With all their work and help, I have spent a wonderful time in the Computer Science Department.

Thanks to Katherine Rose Sabo for her many grammatical suggestions.

I'm truly thankful for my lovely wife Dr. Li Chen who supports me all the time and my parents who gave me the chance to receive the best education.

Abstract

Events occur in every aspect of our lives. An unexpectedly large number of events occurring within some certain measurement (e.g. within some time duration or a spatial region) is called a *burst*, suggesting unusual behaviors or activities. Bursts come up in many natural and social processes. It is a challenging task to monitor the occurrence of bursts whose lasting duration is unknown in a fast data stream environment.

This work describes efficient data structures and algorithms for high performance burst detection under different settings. Our view is that bursts, as unusual phenomena, constitute a useful preliminary primitive in a knowledge discovery hierarchy. Our intent is to build a high performance primitive detection algorithm to support high-level data mining tasks.

The work starts with an algorithmic framework including a family of data structures and a heuristic optimization algorithm to choose an efficient data structure given the inputs. The advantage of this framework is that it is adaptive to different inputs. Experiments on both synthetic data and real world data show the new framework significantly outperforms existing techniques over a variety of inputs.

Furthermore, we present a greedy dynamic detection algorithm which handles the changing data. It evolves the structure to adapt to the incoming data.

It achieves better performance on both synthetic and real data streams than a static algorithm in most cases.

We have applied this framework to several real world applications in physics, stock trading and website traffic monitoring. All the case studies show that our framework has real time response.

We extend this framework to multi-dimensional data and use it in an epidemiology simulation to detect infectious disease outbreak and spread.

Contents

Dedication **v**

Acknowledgments **vi**

Abstract **vii**

List of Figures **xi**

List of Tables **xiv**

1 Introduction **1**

1.1 Motivation 1

1.2 Our Contribution 2

2 Review **4**

2.1 Time Series and Data Stream 4

2.2 Data Representation and Reduction 6

2.3 Novelty, Anomaly, Surprise and Outlier Detection 9

2.4 Burst Modeling and Detection 11

2.5 Elastic Burst Detection and Shifted Binary Tree 14

3 Framework **17**

3.1 Aggregation Pyramid 17

3.2 Shifted Aggregation Tree 23

3.3 Heuristic State-space Algorithm 29

3.4 Empirical Results 36

4 Greedy Dynamic Burst Detection **52**

4.1 Structural Dependency 53

4.2 Greedy Dynamic Detection Algorithm 58

4.3 Empirical Results 63

4.4 Worst Case Analysis 80

5 Case Study **83**

5.1 Gamma Ray Burst Detection in Astronomy 83

5.2 Volume Spike Detection in Stock Trading 87

5.3 Click Fraud Detection in Website Traffic Monitoring 97

5.4 Burst Correlation in Stock Data 103

6 Multi-Dimensional Elastic Burst Detection **106**

6.1 Algorithm for D-Dimensional Elastic Burst Detection 107

6.2 Fast Detection of Infectious Disease Outbreak and Spread . . . 115

7 Conclusion **127**

Bibliography **128**

List of Figures

2.1 An example of a Shifted Binary Tree 15

3.1 An example of an Aggregation Pyramid 19

3.2 Shadow and overlap in an Aggregation Pyramid 20

3.3 Embed a Shifted Binary Tree in an Aggregation Pyramid 21

3.4 Shifted Binary Tree shadow property and detailed search region 22

3.5 Examples of Shifted Aggregation Trees 25

3.6 Shifted Aggregation Tree detailed search region 26

3.7 Shifted Aggregation Tree detection algorithm 27

3.8 State space growth 32

3.9 Theoretical cost model vs. empirical cost model 37

3.10 Alarm probability 42

3.11 The effect of λ in the Poisson distribution 43

3.12 The effect of β in the exponential distribution 44

3.13 The effect of burst probability in the Poisson distribution 46

3.14 The effect of burst probability in the exponential distribution . . 47

3.15 Bounding ratio as a function of window size and burst probability 48

3.16 Effect of search parameter 50

4.1 Algorithm to reformat a Shifted Aggregation Tree 55

4.2 Greedy dynamic detection algorithm 64
4.3 Dynamic algorithm performance under different training sets . . 67
4.4 Dynamic algorithm performance under different parameters . . . 69
4.5 Dynamic algorithm performance under different burst probabilities 70
4.6 Dynamic algorithm performance under different window sizes . . 72
4.7 The effect of different changing rates 73
4.8 The effect of different changing magnitudes 74
4.9 The effect of the maximum allowed shift step 77
4.10 The effect of the size of the alarm region 79

5.1 An example of Gamma Ray Burst 84
5.2 Performance comparison on Gamma Ray Burst Data 86
5.3 S&P 500 Index prices interact with volume spikes 87
5.4 Histogram for the IBM stock data 90
5.5 Effect of different thresholds - IBM data 91
5.6 Effect of different maximum window size of interest - IBM data 92
5.7 Effect of different sets of window sizes of interest - IBM data . . 93
5.8 Robustness test - IBM data 96
5.9 Histogram for the SDSS data 98
5.10 Effect of different thresholds - SDSS data 100
5.11 Effect of different maximum window size of interest - SDSS data 101
5.12 Effect of different sets of window sizes of interest - SDSS data . 101
5.13 Robustness test - SDSS data 104

6.1 Overlap in a D-dimensional Shifted Aggregation Tree 109
6.2 Adaptive D-dimensional Shifted Aggregation Tree 111
6.3 State space algorithm for regular D-dimensional SAT 113

6.4 State space algorithm for adaptive D-dimensional SAT 114
6.5 SIR model 116
6.6 Population distribution of the Tri-State area 119
6.7 Simulation of a disease spread and outbreak detection - Day 1 . 122
6.8 Simulation of a disease spread and outbreak detection - Day 7 . 123
6.9 Simulation of a disease spread and outbreak detection - Day 13 124
6.10 Simulation of a disease spread and outbreak detection - Day 19 125
6.11 Simulation of a disease spread and outbreak detection - Day 25 126

List of Tables

3.1 Shifted Aggregation Tree vs. Shifted Binary Tree 24

3.2 Weights used for different operations 35

3.3 Statistics for testing data sets for search parameters 51

4.1 An example of reformating a Shifted Aggregation Tree 57

4.2 Weights used for different operations in the dynamic algorithm . 59

4.3 Test settings to study the effect of algorithm parameters 76

5.1 Statistics for the IBM stock data 90

5.2 Statistics for the test IBM data for robust test 94

5.3 Test parameters for robust test - IBM data 94

5.4 Statistics for the SDSS SkyServer traffic data 98

5.5 Statistics for the test SDSS data for robust test 102

5.6 Test parameters for robust test - SDSS data 102

5.7 Some highly-correlated stocks at different durations 105

Chapter 1

Introduction

1.1 Motivation

Many aspects of our lives are described by events. An unexpectedly large number of events occurring within some certain temporal or spatial region is called a *burst*, suggesting unusual behaviors or activities. Bursts, as noteworthy phenomena, come up in many natural and social processes.

- A burst of trading volume in some stock might indicate insider trading.
- A burst of gamma rays may reflect the occurrence of a supernova.
- A burst of methane may anticipate a coming volcanic eruption.

To efficiently detect bursts is of critical importance under some circumstances. For example, to detect unusually high tsunami activity as early as possible could save thousands of lives.

If the length of the time period or the size of the spatial region when a burst occurs is known a priori, the detection can easily be done in linear time by

keeping a running count of the number of events. However, in many situations, the window size is not known a priori. For example, gamma ray bursts can last several seconds, several minutes or even several days. The size itself may be an interesting subject to be explored. Furthermore, many data applications require detection of bursts across a variety of window sizes. To detect bursts over m window sizes in a sequence of length N naively requires $\Theta(mN)$ time. This is unacceptable in a data stream environment where the data rates are high.

1.2 Our Contribution

This work explores efficient data structures and algorithms for high performance burst detection under different settings. Our view is that bursts, as an unusual phenomenon, constitute a useful preliminary primitive in a knowledge discovery hierarchy. Our intent is to build a high performance primitive detection algorithm to support high-level data mining tasks.

The work starts with an algorithmic framework for better burst detection over multiple window sizes in a data stream environment [96, 95, 94]. The contribution of this framework includes a family of data structures, called *Shifted Aggregation Trees (SAT)*, and a heuristic algorithm to search for an efficient data structure given the input time series and the window thresholds. The advantage of this framework is that it is adaptive to different inputs. We analyze theoretically and study empirically how different distributions and different thresholds affect the Shifted Aggregation Tree structures and the alarm probabilities. Experiments on both synthetic data and real world data show that the new framework significantly outperforms existing techniques over a variety of inputs.

Based on this family of data structures, we present a greedy dynamic detection algorithm which handles the changing data. The algorithm dynamically evolves the Shifted Aggregation Tree to adapt to the incoming data. It achieves better performance on both synthetic and real data streams than a static algorithm in most cases.

We have applied this framework to several real world applications in physics, stock trading and website traffic monitoring. All the case studies show our framework has real time response.

We also extend this framework to multi-dimensional data and use it in an epidemiology simulation to detect infectious disease outbreak and spread.

This dissertation is organized as follows: Chapter 2 reviews related work in time series and data stream, from low-level data representation and reduction techniques to higher-level burst modeling and detection tasks. Chapter 3 describes our proposed data structures and algorithms for the elastic burst detection problem. Chapter 4 presents the greedy dynamic detection algorithm. Chapter 5 studies several real world applications in physics, finance and website traffic monitoring. Chapter 6 extends our framework to multi-dimensional data. Chapter 7 concludes this work.

Chapter 2

Review

Although this work does not target one-dimensional data only, the review of related work starts with time series and a data stream model in section 2.1. The literature roughly fits into a three-level data processing framework. The burst detection problem is also placed in this three-level framework to show how it fits into the big picture. Low-level data representation and reduction techniques are briefly summarized in section 2.2. Section 2.3 gives a review of a broader class of detection tasks, novelty/anomaly/outlier/surprise detection. Section 2.4 reviews more related work in modeling and detecting bursts. Since our framework is directly based on Yunyue Zhu's work [84], section 2.5 reviews the elastic burst detection problem and the Shifted Binary Tree structure in detail.

2.1 Time Series and Data Stream

Time series data arise in many real world applications, such as stock prices, process control, signal processing, etc. The study of time series data has a long

history in such disciplines as finance, physics, engineering and many others. The research topics include time series analysis, modeling, prediction, searching and mining, just to name a few. In the database community, much research has been done in time series similarity and indexing. [43, 36, 49] give an excellent survey of different similarity measurements and indexing techniques. Mining time series has also attracted lots of research interest as surveyed in [36, 49].

We call a time series a data stream if it is of unbounded length and we want to get information about it as the data arrives. As hardware speeds improve, the rate at which new data arrive increases too. The need to process these massive stream data in real time or near real time requires new data management and processing mechanisms with limited memory and one-pass algorithms.

In the existing literature, there are data stream management systems (DSMS) [1, 2, 5, 9, 11], query processing [20, 64], maintaining different statistics (e.g. variance and k-means [19], frequency count [65], quantile [42], correlation [98], Count/Sum/L_p-norm [29]), data mining [25, 87, 34, 52], prediction [27, 74], classification [88, 33, 16], and clustering [14, 15]. [18, 38, 41, 36, 39, 59] give excellent overviews of issues in data stream management and mining.

The large amount of literature on time series and data streams is beyond the scope of this review. However, in order to see how the burst detection task fits into the big research picture, we can broadly fit these literatures into a general three-level data processing framework.

1. Low-level representation and preprocessing

   This includes data representation, data reduction and summarization, primitive detection, feature extraction, etc. It provides basic data representations and primitives for higher level processing.

2. Middle-level processing

   The middle-level processing is based on the representation and primitives from the low-level processing. This may include data organization and management, such as similarity searching and indexing. It provides extra functions for further processing.

3. High-level analysis and knowledge discovery

   This may include high-level mining tasks, such as clustering, classification, pattern discovery, prediction, etc.

One should note that this is a rough classification. Some tasks may belong to a different level other than stated above depending on their role in the knowledge discovery process. For example, clustering may act as a preprocessing step to extract features, or a tool to create indices, or can be the final goal itself to group similar time series.

In this three-level framework, the burst detection task can be seen as being in between the low level and the middle level. It is based on some low level representation and preprocessing techniques. At the same time, it can also be a basic primitive/feature for middle-level data management, or a high-level knowledge discovery process [87].

2.2 Data Representation and Reduction

Data representation and reduction techniques have been extensively studied in different areas, such as signal processing, time series analysis, data mining, communication theory, statistics, etc. They can be classified from different points of view:

- Time domain vs. transform domain

  A time domain representation can be the raw data itself, or feature representations extracted directly from the time domain, such as landmarks [77], piecewise segment/aggregate approximation [54, 51], etc. Transform domain representations include the widely used Discrete Fourier Transform (DFT), Discrete Wavelet Transform (DWT), Singular Value Decomposition (SVD), etc. — which are linear and orthogonal transformations — and many other non-linear or non-orthogonal transformations, like random projection, ICA, etc.

- Lossy vs. lossless

  Although a lossless representation can preserve all the information in the raw data, lossy representations are often used in many data mining tasks where the data amount is very large. Only the major components/characteristics, for example the first/largest k coefficients in DFT/DWT/SVD, in the data are kept.

- Numerical vs. symbolic

  Although numerical representation preserves more information, symbolic representation maybe more useful in many tasks, such as music retrieval [86], pattern discovery [61], etc.

- Parametric vs. non-parametric

  Depending on whether the data distribution is described by an analytic model, the representation can be classified as parametric or non-parametric [44].

Due to the large amount of data, preprocessing is often used to reduce and/or summarize the raw data. The data can be reduced in two ways:

1. Reduce the size of the data set

   A sampling and/or summarization process can be used to reduce the size of the data set. The random sampling uses a subset of randomly picked data to represent the original data. Other sampling methods are available to give a better approximation, such as selective sampling and adaptive sampling [60].

   While the sampling technique preserves a subset of data from the original data set, it may not preserve the statistics of the original data set. In contrast, the summarization techniques keep only the summarization of the original data set. There are several summarization methods including simple statistics such as different orders of moments [71, 98, 93], histogram [47, 78], wavelet [66, 67], data bubble [23] and clustering-based summarization [93], etc.

   There has been some work on combining the advantages of both methods. The aim is to keep a reduced-size data set that preserves some statistics of the original whole data set, as explained in [85, 35].

2. Reduce the dimension of the data set

   In many applications, the dimensionality of the data sets are high, e.g. hundreds or even thousands. Due to the notorious "Curse of Dimensionality," many algorithms perform badly on high dimensional data. Many dimension reduction methods have been proposed, including global-based (e.g. SVD, factor analysis, projection pursuit, etc.) and local-

based [26, 81]; data-dependent (e.g. SVD) and data-independent (e.g. DFT/DWT); static and adaptive [50, 31]; linear and non-linear [30].

In data stream applications, the sketch-based dimension reduction technique has attracted more and more interest [32, 37, 46, 28].

Given different data representation, reduction and summarization techniques, choosing the proper one is domain- and task-dependent. There is no one-size-fits-all technique.

From the data summarization point of view, the Shifted Aggregation Tree we proposed in the burst detection framework can be seen as an adaptive multi-resolution synopsis over the raw data.

2.3 Novelty, Anomaly, Surprise and Outlier Detection

As a task to detect unusual large numbers of events, burst detection belongs to a broader category of detection tasks: novelty/anomaly/outlier/surprise detection. The novelty/anomaly/outlier/surprise detection has been widely used in fraud detection, network intrusion detection, financial analysis, health monitoring, etc.

Although intuitively novelty/anomaly/outlier/surprise/burst are straightforward concepts, attempted formal definitions are often vague or domain dependent. Following the classification for outlier detection methods, the literature broadly falls into the following categories: depth-based [48], distribution-based [21, 53], distance-based [57, 56, 22, 17, 58], density-based [24, 76], and example-based [97, 75].

The depth-based method is based on computational geometry and computing layers of the k-d convex hull. Objects in the outer layer are identified as outliers.

In the distribution-based method, the data set is fit with a standard distribution, or a model/data structure associated with probabilities [53]. Outliers/surprises [53] are those points with small probability under this distribution model. In [55], a high frequency word is defined as a word whose frequency of usage is substantially higher than others, thus this method can be seen as a distribution-based method.

The distance-based method treats outliers [56, 58, 17, 22] as those points whose distances to their neighbors exceed some threshold usually determined after checking the global distribution characteristics. In [83], the surprise is defined as a large difference between two consecutive averages, obviously a distance-based method. Spatial indexing techniques are usually used to speed up the distance computation.

A limitation of the distance-based method is that it can capture only the "global" outliers, since the threshold is usually determined globally. To address this shortcoming, another type of outlier which is relative to its neighbors was proposed [24]. The density-based method works locally by defining the outliers as those points whose local densities are significantly different from their neighbors.

If we see the detection of outlier/novelty/anomaly as a classification problem, the classification technique in machine learning can be used to identify outliers/novelty. The Support Vector Machine (SVM) classifier has attracted more and more interest [63, 62, 82, 97]. In [97], Zhu et al. approach the outlier detection problem by learning how a user defines an outlier. The user manu-

ally identifies a small set of outliers based on their subjective criteria. A SVM classifier is learned from the small amount of user feedback.

It has been recognized that instead of classifying a point/pattern as either an outlier/surprise or a normal point, it is better to associate some fuzzy degree to the outlier/surprise. This fuzzy degree describes how confident the classification is and the likelihood that it is an outlier/surprise [24, 76, 62].

Our definition of burst is simply a large number of events exceeding a given threshold. It is widely used in many real world applications.

2.4 Burst Modeling and Detection

Among the many topics in time series and data streams, burst modeling and detection is attracting increasing interest. There are several papers that study bursts under different settings.

Wang et al. [89] use a one-parameter model, b-model, to model the bursty behavior in self-similar time series and synthesize realistic trace data. This type of time series includes a large number of real world data applications, such as Ethernet, file system, web, video and disk traffic, etc. Different from those which are usually modeled by a Poisson process, these series are self-similar over different time scales and exhibit significant burstiness. They follow the "80/20 law" in databases: 80% of the queries access 20% of the data. The bias parameter b is used to model the bias percentage of the activities, i.e. 80% or 60%. The bias is applied recursively to a segment of series (starting from a uniformed distribution) to synthesize a trace, i.e. b% of the segment has more activities than the rest of the segment. The entropy is used to describe the burstiness and to fit the model into the training data. The synthetic traces

generated from this model are very realistic compared to real data.

Kleinberg [55] studies the bursty and hierarchical structure in temporal text streams. The goal is to find how high frequency words change over time. The word usage in many text streams, such as email, news articles and research publications, usually exhibits some bursty and hierarchical behaviors. During certain time periods, some words appear more frequently than others and the frequencies change over time. Kleinberg assumes the gaps between two consecutive messages follow an exponential distribution, and uses infinite-state automaton to model the different levels of burstiness in different time scales. Words with high burstiness are those words with significantly higher frequency than others.

While Wang et al. [89] and Kleinberg [55] focus on bursty behaviors and modeling, our focus is a high-performance algorithm to detect bursts across multiple window sizes. Our definition of a burst is simply an aggregate exceeding some threshold, which is a straightforward definition with many applications in real world.

Neill et al. [71, 72, 69, 70] study the problem of detecting significant spatial clusters in multidimensional space. Significant spatial clusters are defined as a square region (extended to a rectangular region in the later papers) with the highest density. They consider a general density function that is a function of the count and the underlying population. The density function could be non-monotonic. They are only interested in the region with the highest density. A top-down, branch-and-bound method is used together with the so-called overlap-kd tree, to prune impossible regions. An overlap-kd tree is a hierarchical space-partition data structure where adjacent regions partially overlap.

By contrast, our work reports all the windows of different sizes which ex-

ceed the corresponding thresholds. The Shifted Aggregation Tree shares with the overlap-kd tree the property that both data structures have adjacent windows/regions overlapping. However, in the overlap-kd tree, the overlapping patterns are fixed and independent of the input data. While the Shifted Aggregation Tree may have different overlapping patterns depending on the input data. Our technique could be applied to their data structure, an area that merits further investigation in the future.

Vlachos et al. [87] mine the bursty behavior in the query logs of the MSN search engine. They use moving averages to detect time regions having high numbers of queries. Only two window sizes are considered, short term and long term. The detected bursts are further compacted and stored in a database to support burst-based queries. We share the view that burst detection should be a preliminary primitive for further knowledge mining process, but we deal with many more window sizes.

Datar et al. and Gibbons et al. [29, 40] study a related problem: estimating the number of 1's in a 0-1 stream and the sum of bounded integers in an integer stream in the last N elements. They use synopsis structures called Exponential Histograms and Waves respectively. These are multiresolution aggregation structures, each unit at the same level has the same aggregate value but may correspond to different window size. Our task is different: to report all the windows of different sizes having bursts. Our Shifted Aggregation Tree is also a multiresolution aggregation structure, however, each unit at the same level corresponds to the same window size, but may not have the same value.

2.5 Elastic Burst Detection and Shifted Binary Tree

The *elastic burst detection* problem [84] is to detect bursts across multiple window sizes. Formally:

Problem 1. *Given a data source producing non-negative data elements* $x_1, x_2, \ldots$, *a set of window sizes* $W = \{w_1, w_2, \ldots, w_m\}$, *a monotonic, associative aggregation function* A *(such as "sum" or "maximum") that maps a consecutive sequence of data elements to a number (it is monotonic in the sense that* $A[x_t \cdots x_{t+w-1}] \leq A[x_t \cdots x_{t+w}]$, *for all* w*), and thresholds associated with each window size,* $f(w_j)$, *for* $j = 1, 2, \ldots, m$, *the elastic burst detection is the problem of finding all pairs* (t, w) *such that* t *is a time point and* w *is a window size in* W *and* $A[x_t \cdots x_{t+w-1}] \geq f(w)$.

A naive algorithm is to check each window size of interest one at a time. To detect bursts over m window sizes in a sequence of length N naively requires $\Theta(mN)$ time. This is unacceptable in a high-speed data stream environment.

In [84], the authors show that a simple data structure called the *Shifted Binary Tree* could be the basis of a filter that would detect all bursts, and perform in time independent of the number of windows when the probability of bursts is very low.

A Shifted Binary Tree is a hierarchical data structure inspired by the Haar wavelet tree. The leaf nodes of this tree (denoted level 0) correspond to the time points of the incoming data; a node at level 1 aggregates two adjacent nodes at level 0. In general, a node at level $i+1$ aggregates two nodes at level i, thus includes 2^{i+1} time points. There are only $\log_2 N + 1$ levels where N is the

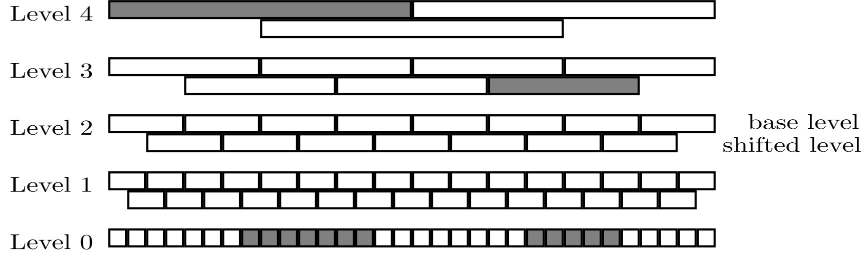

Figure 2.1: An example of a Shifted Binary Tree. The two shaded sequences in level 0 are included in the shaded nodes in level 4 and level 3 respectively.

maximum window size. The Shifted Binary Tree includes a shifted sublevel for each level above level 0. In shifted sublevel i, the corresponding windows are still of length 2^i but those windows are shifted by 2^{i-1} from the base sublevel. Figure 2.1 shows an example of a Shifted Binary Tree.

The overlap between the base sublevels and the shifted sublevels guarantees that all the windows of length w, $w \leq 1+2^i$, are included in one of the windows at level $i+1$. Because the aggregation function A is monotonically increasing, if $A[x_t \cdots x_{t+w+c}] \leq f(w)$, then surely $A[x_t \cdots x_{t+w-1}] \leq f(w)$. The Shifted Binary Tree takes advantage of this monotonic property as follows: the threshold value $f(2+2^{i-1})$ is associated with level $i+1$. Whenever more than $f(2+2^{i-1})$ events are found in a window of size 2^{i+1}, then a detailed search must be performed to check if some subwindow of size w, $2+2^{i-1} \leq w \leq 1+2^i$, has $f(w)$ events. All bursts are guaranteed to be reported and many non-burst windows are filtered away without requiring a detailed check when the burst probability is very low.

However, some detailed searches will turn out to be fruitless (i.e. there is no burst at all). For example, assume the threshold for window size 4 is 100, for 5 is 120, and for 8 is 150. Because each node at level 8 covers window size 4 and

5, if there are 101 events within a level 8 window, a detailed search has to be performed. But there may not be any window of size 4 exceeding the threshold 100. In this case, the detailed search turns out to be fruitless.

After applying the Shifted Binary Tree in several settings, we have observed two difficulties:

1. When bursts are rare but not very rare, the number of fruitless detailed searches grows, suggesting that we may want more levels than the Shifted Binary Tree provides.

2. Conversely, when bursts are exceedingly rare we may need fewer levels than the Shifted Binary Tree provides.

In other words we want a structure that adapts to the input.

In the next chapter, we present our new framework for the elastic burst detection problem. The proposed Shifted Aggregation Tree is a generalization of the Shifted Binary Tree. By using different structures for different inputs, we can achieve better performance, by a factor as large as 35 in some of our experiments.

Chapter 3

Framework

In this chapter, we describe our proposed algorithmic framework in detail. Section 3.1 introduces the concept of Aggregation Pyramid. This acts as a host data structure in which all Shifted Aggregation Trees are embedded. Section 3.2 introduces the Shifted Aggregation Tree and a generalized burst detection algorithm. Section 3.3 describes the cost model and a heuristic state-space search algorithm to find an efficient Shifted Aggregation Tree given the inputs. Section 3.4 presents experiments and results on synthetic data and analyzes how different inputs affect the desired structures.

3.1 Aggregation Pyramid

3.1.1 Aggregation Pyramid as a Host Data Structure

Our generalized framework is based on a dense data structure called the *aggregation pyramid (AP)*. All data structures in our framework contain a small subset of the cells of an aggregation pyramid.

An aggregation pyramid is an N-level isosceles triangular-shaped data structure built over a time window of size N.

- Level 0 has N cells and is in one-to-one correspondence with the original time series.
- Level 1 has $N-1$ cells; the first cell stores the aggregate of the first two data items (say, data items 1 and 2) in the original time series, the second cell stores the aggregate of the second two data items (data items 2 and 3), and so on.
- Level h has $N-h$ cells; the ith cell stores the aggregate of the $h+1$ consecutive data items in the original time series starting at time i.
- The top level has 1 cell, storing the aggregate over the whole time window.

In all, an aggregation pyramid stores the original time series and all the aggregates for every window size starting at every time point within this sliding window. Each cell corresponds to one window, called the *shadow* of the cell. The value (starting time, ending time, length/size) of a cell is the aggregate (starting time, ending time, length/size) of its corresponding shadow window. Figure 3.1 shows an aggregation pyramid built on a sliding window of size 8.

By construction, an aggregation pyramid has the following properties as shown in Figure 3.2.

- All the cells along the 45° diagonal have the same starting time. All the cells along the 135° diagonal have the same ending time.
- A cell ending at time t at level h, denoted by *cell*(h, t), stores the aggregate for the length $h+1$ window starting at time $t-h$ and ending at time t.

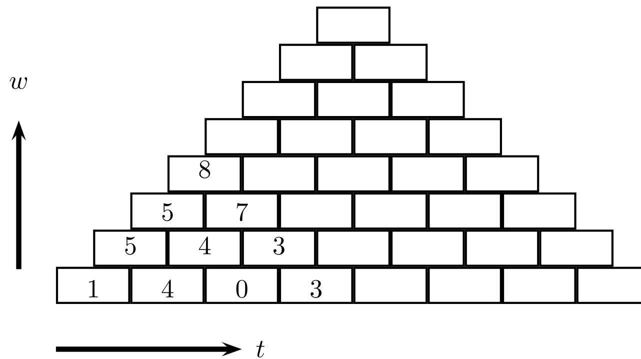

Figure 3.1: An Aggregation Pyramid on a window of size 8

- The shadow window of any cell c in the subpyramid rooted at cell r is covered by the shadow of cell r. We say c is *shaded by* r. Because the aggregates are monotonic, the aggregate in cell c is guaranteed to be bounded by the aggregate in cell r.

- The overlap of two cells is a cell c at the intersection of the 135° diagonal touching the earlier cell c_1 and the 45° diagonal touching the later cell c_2. The shadow window for cell c is the intersection of the shadows of cells c_1 and c_2.

When a new data item arrives at time t, the aggregation pyramid can easily be updated by recursively applying the follow formula from $h = 0$ to the top level.

$$\mathit{cell}(h, t) = \mathit{cell}(h - 1, t - 1) + \mathit{cell}(1, t)$$

If $\mathit{cell}(h, t)$ exceeds the threshold for a window of size $h + 1$, i.e. $f(h + 1)$, a burst ending at time t has occurred.

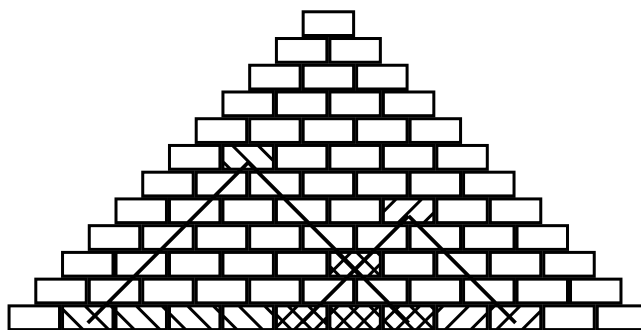

Figure 3.2: Shadow and overlap in an Aggregation Pyramid. The subsequence between the 45° diagonal and the 135° diagonal starting from a cell is the shadow of this cell. The subsequence of cross pattern is the overlap of the cell of forward-diagonal pattern and the cell of backward-diagonal pattern.

3.1.2 Embedding the Shifted Binary Tree into the Aggregation Pyramid

Recall that in a Shifted Binary Tree, level 0 stores the original time series, and level i stores the aggregates of window size 2^i. So, each node in a Shifted Binary Tree has a corresponding cell in the aggregation pyramid. Thus the Shifted Binary Tree can be embedded in the aggregation pyramid. Figure 3.3 shows how. The hatched cells in the aggregation pyramid correspond to the nodes in the Shifted Binary Tree. Notice that level i in a Shifted Binary Tree corresponds to level 2^i in the aggregation pyramid.

An important property of a Shifted Binary Tree is that a window of length w, $w \leq 1+2^i$, is contained in one of the windows at level $i+1$. This is illustrated in Figure 3.4.

By induction, a window of length w, $w \leq 1 + 2^{i-1}$, is contained in one of the windows at level i in a Shifted Binary Tree. Thus, after a node at level $i+1$ is

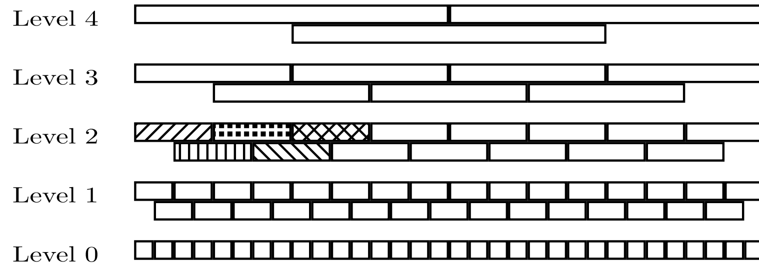

(a) Shifted Binary Tree

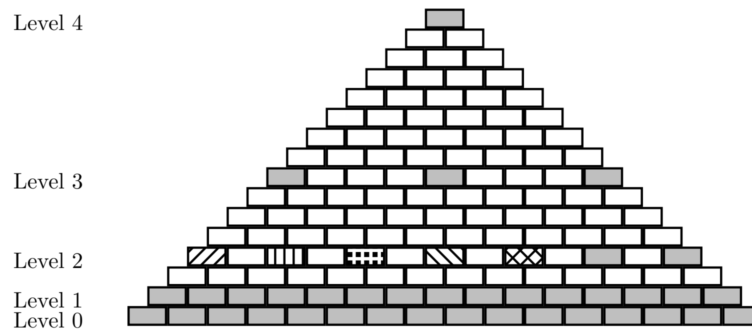

(b) Embed Shifted Binary Tree in Aggregation Pyramid

Figure 3.3: Embedding a Shifted Binary Tree (SBT) in an Aggregation Pyramid (AP). Each hatched cell in the AP corresponds to a node in the SBT. The different patterns in level 2 show the one-to-one correspondence between the nodes in a Shifted Binary Tree and the cells in an Aggregation Pyramid.

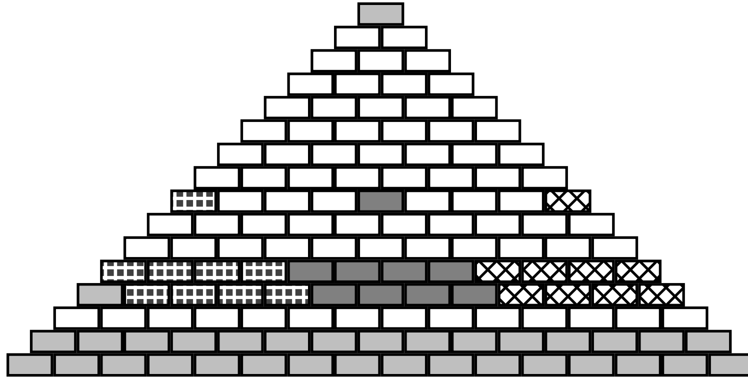

Figure 3.4: The shadow property and the detailed search region in a Shifted Binary Tree. The quadrilateral-shaped region of a specific hatching pattern is the detailed search region for the corresponding node having the same pattern.

updated, if the aggregate exceeds the threshold for size $2+2^{i-1}$, i.e. $f(2+2^{i-1})$, then a detailed search has to be performed for each cell having size between $2+2^{i-1}$ and $1+2^i$. Also when a node at level $i+1$ is updated at time t, we need to search only the cells ending after time $t-2^i$, because the cells ending at or before time $t-2^i$ have been covered by the preceding node at level $i+1$. We call this quadrilateral-shaped region — bounded by the window size range $[2+2^{i-1}, 1+2^i]$ and the time range $[t-2^i+1, t]$ — the *detailed search region (DSR)*. Please see Figure 3.4.

Obviously, there are many other possible embeddings into an aggregation pyramid. As long as a subset includes the level 0 cells and the top-level cell, it can be used together with this update-filter-search framework to detect bursts. In this case, all the bursts are guaranteed to be detected, because the shadow of the top-level cell includes everything. Clearly, it is very likely that the top-level cell will exceed the threshold of window size 1. In that case, it will raise an alarm every time, vastly increasing the need for searches. Such a structure

would be a poor choice.

The Shifted Binary Tree structure reduces the alarm probability by half-overlapping two consecutive nodes at the same level. The trigger for a cell of window size 2^{i+1} to do a detailed search is the threshold for size $2^{i-1}+2$, about a quarter that size. Thus, the probability of raising an alarm is dramatically reduced and more cells are filtered out in the first stage.

Furthermore, by using different embedding structures on different data inputs, we can adjust the probability of raising an alarm and the cost of maintaining the structure. The optimal performance can be achieved by trading off structure maintenance against filtering selectivity.

3.2 Shifted Aggregation Tree

3.2.1 Shifted Aggregation Tree Generalizes Shifted Binary Tree

Like a Shifted Binary Tree, a *Shifted Aggregation Tree (SAT)* is a hierarchical tree structure defined on a subset of the cells of an aggregation pyramid. It has several levels, each of which contains several nodes. The nodes at level 0 are in one-to-one correspondence with the original time series. Any node at level i is computed by aggregating some nodes below level i. Two consecutive nodes at the same level overlap in time.

A Shifted Aggregation Tree is different from a Shifted Binary Tree in two ways:

- The parent-child structure

  This defines the topological relationship between a node and its children,

Table 3.1: Comparing the Shifted Aggregation Tree (SAT) with the Shifted Binary Tree (SBT)

	SBT	SAT
Number of children	2	≥ 2
Levels of children for level $i+1$	i	$\leq i$
Shift at level $i+1$: S_{i+1}	$2S_i$	$kS_i, k \geq 1$
Overlapping window size at level $i+1$: O_{i+1}	window size at level i: w_i	$\geq w_i$

i.e. how many children it has and their placements.

- The shifting pattern

  This defines how many time points apart two neighboring nodes at the same level are. We call this distance the *shift*.

In a Shifted Binary Tree (SBT), the parent-child structure for each node is always the same: one node aggregates two nodes at one level lower. The shifting pattern is also fixed: two neighboring nodes in the same level always half-overlap. In a Shifted Aggregation Tree (SAT), a node could have 3 children and be 2 time points away from its preceding neighbor, or could have 64 children and be 128 time points away from its preceding one. Table 3.2.1 gives a side-by-side comparison of the difference between a Shifted Aggregation Tree and a Shifted Binary Tree. Clearly, a Shifted Binary Tree is a special case of a Shifted Aggregation Tree. Figure 3.5 shows some examples of Shifted Aggregation Trees.

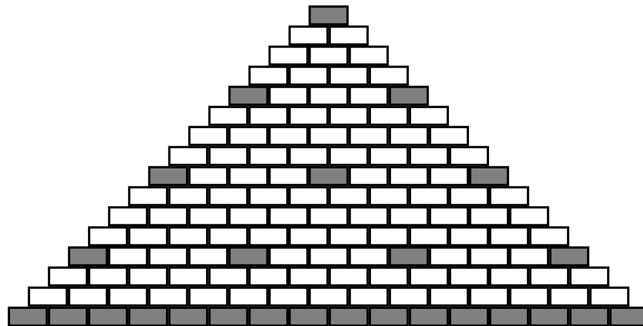

(a) a Shifted Aggregation Tree of size 16

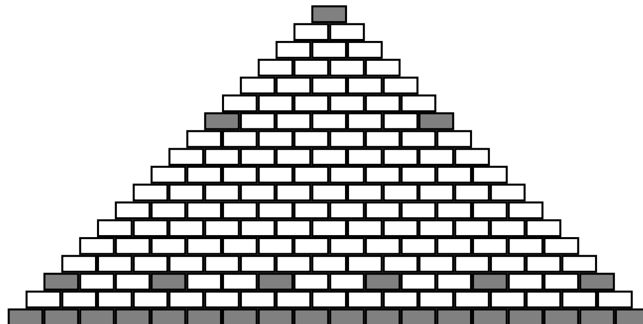

(b) a Shifted Aggregation Tree of size 18

Figure 3.5: Examples of Shifted Aggregation Trees

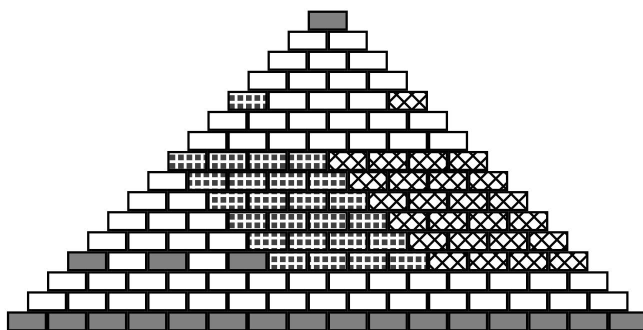

Figure 3.6: Illustration of the shadow property and the detailed search region in a Shifted Aggregation Tree

3.2.2 Shifted Aggregation Tree Shadows and Detection

A Shifted Aggregation Tree shares an important property with a Shifted Binary Tree:

Any window of size w, $w \leq h_i - s_i + 1$, is shaded by a node at level i.

where h_i is the window size at level i, and s_i is the shift at level i. Figure 3.6 illustrates this property in the aggregation pyramid. Because $h_i - s_i$ is the length of the overlapping shadow between two neighboring nodes at level i, the thresholds of all windows of lengths up to $h_i - s_i + 1$ have to be shaded by one of the nodes at level i. By induction, all levels up to $h_{i-1} - s_{i-1} + 1$ have to be shaded by one of the nodes at level $i - 1$. Therefore, after a node at level i is updated, only the windows of sizes between $h_{i-1} - s_{i-1} + 2$ and $h_i - s_i + 1$ need to be checked.

The Shifted Aggregation Tree detection algorithm is similar to that of the Shifted Binary Tree, as shown in Figure 3.7.

The detailed search region $DSR(i, t)$ in a Shifted Aggregation Tree is bounded by the window size range $[h_{i-1} - s_{i-1} + 2, h_i - s_i + 1]$ and the time

```
for every time point t starting from 1
    i = 1;
    while (a window at level i ends at the current time t)
        update node(i, t) by aggregating its children
        if f(h) ≤ node(i, t) < f(h + 1),
            where h_{i−1} − s_{i−1} + 2 ≤ h ≤ h_i − s_i + 1
        then search the portion with sizes w, w ≤ h,
            in the detailed search region DSR(i, t) for real bursts
        endif
        ++i;
    end
end
```

Figure 3.7: Shifted Aggregation Tree detection algorithm

span $[t - s_i + 1, t]$. This generalizes the detailed search region in a Shifted Binary Tree. Part of the detailed search region can be further filtered away, by binary search for the aggregate in a node at level i over the thresholds for sizes between $h_{i-1} - s_{i-1} + 2$ and $h_i - s_i + 1$. The search finds an h, such that $f(h) \leq node(i, t) < f(h + 1)$; this ensures no burst will present in any window of size greater than h.

The detailed search is performed by checking each cell one by one. Notice that two neighboring cells overlap, so, to avoid duplicate computation, we start from one "seed" cell, then by adding/subtracting the difference between two neighboring cells, we can get the aggregate for the neighboring cells. For example, a window of size 10 starting at time point 5 can be used to compute the aggregate at the window of size 10 starting at time point 6, by subtracting the data item at time point 5 from the aggregate at the window starting at time point 5, then adding the data item at time point 15. This process is repeated until the whole DSR is populated.

Because of the properties of a Shifted Aggregation Tree, such a "seed" is guaranteed to be found in or near each DSR without the need to aggregate a long sequence of the original time series. Recall that in a SAT, the shift at level i is a multiple of the shift at level $i - 1$, i.e. $s_{i-1} \leq s_i$, and the time span for $DSR(i, t)$ is s_i. There has to be a node at level $i - 1$ whose shadow window ends between the interval $t - s_i + 1$ and t, call it S. Also recall that in a SAT, the overlap of two neighboring nodes at level i has to cover any node at level $i - 1$, i.e $h_{i-1} \leq h_i - s_i + 1$. If $s_{i-1} > 1$, then $h_{i-1} - s_{i-1} + 2 \leq h_{i-1}$, i.e. level $i - 1$ is between $h_{i-1} - s_{i-1} + 2$ and $h_i - s_i + 1$, thus S lies within the $DSR(i, t)$. If $s_{i-1} = 1$, then S lies one level lower than the $DSR(i, t)$.

Because the shift for each level is fixed, every s_i time points, a node at level

i is updated and its detailed search region is checked if the aggregate exceeds its minimum threshold. Once a node at the top level is updated, all possible bursts will have been checked. Therefore, a burst is reported no later than s_{top} time points after it occurs, where s_{top} is the shift for the top level.

The total running time of the detection algorithm is the sum of the update time and the comparison/search time. Intuitively, if a Shifted Aggregation Tree has more levels and smaller shifts, i.e. a denser structure, it will take a longer time to maintain this structure, but the probability of a fruitless search and the cost of searches will both be reduced. Conversely, a sparser structure takes less time to update, but may take more time to do detailed searches. A good Shifted Aggregation Tree should balance the update time against the comparison/search time to obtain the optimal performance. In the next section, we present a heuristic state-space algorithm to find an efficient Shifted Aggregation Tree given a sample of the input.

3.3 Heuristic state-space algorithm to find an efficient Shifted Aggregation Tree

Given the input series and the window thresholds, the optimization goal is to minimize the time spent both updating the structure and checking for real bursts.

3.3.1 State-space Algorithm

Finding an efficient Shifted Aggregation Tree (SAT) naturally fits into a state-space algorithm framework if we view a Shifted Aggregation Tree as a state and

view the growth from one SAT to another as a transformation.

In a state-space algorithm, the problem to be solved is represented by a set of states and a set of transformation rules mapping states to states. The solutions to the problem are represented by final states which satisfy certain conditions and have no outgoing transformations. The search algorithm starts from one initial state, then repeatedly applies the transformation rules to the set of states currently being explored to generate new states. When at least one final state is reached, the algorithm stops. There are different strategies for choosing the order to traverse the state space. Depth-first search, breadth-first search, best-first search, and A^* search [73, 79] are commonly used ones.

- Initial state

  Since every Shifted Aggregation Tree has to include the original time series, the starting point is the SAT containing only level 0.

- Transformation rule

  If by adding a level onto the top of SAT B, we can get another SAT A, we say state B can be transformed to state A. Recall there are some constraints that the top level of SAT A has to satisfy. First, each node at the top level has to aggregate several children in the lower levels of SAT B. Second, the shadow of all the nodes of the top level has to cover the whole SAT B. Finally, the shift for the new level has to be an integral multiple of the shift of the level below in order to speed up detailed search.

  The transformation rule defines how to grow a complicated SAT from the first simple SAT.

- Final states

Final states are those Shifted Aggregation Trees which can detect bursts in all windows of interest. Since a SAT having top window size h and shift s can cover window sizes up to $h-s+1$, it is a final state if $h-s+1 \geq N$, where N is the maximum window size of interest.

- Traversing strategy

  In order to find an efficient structure, we use the best-first strategy to explore the state space. Each state is associated with a cost which will be discussed in subsection 3.3.2. Since different Shifted Aggregation Trees (SATs) cover different maximum window sizes and have different top-level shifts, a state may have a small cost just because it covers fewer window sizes or has a small top-level shift. So the costs are normalized in order for these SATs to be comparable, i.e. divided by the product of the maximum window size and the top-level shift. The state with the minimum cost is picked as the next state to be explored.

- The final Shifted Aggregation Tree with the minimum cost is picked as the desired structure.

In summary, the algorithm starts with a Shifted Aggregation Tree having level 0 only, then the candidate set of SATs keeps growing in a cost-sensitive manner, until a set of final SATs are reached. Figure 3.8 illustrates how the state space grows.

Given a Shifted Aggregation Tree, there are many ways it can grow. The next candidate level could aggregate multiple nodes from multiple different levels, and have different shifts. For example, for a Shifted Aggregation Tree containing only level 0, the next possible level could have size 2 and shift 1 or 2; alternatively, it could have size 100 and shift 1, 2, $\ldots$, 99, and so on. Such

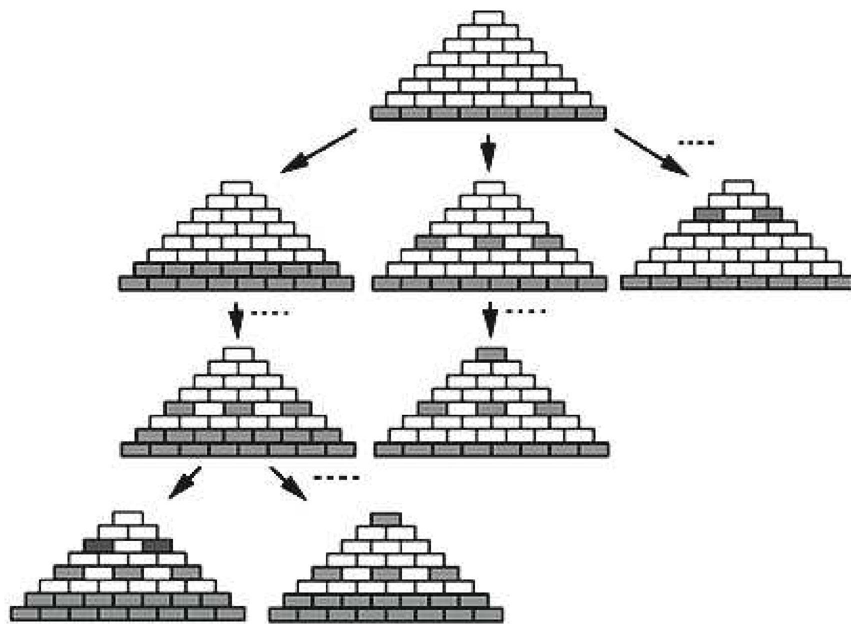

Figure 3.8: State space growth

combinatorial considerations show that there are an exponential number of ways to grow a Shifted Aggregation Tree. Therefore, we introduce some complexity-reducing constraints to avoid an exhaustive breadth first search strategy.

Let the maximum window size of all the explored states be L. Assume S is the current state to be explored. Instead of generating all possible next states for S at once, we generate only states whose maximum window sizes do not exceed $2L$. Then we put S in a list which stores all the states not yet fully explored. Whenever a new state with a larger window size W is generated, L is updated with the new value W. Then we go through each state in the list of partially-explored states and generate new states for them having maximum window sizes up to the new $2L$.

This avoids growing many highly unlikely Shifted Aggregation Trees at the early stage (say with a very large window size 10000 and shift 5000), but it allows us to gradually grow the intermediate structures and explore the more reasonable ones first. Note that this does not prune the search space, but controls the order of traversal of the search space. Our experiments (Figure 3.16) show that the best-first strategy works well.

We also restrict the number of states having the same shadow size and the number of final states. For example, if we have visited 500 states whose maximum shadow is of size 100, we do not explore any new such states. And if we have visited say 10000 final states, the algorithm stops.

3.3.2 Cost model

The cost associated with each state is used to indicate which structure to choose in terms of running time. One can measure this cost empirically by running this

Shifted Aggregation Tree on a small set of sample data and using the actual CPU time as the cost. Another method is to use the expected number of operations in a theoretical cost model to model the CPU's running time. Our model is a simple RAM model.

Let s_{top} be the shift at the top level; recall that every s_{top} time points, a node at the top level is updated and bursts below are covered. Thus, we need to consider the number of operations only every s_{top} time points, namely in one update-filter-search *cycle*. The expected number of operations in one cycle is the sum of the number of operations in the update phase, the filtering phase (to decide if a detail search is needed) and the detailed search phase.

- Cost in the update phase

  The number of update operations is just the number of nodes that are updated in a Shifted Aggregation Tree every s_{top} time points.

- Cost in the filtering phase

  For a node at level i, we need to find out h, $h_{i-1}-s_{i-1}+2 \leq h \leq h_i-s_i+1$, such that $f(h) \leq node(i,t) < f(h+1)$. This can be done using binary search. The number of comparison operations is

$$\sum_i \left(\log_2(h_i - s_i - h_{i-1} + s_{i-1} - 1) + 1\right)$$

- Cost in the detailed search phase

  The number of detailed search operations is the expected number of cell accesses in the detailed search region. Let $\Pr(w|h_i)$ be the probability of checking a cell of size w given a node at level i with window size h_i, s_i be the shift at level i, the expected number of cell to be checked is

$$\sum_i \sum_w \Pr(w|h_i) \cdot s_i$$

Table 3.2: Weights used for different operations

updating	filtering	detailed search
4.6	1	2.1

$\Pr(w|h_i)$ can be estimated from the statistics in the sample data.

In different real implementations and applications, the costs for various operations may differ. In order to take this into consideration, one can associate a weight with each type of operation. The weight can be obtained by a test run method: run millions of operations of each type and count the total running CPU time, and the averaged CPU time is used as the weight for each type. Table 3.3.2 shows the weights we used in our implementation.

The advantage of the theoretical cost model is that it is not subject to the fluctuation of the CPU usage in the empirical model when testing on the sample data. In the early stages of the state-space algorithm, the fluctuation in CPU usage could assign an inaccurate cost to a state, so that some worse state and its descendants get explored first in the best-first strategy. As stated above, because we limit the number of states having the same window size and the number of final states in order to prune the exponential state space, the actual better state and its descendants may be pruned afterwards, thus a better solution would be missed in this case. Another advantage of the theoretical model is that it is much faster than the empirical model, up to thousands of times faster depending on the amount of training data.

Our experiment (Figure 3.9) shows the theoretical model performs better than the empirical model for many different settings, i.e. different burst probabilities, different maximum window sizes of interest and different distribution

parameters. The theoretical cost model models the actual CPU running time well for Poisson and exponential distributions. The data setup is explained in the next section.

3.4 Empirical Results

In this section, we study how Shifted Aggregation Trees perform under different data distributions and different window thresholds. We first test on a set of synthetic data drawn from two classes of distributions common in the real world: the Poisson distribution and the exponential distribution. We analyze the alarm probability, then demonstrate empirically how different distributions and different window thresholds affect the desired Shifted Aggregation Trees, which in turn affect the alarm probability. The experiments on the real data can be found in the Case Study chapter. The experiments show that the Shifted Aggregation Tree-based detection always outperforms the Shifted Binary Tree-based detection, by a multiplicative factor as large as 35 in some of our experiments (Figure 3.14).

All the experiments were performed on a 2Ghz Pentium 4 PC having 512 megabytes of main memory. The operating system is Windows XP and the program is implemented in C++. The theoretical cost model (i.e. the expected number of operations) is used in the experiments. The CPU time shown in each test is the total wall clock time spent on each testing data set.

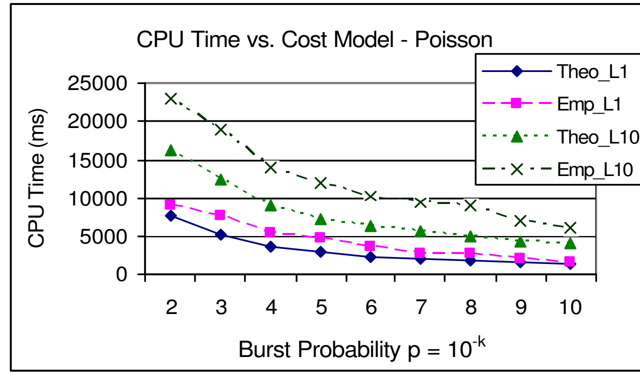

(a) Two Poisson distributions with $\lambda = 1, 10$ respectively (L1:$\lambda = 1$,L10:$\lambda = 10$)

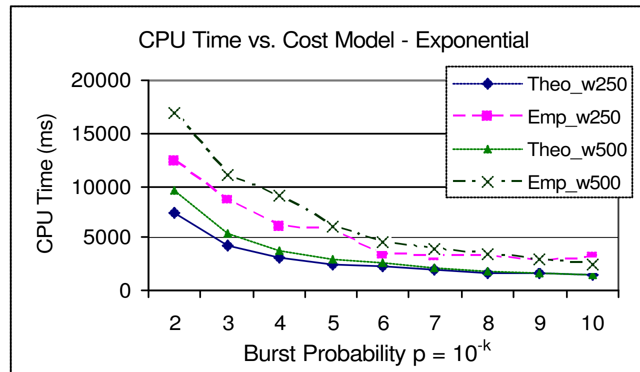

(b) Two exponential distributions with maximum window sizes 250 (w250) and 500 (w500) respectively

Figure 3.9: Comparison of the theoretical cost model and the empirical cost model on Poisson data and exponential data

3.4.1 Shifted Aggregation Tree Density and Alarm Probability

In order to see how the input affects the desired structure, we first define two variables to describe the characteristics of a Shifted Aggregation Tree: *density* and *alarm probability*.

Let s_{top} be the shift at the top level. As noted above, every s_{top} time points, an update-filter-search cycle is finished. The *density* D is defined as

$$D = \frac{Number\, of\, nodes\, in\, the\, SAT\, in\, one\, cycle}{Number\, of\, cells\, in\, the\, pyramid\, in\, one\, cycle}$$

Intuitively, the density describes the ratio between the number of cells to be updated in the updating phase and the number of cells to be filtered or searched in the detailed search phase. As the name suggests, it describes how dense a Shifted Aggregation Tree structure is when embedded in the aggregation pyramid.

While the density characterizes a static structural property of a Shifted Aggregation Tree, the alarm probability describes the dynamic statistical property of a Shifted Aggregation Tree running on a data set. Recall that if a node exceeds the minimum threshold within its detailed search region, it will raise an alarm and start a detailed search. The *alarm probability* P_a^i at level i is defined as

$$P_a^i = \frac{Number\, of\, nodes\, raising\, alarms\, at\, level\, i}{Number\, of\, nodes\, updated\, at\, level\, i}$$

Since the actual CPU cost is positively related both to alarm probability and to the size of the detailed search region, we define the alarm probability of a Shifted Aggregation Tree as the weighted sum of the alarm probability for each level multiplied by the number of cells in their detailed search regions. Intuitively,

the larger the alarm probability, the more detailed searches are performed thus requiring more CPU time. This gives a dynamic statistical description of how a Shifted Aggregation Tree performs on a data set.

3.4.2 Synthetic Data

A set of synthetic data was generated using a random number generator. Two classes of probabilistic distributions which have been widely used to model many real world phenomena were chosen to generate the synthetic data: the Poisson distribution and the exponential distribution.

- Poisson distribution

  Many real world phenomena can be modeled as a Poisson process, such as customers arriving at a service station, emissions from radioactive material, etc. [68]. It is well known in a Poisson process that the number of events happening within the time interval $[0, t]$ follows the Poisson distribution. Also the normal distribution is the limit distribution of the Poisson distribution.

- Exponential distribution

  One class of data application that does not follow the Poisson distribution but characterizes the behaviors of phenomena like network traffic is self-similar or fractal data [89] [55] [90]. For example, a fractal process, following the "80/20 law," 80% of the time there is no activity, 20% of the time there is some activity; within the latter 20% of the time, 80% of that time has little activity and 20% of that time there is high activity; and so on. In such a case, the number of activities within one unit time follows the exponential distribution.

For each distribution, we synthesized a set of data with different distribution parameters in a broad range. Each testing data set includes 5 million data points. The first 20,000 data points are used as the training data in the state-space algorithm to find a desired structure. To make our task challenging, in these tests, we want to find bursts for every window size between 1 and 250.

Because the Central Limit Theorem says that the sum of N independent identically distributed random variables approaches the normal distribution when N is large, we use the normal distribution in the following analysis of the alarm probability. Note that the normal distribution assumption is for qualitative analysis only. In real data, the distribution may not follow the normal distribution. Thus in our algorithm, the statistics to estimate the alarm probability are collected from the sample data, instead of using the formula directly.

Assume that each point in the input time series has a number of events characterized by a mean μ and a standard deviation σ. Then a sliding window of the time series of size w has mean $w\mu$ and standard deviation $\sqrt{w}\sigma$. Assume that for each window size, the probability of exceeding the threshold should be some value p. We can characterize this by saying that $Pr[S_o(w) \geq f(w)] \leq p$, where $S_o(w)$ is the observed number of events for window size w and $f(w)$ is the threshold for window size w.

Let $\Phi(x)$ be the normal cumulative distribution function, for a normal random variable X,

$$Pr[X \geq -\Phi^{-1}(p)] \leq p$$

We have

$$Pr\left[\frac{S_o(w) - w\mu}{\sqrt{w}\sigma} \geq -\Phi^{-1}(p)\right] \leq p$$

Therefore, $f(w)$ should set to be $w\mu - \sqrt{w}\sigma\Phi^{-1}(p)$.

The alarm probability P_a for an aggregate of window size W to exceed the threshold for size w, is $Pr[S_o(W) \geq f(w)]$. Therefore,

$$
\begin{aligned}
P_a &= Pr[S_o(W) \geq f(w)] \\
&= Pr[\frac{S_o(W) - W\mu}{\sqrt{W}\sigma} \geq \frac{f(w) - W\mu}{\sqrt{W}\sigma}] \\
&= \Phi(-\frac{f(w) - W\mu}{\sqrt{W}\sigma}) \\
&= \Phi(\frac{(W-w)\mu}{\sqrt{W}\sigma} + \frac{\sqrt{w}\sigma\Phi^{-1}(p)}{\sqrt{W}\sigma}) \\
&= \Phi((\sqrt{T} - \frac{1}{\sqrt{T}})\sqrt{w}\frac{\mu}{\sigma} + \frac{\Phi^{-1}(p)}{\sqrt{T}})
\end{aligned}
$$

where $T = W/w$, denotes the *bounding ratio*. The smaller T is, the tighter the bounding, and vice versa.

So P_a is determined by the distribution parameters μ and σ, the threshold parameter p, the bounding ratio T and the level w in the underlying aggregation pyramid. We can draw the following conclusions from the formula above.

- The larger the ratio μ/σ is, the larger the alarm probability P_a.

  This is illustrated conceptually in Figure 3.10. Figure 3.10 shows the probability density functions (pdf) for two normal random variables, one for the number of events in a window of size w which has mean $w\mu$ and standard deviation $\sqrt{w}\sigma$, another similar one for a window of size W. The threshold line shows where $f(w)$ lies. When a distribution realization for size W appears to the right of the threshold line, the aggregate is greater than the threshold for size w, and an alarm is raised. So the value of P_a is the area below the probability density function of size W but to the right

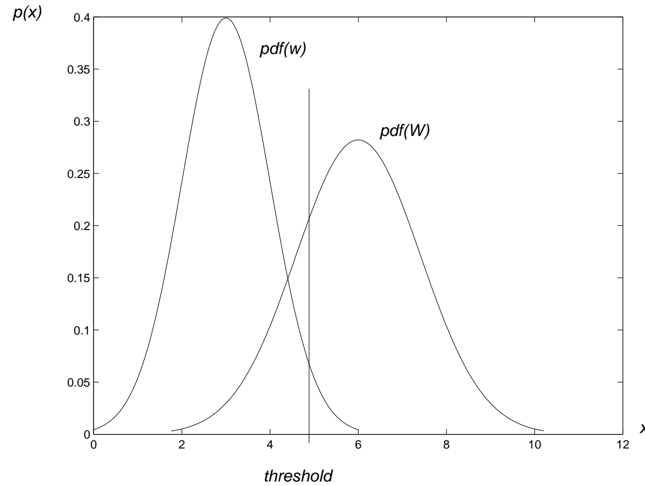

Figure 3.10: Illustration of the alarm probability for a window of size W to exceed the threshold for size w, i.e. the portion under the probability density function of size W and to the right of the threshold line for size w.

of the threshold line.

As μ increases, both the threshold line and the curve peaks move to the right along the x axis, but the gap between the two peaks increases. There are more portions to the right of the threshold line under the pdf of size W. There are more chances to raise an alarm. As σ increases, both curves stretch along the x axis, and the threshold line moves to the right. The portion to the right of the threshold line under the probability density function of size W decreases. There are fewer chances to raise an alarm.

For a Poisson distribution with shape parameter λ, the mean μ is λ and the standard deviation σ is $\sqrt{\lambda}$, so the ratio is $\sqrt{\lambda}$. Different λ ranging from 10^{-3} to 10^{3} were tested. In this test, the burst probability is set to be 10^{-6}. Figure 3.11 shows the CPU time, the alarm probabilities and the densities for different λ.

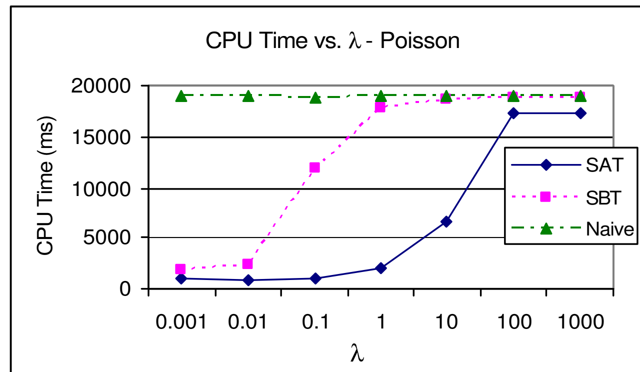

(a) CPU time

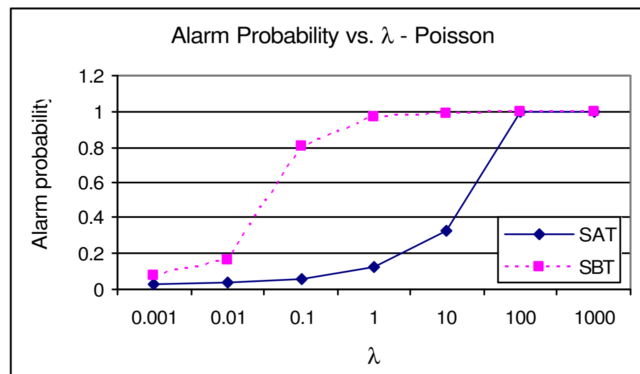

(b) Alarm Probability

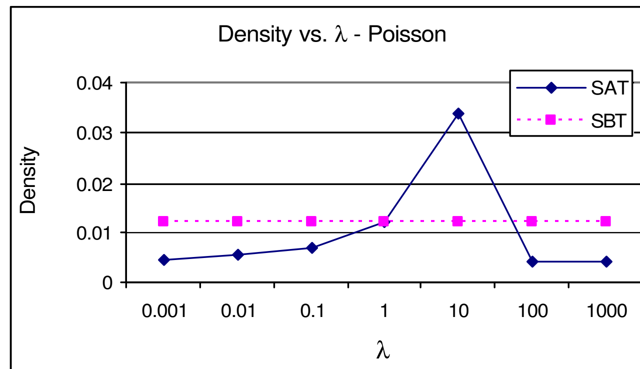

(c) Density (i.e. the ratio between the number of cells to be updated and the number of cells to be filtered or detailed searched in one cycle)

Figure 3.11: The effect of λ in the Poisson distribution

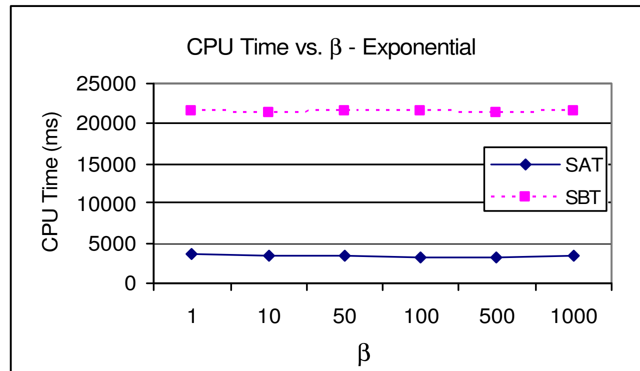

(a) CPU time

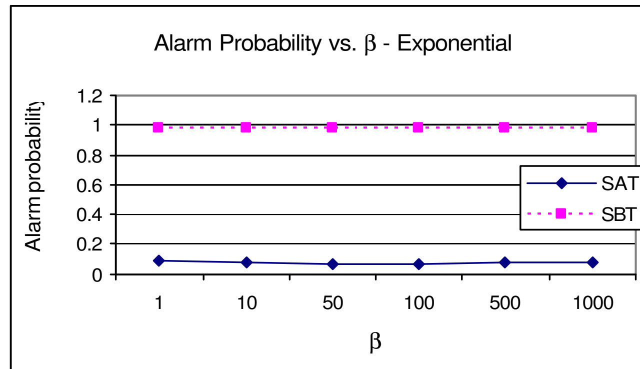

(b) Alarm Probability

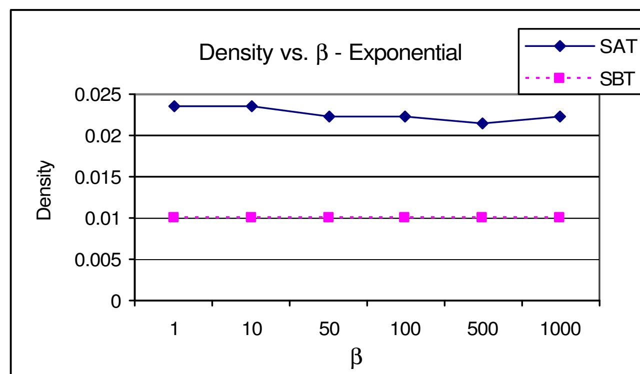

(c) Density

Figure 3.12: The effect of β in the exponential distribution

As λ, i.e. $(\mu/\sigma)^2$, increases, P_a increases. More detailed searches are performed so the CPU time increases. To mitigate this, the Shifted Aggregation Tree must become denser in order to bring down the alarm probability. When λ becomes very large, the alarm probability is close to 1 anyway, so the Shifted Aggregation Tree becomes sparse again to reduce the updating time, but is essentially useless.

For an exponential distribution with scale parameter β, both μ and λ are β, so the ratio is the constant 1. This means that changing β should have no effect on the alarm probability. Figure 3.12 shows the effect of different β. The experiments show that varying β has no noticeable effect.

- The smaller the burst probability p, the larger the threshold, the smaller P_a.

  This essentially moves the threshold line of size w to the right in Figure 3.10. So P_a decreases.

  Figure 3.13 and 3.14 show the effect of different thresholds for the Poisson distribution and the exponential distribution respectively. The burst probabilities range from 10^{-2} to 10^{-10}. As the burst probabilities go down, both the alarm probabilities and the densities decrease, because there are fewer bursts to worry about, so speed depends on reducing the update time.

- As the bounding ratio T decreases, so does P_a.

  In a Shifted Aggregation Tree, T could be very close to 1, e.g. $W = w+1$, whereas T in a Shifted Binary Tree is designed to be about 4. Figure 3.15.a shows the bounding ratios at different levels of a Shifted Aggregation Tree

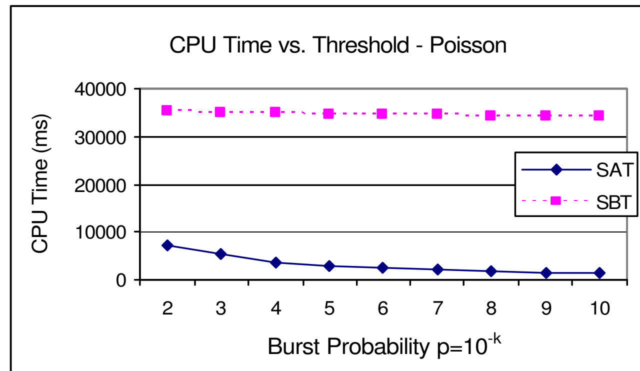

(a) CPU time

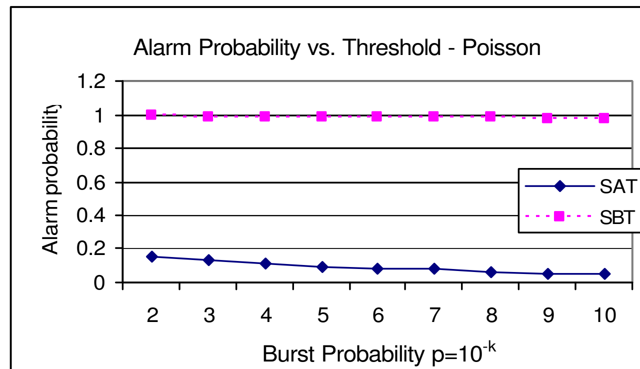

(b) Alarm Probability

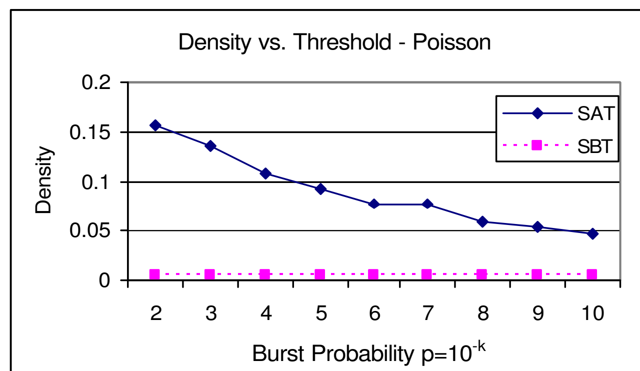

(c) Density

Figure 3.13: The effect of burst probability in the Poisson distribution

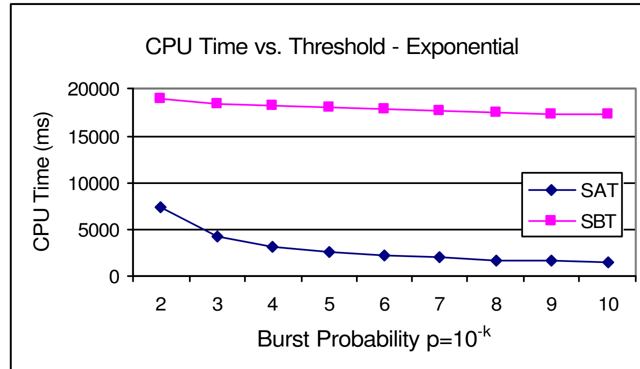

(a) CPU time

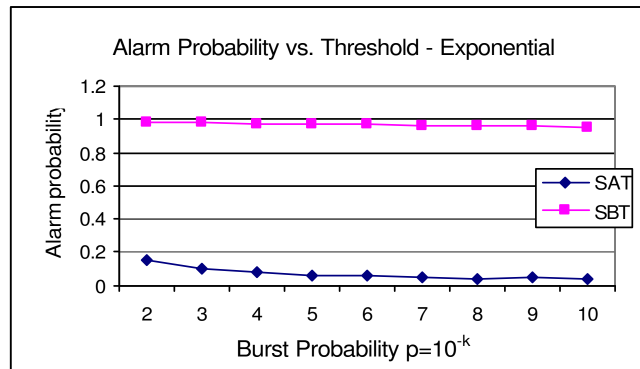

(b) Alarm Probability

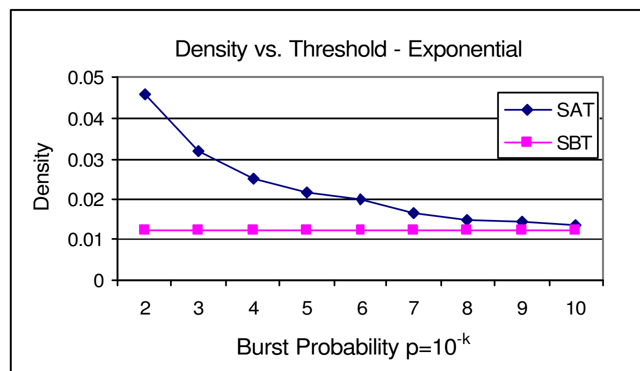

(c) Density

Figure 3.14: The effect of burst probability in the exponential distribution

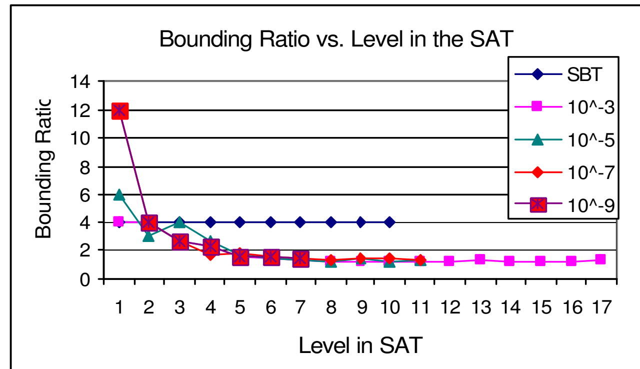

(a) The bounding ratio for different levels in a Shifted Binary Tree and Shifted Aggregation Trees for different burst probabilities

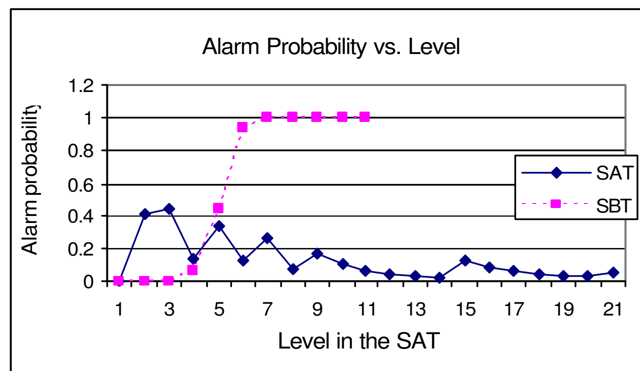

(b) Alarm probability as a function of window size in the Shifted Binary Tree vs. the Shifted Aggregation Tree

Figure 3.15: How the bounding ratio in a Shifted Aggregation Tree adjusts as a function of window size and the burst probability in order to reduce the alarm probability.

and a Shifted Binary Tree under different burst probabilities. Notice how the bounding ratio changes in a Shifted Aggregation Tree: it is high at the lower levels where the window size w is small, while low at the higher levels where the window size w is large, in order to bring down the alarm probability. As the burst probability becomes smaller, there are fewer bursts. Thus, the bounding ratio becomes a little larger, and the Shifted Aggregation Tree becomes sparser.

- As the size w increases, so does P_a.

  Figure 3.15.b shows the alarm probabilities at different levels in a Shifted Binary Tree and a Shifted Aggregation Tree. The Shifted Binary Tree always has a high alarm probability at the high levels, while in a Shifted Aggregation Tree, by using a small bounding ratio T, the alarm probability remains low. Thus the Shifted Aggregation Tree has more filtering power than the Shifted Binary Tree.

In summary, because the Shifted Aggregation Tree can adjust its structure to reduce the alarm probability, it achieves far better running time than the Shifted Binary Tree.

Search parameters in the state-space algorithm

We want to study how different search parameters affect the desired Shifted Aggregation Tree structures in the state-space algorithm. We tested on different data settings with different numbers of final states and different number of states with the same maximum window size, to see when there are diminishing returns from broadening the search.

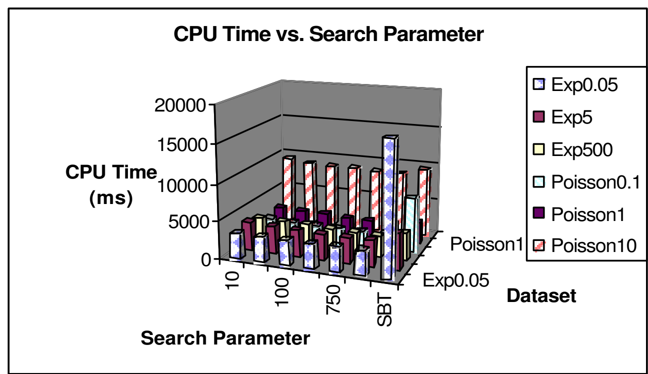

Figure 3.16: CPU time for Shifted Aggregation Trees found using different search parameters

The number of states with the same maximum window size, and the number of final states are set to be 10, 50, 100, 500, 750, 1000 respectively. Other parameters are chosen randomly to cover a broad parameter range. Table 3.3 summarizes the parameter settings. Three pieces of training data are picked for the Poisson distribution and the exponential distribution respectively. Figure 3.16 shows the CPU running times for the Shifted Aggregation Trees found using these parameters. It also shows the CPU running time for the Shifted Binary Tree as a reference.

The experiments show that even with small values of these parameters, the Shifted Aggregation Trees discovered are close to those discovered with much larger values of the parameters. The best-first search strategy works well in this situation. In practice, we believe that setting both parameters to be 500 works most effectively.

Table 3.3: Statistics for testing data sets for search parameters

	Mean	StdDev	Max Size	Number of Sizes	Burst Probability
Poisson0.1	0.1	0.316	250	250	10^{-3}
Poisson1	1	1	750	25	10^{-5}
Poisson10	10	3.16	500	100	10^{-6}
Exponential0.05	0.05	0.05	500	500	10^{-5}
Exponential5	5	5	750	75	10^{-7}
Exponential50	500	500	1000	50	10^{-8}

Chapter 4

Greedy Dynamic Burst Detection

The previous chapter shows a framework to train a Shifted Aggregation Tree given a sample input time series and window thresholds. However in real world situations, the incoming data often changes constantly.

In a situation where the input time series keep changing, the performance would be poor if the training data used to find the Shifted Aggregation Tree differed significantly from the data to be detected. For example, if the training data has fewer bursts, as with a trained Shifted Aggregation Tree that is sparse, while the test data has far more bursts, it would require a denser structure. If the training data has the same mean and standard deviation as those of the test data, we call it an *unbiased* data (thus an "ideal" training data), otherwise we call it a *biased* data. Our experiment (Figure 4.3) shows that given fixed thresholds, the detection time training with a biased data can be 10 percent to 2.5 times more than that training with an unbiased data. In this case, it would be preferable if we could dynamically adjust the structure in order to achieve

better performance.

In this chapter, we present a greedy dynamic detection algorithm which dynamically evolves the Shifted Aggregation Tree to adapt to the incoming data. This algorithm starts with a Shifted Aggregation Tree trained with a sample data set from the incoming data, then changes the structure dynamically based on the alarms to trigger a detailed search. The dynamic structure either filters out more detailed searches or reduces the number of updates, and thus has better detection time. The experiments show that the dynamic algorithm overcomes the discrepancy resulting from a biased training set and achieves even better performance than the static algorithm training with an unbiased sample data in most cases.

This chapter is organized as follows: Section 4.1 describes the structural dependency between different levels in a Shifted Aggregation Tree and defines a more flexible dependency structure which can be easily changed dynamically. Section 4.2 presents the greedy dynamic detection algorithm. The experimental results are shown in Section 4.3 comparing the greedy algorithm with the static algorithm over different settings and different types of data. A worst-case analysis comparing the greedy algorithm with the clairvoyant algorithm is presented in Section 4.4.

4.1 Structural Dependency

In the state-space search algorithm, the candidate Shifted Aggregation Tree keeps growing by adding one level onto the top of the existing candidate tree. For example, a level of window size 256 can be added onto the top of a Shifted Binary Tree with maximum window size of 192 by adding an extra window of

size 64. There is a structural dependency between the levels. For example, a window of size 256 won't be computed without its children subwindows of size 192 and size 64, therefore we cannot remove the level of size 192 if the level of size 256 is still in the tree. Because each level depends on one level below, we don't have complete freedom in removing levels.

However, it is easy to see that one window can be composed of different sets of subwindows, for example, a window of size 256 can be composed of one of size 192 and one of size 64, or two of size 128. Therefore, we can construct the Shifted Aggregation Tree in such a way that only a small set of backbone levels are used to compose other levels. An example of the backbone levels are levels of sizes 16, 32, 64, 128, etc. By aggregating these backbone levels, we can get other window sizes such as 48, 96, 192, etc. These window sizes in turn can act as the secondary backbone levels to compose more window sizes, for example a window of size 112 (aggregating size 16 and 96).

Figure 4.1 shows the algorithm to reformat a Shifted Aggregation Tree generated by the state-space algorithm in order to reduce the structural dependency. "Reformatting" entails changing the dependency relationships among levels. "Occurrence" in this context means how many times a level appears as a child of higher levels. For example, in the original structure shown in Table 4.1, the occurrence of size 8 is 2, the occurrence of size 16 is 6, the occurrence of size 48 is 1, etc.

The basic idea is first to pick a level L with the most occurrences in the tree but having the minimum window size. That level L is reformated to depend on the 0th level. L is then called the base level. In general, a level which can be computed from the set of reformated levels only and having the minimum number of unique children is reformated to depend on these children. This

```
count the occurrences of the child levels of every level
L = {all levels but level 0}; // levels to be reformated
R = {}; // reformated levels
while L not empty
    let k be the level in L with the most occurrences
        but having the minimum window size
    reformat k to depend on level 0 only
    move k from L to R
    D = {l: l ∈ L, level l can be composed of by levels in R only}
    while D not empty
        m = the level in D having minimum number of unique children
        reformat m to be the aggregate of these children
        move m from L to R, remove m from D
        update D
    end while
end while
```

Figure 4.1: Algorithm to reformat the parent-child structures in order to reduce the structural dependency in a Shifted Aggregation Tree

process is repeated until all the levels are reformated.

Table 4.1 shows an example of how the algorithm reformats a Shifted Aggregation Tree. The algorithm first picks the level of size 16 as the base level. Because size 16 depends on size 1 only, size 8 is removable. Next size 32 which depends on size 16 only is picked as the second level, and similarly for size 64 and size 128 in turn. Finally, other levels are reformated to depend on these reformated levels only.

In this way, we organize all the window sizes in dependency hierarchies. The bottom hierarchy contains the backbone levels; the second hierarchy contains the levels that are dependent only on the bottom hierarchy; the levels in a higher hierarchy depend only on the levels in the same or lower hierarchies; and so on, until the top hierarchy which has no other levels depending on them. This way there are fewer dependencies between different levels, giving us the freedom to add or remove levels on the fly. We can change the structure from a very sparse one that contains only the initial backbone levels to a very dense one that contains many derivative levels, or any structure in between. In other words, we can create multiple different structures on the fly with different maintenance costs and different pruning power to adapt to different incoming data.

When trying to add a level in between two levels, say of size 128 and size 256, we want to add the level in such a way that it has good pruning power (to potentially save more detailed search time) and it has low updating cost and less dependency (to save more updating time). We prefer a level which is evenly spread out in between these two levels and belongs to as low of a hierarchy as possible. For example, we prefer to add a level of size 192 between size 128 and size 256, instead of 144, because given the same cost to update, a window of size 192 can avoid more detail searches if there is no alarm raised. We prefer

Table 4.1: An example of reformating a Shifted Aggregation Tree to reduce structural dependency

Step 0: original structure

size	children
1	1
8	depending on size 1 only
16	8+8
32	16+16
48	16+32
64	16+48
80	16+64
96	16+80
128	32+96

Step 1: size 16 picked as the base level

size	children
1	1
8	depending on size 1 only
16	depending on size 1 only
32	16+16
48	16+32
64	16+48
80	16+64
96	16+80
128	32+96

Step 2: size 32, 64 and 128 reformated

size	children
1	1
8	depending on size 1 only
16	depending on size 1 only
32	16+16
48	16+32
64	32+32
80	16+64
96	16+80
128	64+64

Step 3: other levels reformated

size	children
1	1
8	depending on size 1 only
16	depending on size 1 only
32	16+16
48	16+32
64	32+32
80	16+64
96	32+64
128	64+64

not to add a level of size 193, because its pruning power is similar to 192, but depends on more levels, thus requiring more updating cost and restricting the removal of other levels. We denote the candidate level to be added between two levels of size h_i and h_{i+1} as $cand(h_i, h_{i+1})$. $cand(h_i, h_{i+1})$ is chosen from all the possible levels between h_i and h_{i+1}, based on the above criteria. After $cand(h_i, h_{i+1})$ is chosen, the same process is used to choose the new candidate level between h_i and $cand(h_i, h_{i+1})$, and the one between $cand(h_i, h_{i+1})$ and h_{i+1}. This is repeated until no more levels can be added between two adjacent levels. In order to efficiently retrieve the candidate levels, in the initialization phase, a map is constructed; this map maps two adjacent levels to the candidate level to be added in between.

4.2 Greedy Dynamic Detection Algorithm

Before going into the algorithm details, we first explain the cluster and delay phenomenon when an alarm happens. This phenomenon is used as a heuristic in the dynamic algorithm.

Alarms are likely to happen in clusters, across multiple window sizes and multiple neighboring windows. When a large number of events happen in a short period of time, the number of events in any window containing this period of time is likely to be large too, due to the monotonicity property. For example, a window of size 5 contains 30 events and raises an alarm because it exceeds the threshold of 10 events for size 5. A window of size 10 containing this window of size 5 would likely contain a large number of events and thus also raise an alarm. In this case, multiple neighboring windows of different sizes may exceed their minimum thresholds and raise alarms. Furthermore, when a burst happens in a

Table 4.2: Weights used for different operations in the dynamic algorithm

updating	filtering	detailed search	changing structure
4.6	1	2.1	10

small window, a larger window starting with this small subwindow likely raises an alarm some time later when the larger window ends. In the above example, the alarm at size 10 will be raised 5 time points later than the alarm at size 5. In other words, there is some delay for an alarm at a larger window size following an alarm at a smaller window size.

This phenomenon suggests when an alarm happens at level k, we may expect more alarms at levels higher than k in the near future. Accordingly, the structure should be changed so as to anticipate this.

The basic idea behind the dynamic detection algorithm is to change the Shifted Aggregation Tree if a change helps to reduce the overall cost. In order to compute the cost, we use the theoretical model as described in the previous chapter. Besides the costs for updating, checking/filtering and detail searches, there will be a cost for changing the structure. We use a similar test run method as described in the theoretical model section to quantify this cost. We run the operation a million times to change one level (i.e. add/remove a level or widen/narrow a shift as defined below) in the Shifted Aggregation Tree. The average CPU time is used as the unit cost for changing a level. Table 4.2 shows the cost for changing the structure compared to other operation costs. Note that the cost to change one level is not that significant compared to other costs. This allows us to change the structure relatively frequently.

Intuitively, when considering one level alone, if by adding a level, the total saved detailed search cost is more than the total updating/filtering cost plus

the cost to change the structure, we should add this level. Similarly, if the updating/filtering cost for a level is greater than the detailed search cost it saves and the changing cost, we should remove this level. However, when considering multiple levels together, this removed level may have been helpful for supporting another higher level which would in turn have saved more detail searches. For example, a level of size 64 may support a level of 192 which aggregates size 64 and size 128.

We adopt a greedy strategy when trying to make the structure denser, i.e. whenever the saved detail search cost is greater than the updating/filtering cost, make the structure denser. On the other hand, because of the cluster and delay phenomenon, we use a delayed greedy strategy when trying to make the structure sparser: if an alarm is raised at level k at time t, we won't remove any level lower than $k + \delta k$ until time $t + \delta t$, where $\delta k \geq 0, \delta t \geq 0$. This is to anticipate any potential secondary alarm after an alarm occurs and to avoid unnecessary changes to the structure. We call this region determined by δk and δt an *alarm region*. The alarm region extends further if a new alarm occurs in the alarm region. We will study the effect of different δk and δt in the experiment section.

To make a structure denser, we can add a level or make a shift smaller; conversely, we can remove a level or make a shift larger to make a structure sparser. Recall that a shift is defined as the number of time points separating two neighboring nodes at the same level. The closer two neighboring nodes are, the denser the structure is. Due to the Shifted Aggregation Tree property, the shift at level $k+1$ has to be an integral multiple of the shift at level k. So, when changing a shift S_k, we make the new shift either $2S_k$ (i.e. double the current shift) or $\frac{S_k}{2}$ (i.e. half the current shift). This normally satisfies the integral

multiple property (it always does for halving and often does for doubling in our construction method).

To be more specific, we need to decide the following:

- Which structure to start with:

  Given the inputs, we first train a Shifted Aggregation Tree using any sample data set. Then we reformat the Shifted Aggregation Tree to reduce the structure dependency as described in the structural dependency section. The dynamic algorithm starts with the reformatted structure.

- How to change the structure:

  We define four possible actions to change level k in the existing structure:

  - Add a level between level k and level $k-1$
  - Remove level k
  - Widen the shift at level k, denoted by S_k, to be $2S_k$
  - Narrow the shift at level k, denoted by S_k, to be $\frac{S_k}{2}$

  Notice that all these actions have to conform to the dependency rules. Also the structure after the change has to be another valid Shifted Aggregation Tree, i.e. they have to satisfy the properties of a Shifted Aggregation Tree as described in the framework chapter.

  Theoretically, we can narrow or widen the shift of a level as long as the structure after the change is still a valid Shifted Aggregation Tree. However in the actual implementation, a memory buffer is allocated to store the aggregate for one level. The narrow operation requires a memory reallocation and re-creation of the parent-children structure which

are expensive operations. One way to avoid the memory reallocation is to allocate a larger buffer than needed when first creating this level. We still need to restrict the maximum allowed shift step ms such that $\frac{1}{ms} \leq \frac{shift\ at\ any\ time}{initial\ shift} \leq ms$, i.e. the shift won't be ms times more than the initial shift or $1/ms$ times less than the initial shift. It actually limits how many times we can consecutively widen or narrow a shift from the initial shift, thus how far a structure can change away from the initial structure. For example, the initial shift for a level is 32 time points, if ms is set to be 1, the shift can be 16, 32 and 64; if ms is set to be 2, the shift can be 8, 16, 32, 64 and 128; and so on. We will show the effect of the maximum allowed shift step in the experiment section. A too large ms actually may lead to poor performance depending on how far the training data deviates from the test data.

- When to change the structure:
  - When an alarm is raised at some level $k+1$ and a detailed search is triggered, we check if adding $cand(h_k, h_{k+1})$ will help to reduce the cost for detailed search. If the cost saved on the detailed search is greater than the updating/filtering cost, we add this candidate level between level k and $k+1$.
  - If the candidate level cannot be added because some of its children are not in the tree, then add those children into the tree.
  - If the candidate level cannot be added because its shift makes the resulting structure invalid, we try to narrow the shifts of levels below $k+1$ if narrowing the shifts is helpful to fit the candidate in. For example, based on the Shifted Aggregation Tree properties, we cannot

add a level of size 20 with shift 8 between a level of size 24 with shift 8 and a level of size 16 with shift 8, because the overlapping size of the level of size 20 has to be greater than or equal to size 16. In this case, we first narrow the shifts at these three levels (16, 20, 24) to be 4. This allows more candidate levels to be added in.

– If the aggregate at level $k+1$ does not exceed the minimum threshold for level k, i.e. keeping the level k does not help to reduce the detailed search time, we remove level k if it is not in an alarm region.

– If level k cannot be removed due to the dependency and it is not in an alarm region, we try to widen and double the shift at level k if possible.

Figure 4.2 shows the full detection algorithm.

4.3 Empirical Results

We have tested the greedy dynamic detection algorithm on different types of data distributions and different parameter settings. The experiments show that the greedy dynamic detection algorithm overcomes the discrepancy resulting from a biased training data and achieves better performance in most cases than the static algorithm even training with unbiased sample data. But it may not work as well as the static algorithm in some cases, for example when the bursts are very rare or very frequent.

First we compare the performance of the dynamic algorithm and the static algorithm under different parameter settings. Then we also study the effect of different parameters in the dynamic algorithm: the maximum allowed shift step

```
for every time point t starting from 1
    a_l = 0; a_s = 0; alarm region = null;
    for the window ending at the current time t at every level i
        update node(i, t) by aggregating its children
        if node(i, t) raises an alarm then
            if legal to add cand(h_{i-1}, h_i)
                compute the aggregate at cand(h_{i-1}, h_i)
                if the updating/filtering cost < the saved
                    detailed search cost by adding cand(h_{i-1}, h_i) then
                    add cand(h_{i-1}, h_i) between level i - 1 and i
                    if cand(h_{i-1}, h_i) raises an alarm then
                        search the DSR of cand(h_{i-1}, h_i) for real bursts
            else if cannot add because the children are not in the tree
                add those children into the tree
            else a_l = i; a_s = the shift to make cand(h_{i-1}, h_i) fit in
            if there is still an alarm in the DSR of node(i, t)
                search DSR(i, t) for real bursts
            update the alarm region
        else if node(i, t) < the minimum threshold in DSR(i - 1, t)
                and node(i - 1, t) not in the alarm region then
                if legal to remove level i - 1 then remove it
                else legally double the shift at level i - 1
    for i = 1 to a_l
        if shift_i > a_s and legal to narrow shift_i, then narrow shift_i
```

Figure 4.2: Greedy dynamic detection algorithm

and the size of the alarm region.

In the following experiments, we use the synthetic data with Poisson distribution and exponential distribution as described in the previous chapter. The experiments on the real world data can be found in the next chapter.

4.3.1 Performance Test

We want to compare the performance of the dynamic algorithm with that of the static algorithm under different parameter settings: different training data in the static algorithm, different distribution parameters, different burst probabilities and different sets of window sizes. Further, we study how the dynamic algorithm performs under different changing rates and different changing magnitudes in the data. In the dynamic algorithm, the maximum allowed shift step is set to be 1 and the size of the alarm region is set to be $\delta k = 1$, δt is set to be the size difference between level k and level $k+1$ (as explained later).

Performance comparison using different training sets

Given the fixed thresholds and the test data, we are interested in how different training data affect the performance of the static algorithm and how the dynamic algorithm performs compared to the static algorithm.

A set of Poisson data of 10,000 points are synthesized with different λ: 0.8, 0.9, 1.0, 1.1, 1.2. They are used as the training data in the static algorithm. A synthesized data of 5 million points with $\lambda = 1$ is used as the test data. The thresholds are computed based on $\lambda = 1$ and burst probability 10^{-6}. A burst probability of p means that for every window size, the probability at any timepoint that a burst occurs is p. Put another way, we set the threshold for

any window size w so that, given the distribution assumptions, the burst occurs with probability p. The maximum window size is set to be 250; the task is to detect bursts at every window size.

We use the synthesized data and the same thresholds to train a Shifted Aggregation Tree in each case. Then the static algorithm is tested with the trained structure to detect the same test data. Thus except for the training data having $\lambda = 1$, all other training data have different statistics from the test data, i.e. they are all biased training data.

Similarly, we synthesized a set of training data of exponential distribution with different β: 0.8, 0.9, 1.0, 1.1, 1.2. Other parameters are set up in the same way as those for the Poisson data.

Figure 4.3 shows that for the static algorithm, using biased training data could require 10 to 250 percent more detection time compared to using a unbiased training data. The dynamic algorithm can reduce the detection time by up to two-thirds, when the training data differs from the test data significantly. It even performs about 20 percent better than the static algorithm using the unbiased training data.

Since biased data always gives worse performance than an unbiased data, in the next experiments, we show only the comparison between the dynamic algorithm and the static algorithm using unbiased sample data unless otherwise stated.

Performance comparison using different distribution parameters

We want to study how the dynamic algorithm performs compared to the static algorithm using unbiased sample data under different distribution parameters. As shown in the previous chapter, the parameter in the exponential distribution

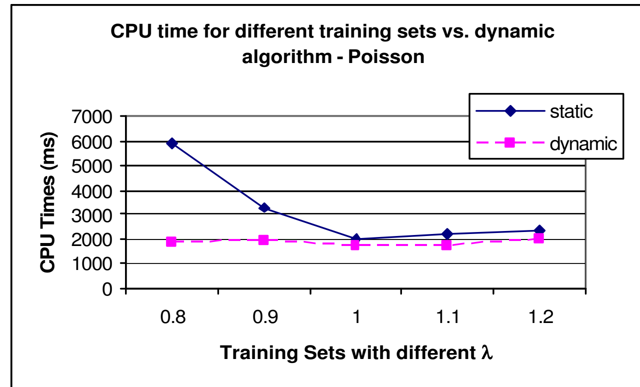

(a) Poisson distribution

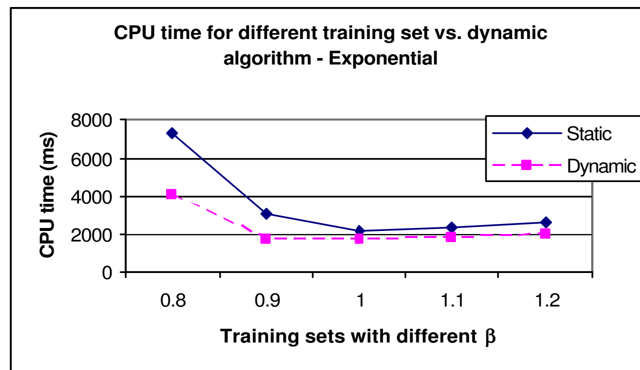

(b) Exponential distribution

Figure 4.3: Performance comparison between the dynamic algorithm and the static algorithm using different training sets

has little effect on the alarm probability. So we show only the results for the Poisson data.

We synthesized a set of training data with different λ values ranging from 10^{-3} to 10^{3}. Different thresholds and test data are generated based on the corresponding λ. The burst probability is set to 10^{-6}. The maximum window size is set to be 250; the task is to detect bursts at every window size.

Notice that the differences between this test and the previous one are the different thresholds and different test data used. In this test, for $\lambda = 10^{-1}$, the thresholds are generated using mean 10^{-1} and standard deviation $\sqrt{10^{-1}}$; while in the previous test, the thresholds are generated using mean 1 and standard deviation 1. Similarly, the test data are generated using $\lambda = 10^{-1}$, instead of using $\lambda = 1$. Thus, in this test, the training data are all unbiased.

Figure 4.4 shows the results. When λ is smaller than 100, the dynamic algorithm performs about 10 percent better than the static algorithm. When λ is equal to and greater than 100, the dynamic algorithm performs slightly worse than the static algorithm. The reason is that when λ is large, the alarm probability is always large, thus the desired structure is sparse to save some updating time. (Please refer to the previous chapter for the explanation.) The dynamic algorithm checks to determine if adding a level is helpful each time an alarm is raised, but most checks are fruitless and a level is seldom added. The dynamic algorithm saves little by adding a level, instead, it has to spend extra time on checking to see if adding a level is helpful.

Performance comparison under different burst probabilities

This test compares the dynamic algorithm against the static algorithm using unbiased data under different burst probabilities.

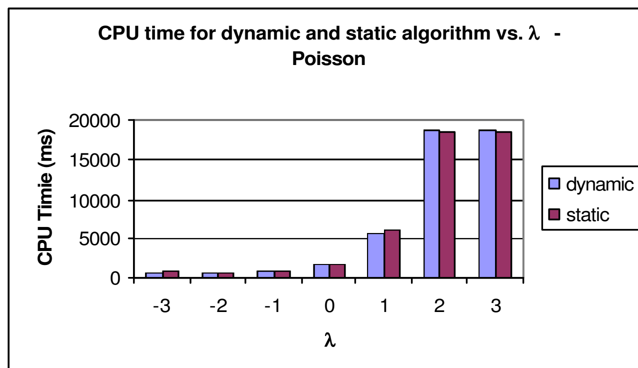

Figure 4.4: Performance comparison between the dynamic algorithm and the static algorithm using unbiased data under different distribution parameters

λ is set to be 1 in the Poisson distribution and β is set to be 10 in the exponential distribution. The burst probabilities range from 10^{-2} to 10^{-10}. The maximum window size is set to be 250; the task is to detect bursts at every window size.

The results in Figure 4.5 show that under different burst probabilities using unbiased training data, the dynamic algorithm always performs 10 to 20 percent better than the static algorithm.

Performance comparison under different sets of window sizes of interest

In this experiment, different sets of window sizes of interest are used to see how the dynamic algorithm performs compared with the static algorithm when training with unbiased data.

Instead of detecting bursts at every window size, this test detects bursts only for a set of n window sizes exponentially evenly-spaced up to the maximum window size of interest, i.e. $\{N^{\frac{1}{n}}, N^{\frac{2}{n}}, N^{\frac{3}{n}}, \ldots, N\}$, where N is the maximum

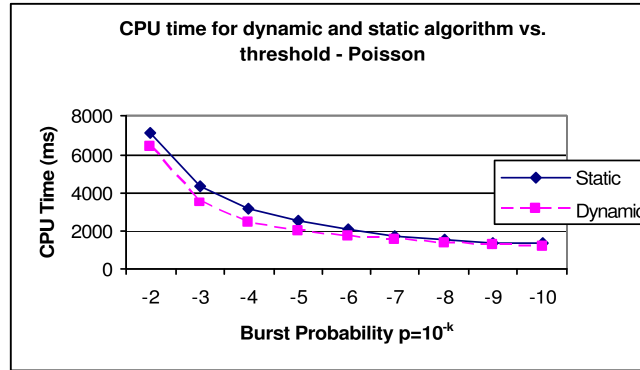

(a) Poisson distribution

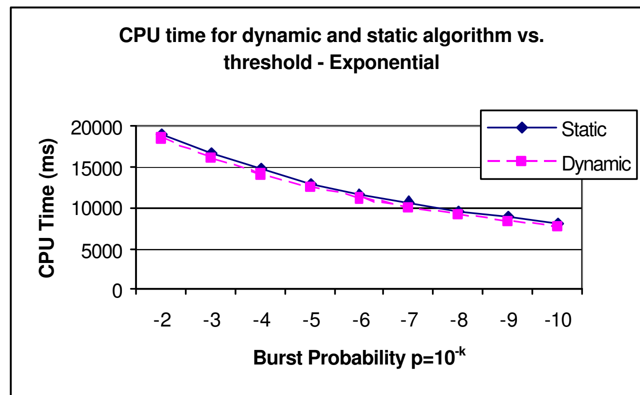

(b) Exponential distribution

Figure 4.5: Performance comparison between the dynamic algorithm and the static algorithm training with unbiased data under different burst probabilities

window size of interest. In this test, N is set to be 1000 and n is set to be 10, 25, 50, 75, 100 respectively. λ is set to be 0.1 and the burst probability is set to be 10^{-4} for the Poisson distribution; β is set to be 10 and the burst probability is set to be 10^{-7} for the exponential distribution.

Figure 4.6 shows the results. When n is small, there are fewer window sizes of interest, and the structure is sparse. In this case, there is little saving for the dynamic algorithm. Instead, it has to spend more time checking whether or not it is beneficial to add a level. When n is large, the dynamic algorithm shows its strength by filtering out unnecessary detailed searches and thus achieves better performance than the static algorithm.

Performance comparison under different changing rates

The purpose of this experiment is to study how the dynamic algorithm performs on data with different changing rates. We synthesize five pieces of test data with different changing rates. Each piece of data contains several segments of data, each segment has length L. The λ parameter for the ith segment is 0.1 when i is odd or 1 when i is even, i.e. λ changes every L time points. A larger L means a slower change in the data, and vice versa. L is set to be 500, 1000, 2000, 4000, 8000 respectively for each piece of data. The total length of each piece of test data is set to be same, one million points. A segment of 32000 points in each piece is used as the training data. The maximum window size of interest is set to be 250; the task is to detect bursts at every window size. The burst probability is set to be 10^{-5}.

Figure 4.7 shows the results for both the static algorithm and the dynamic algorithm, together with the difference of the CPU times. For the static algorithm, the experiments show that as L increases, i.e. the changing rate de-

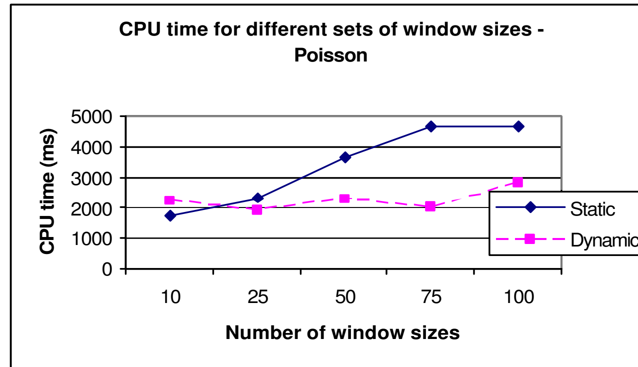

(a) Poisson distribution

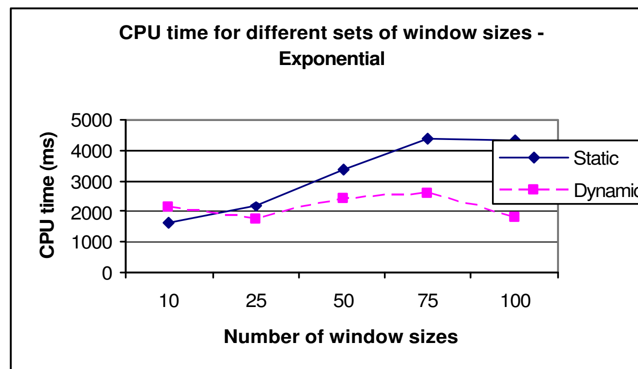

(b) Exponential distribution

Figure 4.6: Performance comparison between the dynamic algorithm and the static algorithm using unbiased data under different sets of window sizes

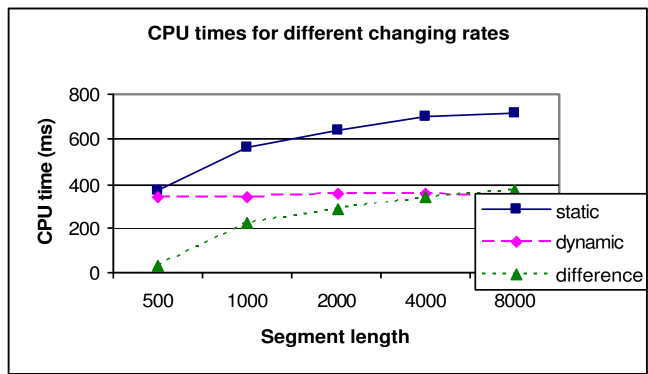

Figure 4.7: The effect of different changing rates. The longer each segment length, the slower the changing rate.

creases, the CPU time increases, although the number of real bursts actually decreases from $L = 1000$ to $L = 8000$. This occurs because when L is large, there are more aggregates that have large values, for example, in a segment of 10 consecutive 1s followed by 10 consecutive 0.1s, there are 5 aggregates of size 6 whose value is greater than 5; while in a segment of length 20 with 1 and 0.1 alternating, there is no aggregate of size 6 whose value is greater than 5. Thus, there are likely more aggregates exceeding their minimum thresholds and more detailed searches triggered.

On the other hand, there is no such effect using the dynamic algorithm, because whatever value L has, the dynamic algorithm can add the levels necessary to filter out unnecessary detailed searches. Therefore, as L increases, the time the dynamic algorithm saves compared to the static algorithm increases too.

Performance comparison under different changing magnitudes

In this experiment, we want to study how the dynamic algorithm performs on data with different changing magnitudes. We synthesize five pieces of test

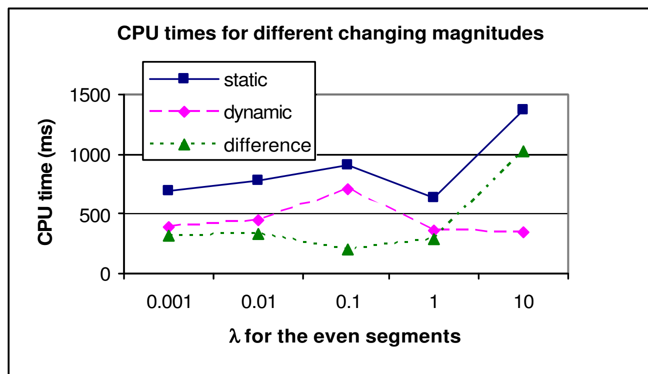

Figure 4.8: The effect of different changing magnitudes. The more λ deviates from 0.01, the larger the changing magnitude.

data with different changing magnitudes. Each piece of data contains several segments of data, each having a fixed length of 2000. λ for the ith segment is set to be 0.1 when i is odd, or 0.001, 0.01, 0.1, 1, 10 respectively for each piece of data when i is even, to simulate different changing magnitudes. That is, λ is 0.001 for i at 2, 4, 6, etc. in the first data, and λ is 0.01 for i at 2, 4, 6, etc. in the second data, and so on. In other words, the first data set consists of alternating segments characterized by parameters 0.1 and 0.001, the second data set consists of alternating segments characterized by parameters 0.1 and 0.01, and so on. So, 0.1 means no change at all between the odd segments and the even segments, while 0.001 and 10 have the largest changing magnitudes. The total length of each piece of test data is set to be the same, one million points. A segment length of 32000 points in each piece is used as the training data. The maximum window size of interest is set to be 250; the task is to detect bursts at every window size. The burst probability is set to be 10^{-5}.

Figure 4.8 shows the results for both the static algorithm and the dynamic algorithm, together with the difference of the CPU times. Although the number

of real bursts are different in each test data, the experiments show that as the changing magnitude increases, the time the dynamic algorithm saves compared to the static algorithm increases too. Because each test data is composed of two sets of data with different parameter settings, each set of data is best served by a different Shifted Aggregation Tree. When there is a large difference between the parameters, i.e. the magnitude change is large, there is also a large difference between the desired structures. While the static algorithm has to use a structure compromising between these two desired structures, the dynamic algorithm can change from one structure to another on the fly, and thus save more running time.

In summary, the dynamic algorithm overcomes the discrepancy resulting from a biased training data. In most cases, it performs better than the static algorithm training even with unbiased data. However, when the bursts are either very rare or very frequent, it may perform worse than the static algorithm. The greater the change in magnitude, the slower the changing rate, the more the dynamic algorithm saves compared with the static algorithm.

4.3.2 The effect of the parameters in the dynamic algorithm

In this section, we study the effect of the parameters in the dynamic algorithm. We picked 6 test settings to simulate different scenarios as shown in Table 4.3.

The effect of the maximum allowed shift step

As stated in the algorithm section, the dynamic algorithm allows changing a structure by widening or narrowing the shifts. A shift is the number of time

Table 4.3: Test settings to study the effect of algorithm parameters

	Training data parameter	Test data parameter	Max size	Number of sizes	Burst probability
Poisson1	1	0.5	250	250	10^{-3}
Poisson2	1	1	750	25	10^{-5}
Poisson3	5	10	500	100	10^{-6}
Exponential1	0.8	1	250	250	10^{-6}
Exponential2	5	5	750	75	10^{-7}
Exponential3	50	5	1000	50	10^{-8}

points separating two neighboring nodes at the same level. Because of the memory reallocation and re-creation of the parent-children structure when changing a shift, we restrict the maximum allowed shift step, i.e. how many times we can consecutively widen or narrow a shift from the initial shift. For example, one shift step allowed means that the legal shift can be 16, 32 or 64 if the initial shift is 32. It can never take other values. This experiment studies how the maximum allowed shift step affects the performance.

We set the maximum allowed shift step ms to be 0, 1, 2 respectively. The larger the value, the more a structure is allowed to deviate from the initial structure. Zero means no widening/narrowing is allowed. Figure 4.9 shows the results. The CPU running time of the static algorithm is included as a reference.

For some setting where the training data differs greatly from the test data (for example, Exponential1), the initial structure deviates greatly from the desired structure. For example, the initial shift at a level is 256, but a better structure would have a shift of 4. A small maximum allowed shift step, say 1, allows the shift to be 128, 256, or 512, which are still far from the desired shift.

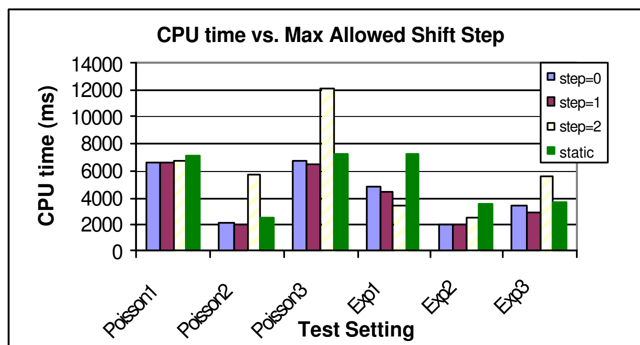

Figure 4.9: The effect of the maximum allowed shift step. The larger the step, the more a structure is allowed to deviate from the initial structure.

By contrast, a large maximum allowed shift step allows changing the initial structure greatly, bringing it closer to the optimal structure, and thus achieves better performance compared to a small value.

However for other settings, the desired structure is close to the initial structure. When ms is too large, the structure can become very sparse when there is no burst for a long period of time. In this instance, if a burst starts to happen, because a shift is only doubled or halved once when a node is updated, the structure cannot become dense quickly enough to filter out unnecessary detailed searches and thus has to spend more time in detailed searches. In practice, we believe generally it works best to set the maximum allowed shift step to be 1, unless it is known that the training data differs from the test data greatly.

The effect of the size of the alarm region

As described in the algorithm section, when an alarm is raised at level k at time t, we do not remove any level lower than $k + \delta k$ until time $t + \delta t$, where $\delta k \geq 0, \delta t \geq 0$. The purpose is to be prepared for more coming alarms and thus

avoid unnecessary structural changes when an alarm occurs. We want to study how different δk and δt values affect the performance.

We set δk to be 0, 1, 2 respectively to see the effect of different size ranges, and set δt to be 0, the size difference between level k and level $k+1$, the size of level k, respectively, to see the effect of different time ranges. Smaller δk and δt allow the algorithm to remove a level or widen a shift sooner, but may lead to frequent structural changes. Frequent structural changes may cause the structure to become sparse and then be unable to become dense quickly enough to filter out unnecessary detailed searches. By contrast, large δk and δt avoid frequent structural changes but may be too conservative to make a structure sparser. The maximum allowed shift step is set to be 1 in this test.

Figure 4.10 shows the results. The CPU running time of the static algorithm is included as a reference. The results show that medium δk and δt work better than small or large δk and δt. The small δk and δt have to spend more time changing the structure and detailed searching, while the large δk and δt cannot remove the unnecessary levels quickly and have to spend more time updating the structure.

Given the above experimental results, we recommend the following about the dynamic algorithm:

- If the bursts are very rare or very frequent, e.g. the burst probability is very low or very high, or the number of window sizes is very few, use the static algorithm only.

- If it is known the training data deviates greatly from the test data, use a large maximum allowed shift step with the dynamic algorithm. The more the difference is, the larger this value should be. Otherwise, it is better to

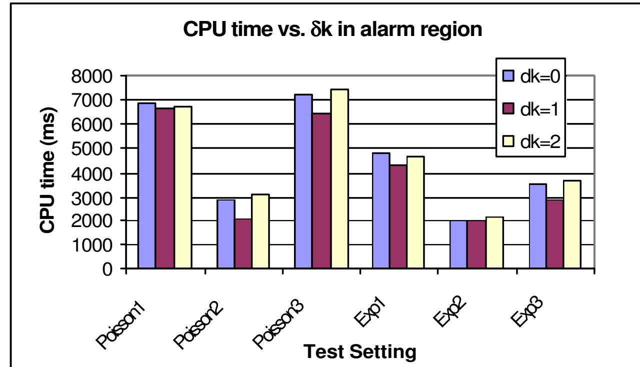

(a) Different δk

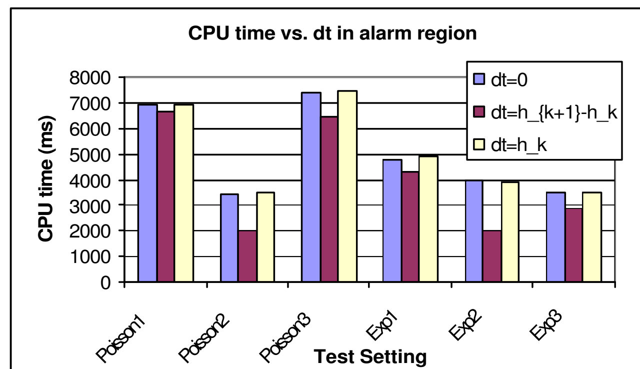

(b) Different δt

Figure 4.10: The effect of the size of the alarm region. The larger δk and δt, the larger the alarm region.

use a maximum allowed shift step of 1.

- It is recommended to use a medium size alarm region.

4.4 Worst Case Analysis

In this section, we analyze the greedy dynamic detection algorithm compared with the clairvoyant dynamic detection algorithm which knows when and where an alarm is going to happen and thus knows when and how to change the structure in advance.

Consider the following two scenarios:

- At some time t, an alarm is raised at level k, the greedy algorithm may not be able to add a level (say of size 192) between k and $k-1$ because the lower level to support size 192 (say size 64) is not in the tree. (At time $t-128$, there may be no sign an alarm is going to occur, thus no reason to add level 64.) However, the clairvoyant algorithm knows about the alarm at level k in advance, thus may add the level of size 64 at time point $t-128$. When the alarm is raised at time point t, the clairvoyant algorithm is able to add the level of size 192 and potentially filter out an unnecessary detailed search at this node.

  In this case, the greedy algorithm has to spend more time in the detailed search than the clairvoyant algorithm, until 128 time points later, when another window of size 128 ends. At that point, both windows of size 64 and size 128 are available to support the level at size 192. In the worst case, the candidate level is at the top level, and the extra detailed search

has to be performed within the time period from t up to $t + W$, where W is the maximum window size of interest.

Notice this could happen at multiple levels at the same time. Therefore the extra detailed search time is of $\Theta(mW)$, where m is the number of window sizes of interest.

- After an alarm is raised at t, the greedy algorithm will not remove a level within the alarm region at level $k + \delta k$ until time $t + \delta t$, while the clairvoyant algorithm may know that there will be no more alarms and thus will remove this level right away.

  In this case, the greedy algorithm has to spend more time in the updating/filtering phase than the clairvoyant algorithm, until the alarm region ends. Assuming the underlying data is independent, a window of size W contains no information about a window of size W following it. Thus δt should be less than W. The extra updating/filtering cost should be the cost within a window of size at most W.

Put them together and the worst case scenario would be that the clairvoyant algorithm does not need any detailed search (i.e. there is no real burst at all), but the greedy algorithm has to spend more detailed search time when an alarm starts to occur and more updating/filtering time in the alarm region.

Let t_u, t_s, t_c denote the total updating/filtering time, searching time and structure-changing time respectively for the greedy algorithm. Similarly, we use t_u^C, t_s^C, t_c^C to denote the same costs for the clairvoyant algorithm. As explained above, we need to consider only the costs in a time period of $2W$: W for the period from the start of an alarm to the addition of a candidate level, and another W for the alarm region.

Within the time period $2W$, the number of nodes in the tree is of $\Theta(W)$, so are t_u and t_u^C, since each updating/filtering operation is associated with a node. Because a change to the structure only happens after a node is updated, t_c and t_c^C have the complexity of $\Theta(L)$, where L is the number of levels in the tree, $L < W$. As explained above, the detailed search cost t_s for the greedy algorithm has the complexity $\Theta(mW)$, while t_s^C is 0 for the clairvoyant algorithm. So in the worst case, the greedy algorithm has the complexity of $\Theta(mW)$, while the clairvoyant algorithm has the complexity of $\Theta(W)$. The performance ratio is up to m, the number of window sizes of interest.

Chapter 5

Case Study

In this chapter, we study several real world burst detection applications in physics, finance and website traffic monitoring. We also show how bursts can be a primitive for higher-level data mining tasks, such as burst correlation. Real world applications all confirm the excellent performance of our algorithmic framework. The experiments show that the average processing time to process a new datum is less than 0.1 ms, therefore, the Shifted Aggregation Tree framework is suitable for real data stream environments.

5.1 Gamma Ray Burst Detection in Astronomy

Gamma rays are high-energy electromagnetic radiation produced by radioactive decay or other nuclear processes. In the cosmos, different processes can generate gamma ray emissions, such as cosmic ray interactions with interstellar gas, supernova explosions and interactions of energetic electrons with magnetic fields

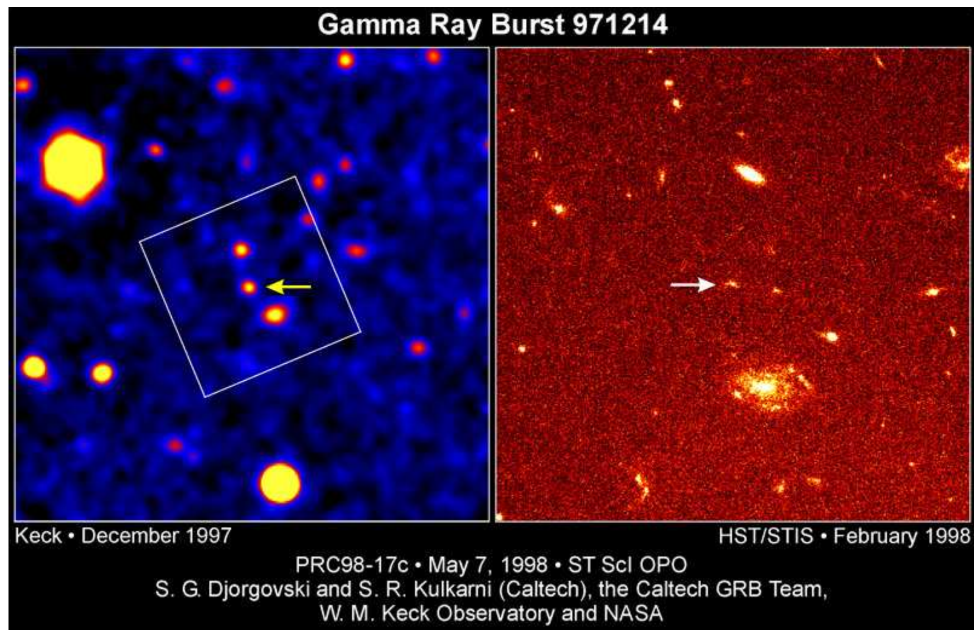

Figure 5.1: Gamma Ray Burst 971214 (image from Hubble Space Telescope website [4])

to name a few. Gamma Ray Bursts (GRB) are flashes of gamma rays. They are the brightest source of cosmic gamma-ray photons in the observable Universe, hundreds of times brighter than a typical supernova and about a million trillion times as bright as the Sun. Since the first GRB discovered in the late 1960s, Gamma Ray Bursts have been important phenomena and useful vehicles for physicists to study the activity of the Universe. Figure 5.1 shows a picture of a GRB observed by the Hubble Space Telescope [4].

Gamma Ray Bursts occur roughly once per day from wholly random directions of the sky. A Gamma Ray Burst can last anywhere from milliseconds to minutes, even days. For example, the GRB 060218 discovered in February 2006 lasted for 33 minutes, while the GRB 050509 detected in May 2005 only lasted for a tiny fraction of a second. They can be classified as long-duration bursts

(> 2 seconds) or short duration bursts (< 2 seconds).

The MILAGRO astronomical telescope is one of the Gamma Ray observers. It was built by Los Alamos National Laboratory and several universities to detect the so-called VHE GRBs and measure their arrival directions and energy. MILAGRO [7] consists of an array of 723 light-sensitive detectors in a football-field-size pool of water. When a VHE gamma ray enters the earth's atmosphere, it interacts with the atmosphere to produce new particles which in turn interact themselves producing even more particles. Those particles are detected by the array of light-sensitive detectors. The intensity of the particles and the time at which they are detected are used to infer the position and energy of the original gamma ray.

Because the location of a Gamma Ray Burst occurs is completely random, the whole sky is partitioned into a 1800×900 grid structure and every cell is constantly monitored. Each cell records occurrences of particles in this region. A Gamma Ray Burst is detected if the number of particles received within a time duration exceeds a pre-defined threshold.

Because the burst period could last from milliseconds to days, the events have to be monitored at multiple window sizes. The rate at which events arrive is very high, up to 2000 events per second. The data throughput rate could reach about 5 megabytes per second at this rate [7].

The fast incoming data rate and the large number of the cells to be monitored present an enormous challenge to data processing. All the events have to be processed in real time. Once a Gamma Ray Burst is discovered, it should be reported right away in order to confirm the occurrence of the burst.

In the original system, a naive algorithm had been used to maintain a running sum over each window size. We have applied the new Shifted Aggregation

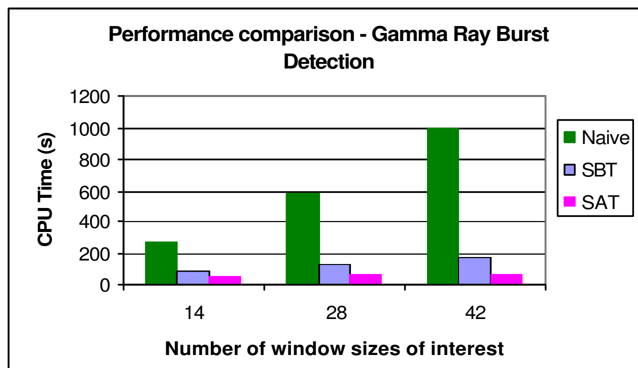

Figure 5.2: Performance comparison between the Shifted Binary Tree and the Shifted Aggregation Tree on the Gamma Ray Burst data

Tree framework to this situation.

The test data set includes 5 offline raw data files. Each data file contains the raw observed events including the observed time, signal intensity, position, etc. There are in total about 2.5 million events. These raw events are first allocated into one of the 1800×900 cells. Then the bursts are detected within each cell. N window sizes of interest are monitored, N was set to be 14, 28, 42 in this test. The minimum time resolution to distinguish a burst is 0.01 second. The minimum window size of interest $N_{\min}$ is 0.1 second, and the maximum window size of interest $N_{\max}$ is 39.8 seconds. The window sizes of interest are exponentially even-spaced between the minimum window size and the maximum window size, i.e. $\{\exp(N_{\min} + \frac{\ln(N_{\max}-N_{\min})}{n}), \exp(N_{\min} + \frac{2\ln(N_{\max}-N_{\min})}{n}), \exp(N_{\min} + \frac{3\ln(N_{\max}-N_{\min})}{n}), \ldots\}$. The thresholds are updated dynamically based on the background signals in the sky.

We use a small sample of 10K data from the first file to train a Shifted Aggregation Tree. We use the empirical cost model: run 1000 times detection over this training data and use the actual CPU time as the cost. The trained Shifted

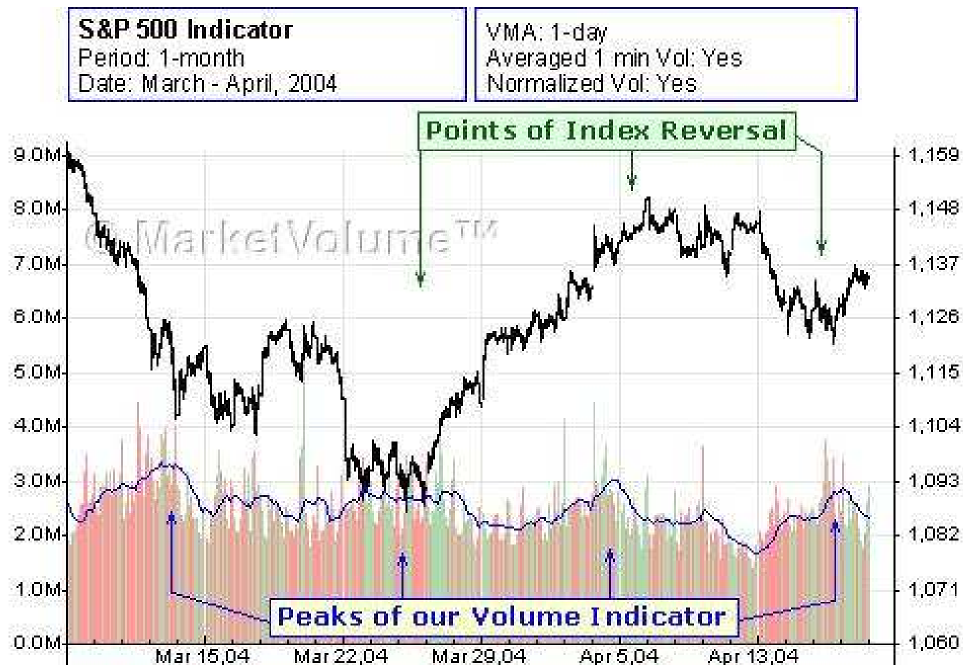

Figure 5.3: An example how the price of the S&P 500 Index interacts with the volume spikes (chart from MarketVolume.com [6])

Aggregation Tree is used for burst detection on the five test data files. Figure 5.2 shows the result. The Shifted Binary Tree outperforms the naive approach by a factor of 3 to 6, furthurmore, the Shifted Aggregation Tree framework achieves a 1.5 to 3 times speedup over the Shifted Binary Tree. More speedup can be achieved if there are more window sizes of interest, which is helpful to avoid missing any possible burst.

5.2 Volume Spike Detection in Stock Trading

In stock trading, the trading volume is the number of shares or contracts of a security traded during a given length period. Volume indicates the interest of

traders in buying or selling a security. It is the underlying force behind price movements. For example, a large volume on the buy side suggests a strong buy interest, thus the price is likely to rise; conversely, a small volume means a weak interest, suggesting the rise has lost its momentum and the price is likely to fall. The volume behavior and the price behavior are closely interrelated. The price pattern can be anticipated by a proper understanding of the volume pattern. There is a long history of traders using volume as a technical indicator to analyze stock behavior.

A commonly used volume indicator is Volume Moving Average (VMA). Similar to the price moving average, Volume Moving Average is the average of the trading volume over a given period of time. The VMA can be computed over several seconds to several months to capture the patterns over different time scales. Within the smoothed view of the trading volume, a large peak in the VMA, called Volume Spike, is of particular interest. A volume spike indicates a burst of trading activity. It is usually triggered by some political or economic news, earning reports, etc., and may drive the price to change substantially. Figure 5.3 shows an example of how the price reversals of the Standard & Poor 500 Index interacts with volume spikes.

Due to the time-sensitive nature of the stock market, it is very important for traders to be able to detect volume spikes as early as possible. In the modern security industry, there are hundreds of thousands of securities traded on different exchanges or over-the-counter, and the message rates for a single stock are ultra high. For example, a normally-traded stock could have more than 100 volume changes per second during a busy time. For an index, say the Russell 2000, the number of updates could reach 200,000 updates per second. Therefore to track the volume spikes over multiple stocks simultaneously is a

challenging task. Furthermore, as more and more traders adopt program trading — The NYSE has reported the percentage of program trading has risen from about 20% in 1999 to 60% in 2006 [8] — the required response time has been reduced from seconds in manual trading to a few milliseconds. Any trading program will benefit from the even one millisecond saved by a fast volume spike detection algorithm.

Our elastic burst detection framework is well suited for volume spike detection. The average function satisfies the monotonicity property. Multiple window sizes can be monitored simultaneously.

Data Setup

We have downloaded the NYSE TAQ stock data from the Wharton Research Data Services (WRDS) [13]. This data set includes tick-by-tick trading activities of the IBM stock between January 1st, 2001 to May 31st, 2004. There are a total of 6,134,362 ticks, and each record contains the time precise to the second, as well as each trade's price and volume. The preprocessing aggregates all the trading volumes within the same second and pads the second with a 0 if there is no activity within this second. A standard work week's (five day) worth of data is used as the training data. The training data has a similar mean and standard deviation as those of the test data.

Table 5.1 gives the basic statistics. Figure 5.4 shows the histogram of the IBM data set. The histogram shows that the IBM stock trading volume data is close to the exponential distribution.

Table 5.1: Statistics for the IBM stock data

Size	23,085,000
Mean	287.06
Standard deviation	2,796.05
Min	0
Max	2,806,500

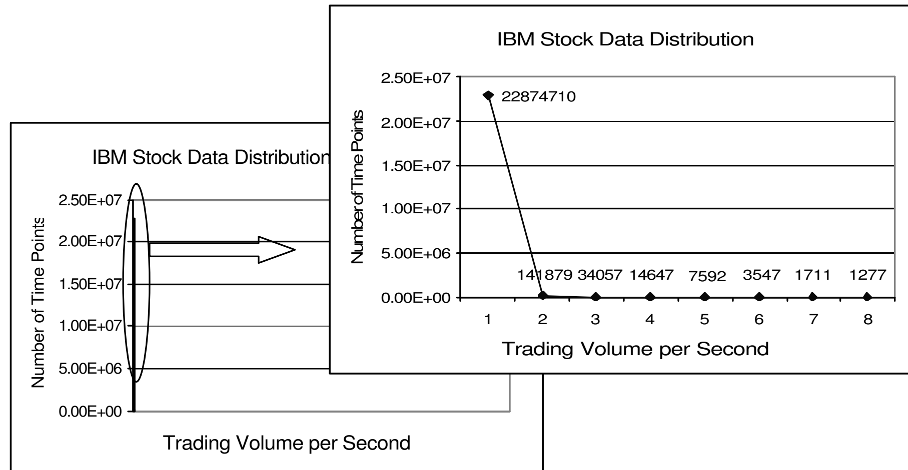

Figure 5.4: The histogram distribution of the IBM stock data. Each bin in the enlarged figure stands for 5000 shares, i.e. the first bin stands for volume 0-5000, the second bin stands for volume 5000-10000, and so on.

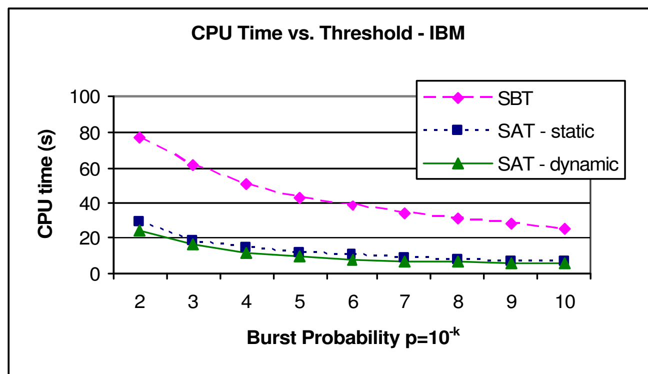

Figure 5.5: The effect of different thresholds in the IBM data

Performance Tests

We are interested in comparing the Shifted Aggregation Tree using the static and dynamic algorithms with the Shifted Binary Tree under different settings.

Unlike the thresholds used in the test on the synthetic data which are fixed during the whole detection process, the thresholds used in the following tests change dynamically based on the most recently observed data. The reason is obvious: the thresholds set for a region with less activity can be easily exceeded during a region with much more activity. People are usually interested in a burst of activity relative to the most recent activity.

A burst probability p is selected to reflect the probability of a burst happening at each window size. The mean μ and standard deviation σ are computed for each week, and used to compute the thresholds for the following week. The threshold for window size w is set to $w\mu - \sqrt{w}\sigma\Phi^{-1}(p)$, where Φ is the normal cumulative distribution function.

- Different thresholds

  The thresholds are set to reflect a burst probability ranging from 10^{-2}

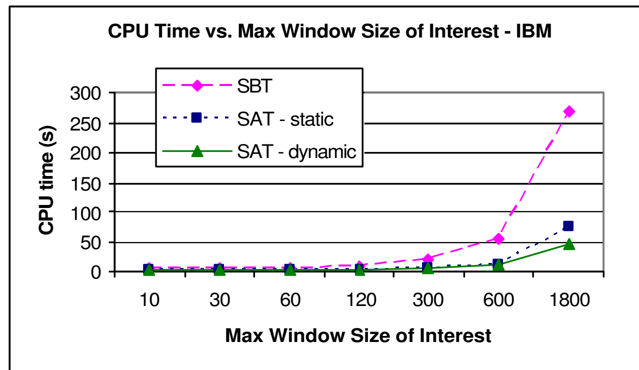

Figure 5.6: The effect of different maximum window size of interest in the IBM data

to 10^{-9}. The maximum window size is set to 500. The task is to detect bursts at every window size.

Figure 5.5 shows that as the burst probability decreases, the CPU time for the Shifted Aggregation Tree decreases quickly. The Shifted Aggregation Tree performs 3 to 4 times better than the Shifted Binary Tree. The dynamic algorithm also performs slightly better (10 to 20 percent less time) than the static algorithm.

- Different maximum window sizes of interest

  The maximum window sizes are set from 10 seconds up to 1800 seconds. The burst probability is set to 10^{-6}. The task is to detect bursts at every window size.

  Figure 5.6 shows the results. As the maximum window size increases, there are more candidate levels in the desired structure, i.e. the bounding ratio can be much more smaller compared to that in the Shifted Binary Tree, and thus the speedup for the Shifted Aggregation Tree over the

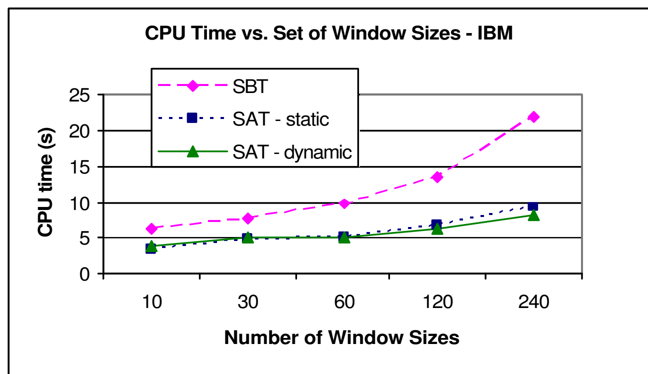

Figure 5.7: The effect of different sets of window sizes of interest in the IBM data

Shifted Binary Tree increases. Similarly, the dynamic algorithm achieves more speedup (a factor of 1.5) as the maximum window size increases, because adding a level of large window size can reduce the detailed search time.

- Different sets of window sizes of interest

  Instead of detecting bursts at every window size, we want to see how the Shifted Aggregation Tree performs with different sets of window sizes. The test is performed to detect bursts for a set of n window sizes exponentially evenly-spaced up to the maximum window size of interest, i.e. $\{N^{\frac{1}{n}}, N^{\frac{2}{n}}, N^{\frac{3}{n}}, \ldots, N\}$, where N is the maximum window size of interest. In this test, N is set to be 3600 and n is set to be 10, 30, 60, 120, 240 respectively. The burst probability is set to be 10^{-6}.

  Figure 5.7 shows that as the set of window sizes becomes sparser, there are fewer bursts to worry about, thus both the Shifted Binary Tree and the Shifted Aggregation Tree take less time. As the set of window sizes

Table 5.2: Statistics for the test IBM data for robust test

	Mean	Standard deviation
IBM_w12	376.21	2147.10
IBM_w20	279.20	5430.01
IBM_w29	401.35	2307.30
IBM_w70	250.81	1716.69
IBM_w100	306.83	1760.76
IBM_w150	163.15	1184.95

Table 5.3: Test parameters for robust test - IBM data

	Max Window Size	Burst Probability	Number of Window Sizes
IBM_setting1	250	10^{-3}	250
IBM_setting2	500	10^{-6}	100
IBM_setting3	750	10^{-7}	75
IBM_setting4	1000	10^{-8}	50

becomes sparser, both the structure and the bursts become very sparse. Thus there is little saving for the dynamic algorithm, but extra cost is spent to check if a change is needed. The dynamic algorithm performs slightly less well than the static algorithm in this case, taking about 10 percent more time. However, when the number of window sizes increases, the dynamic algorithm performs better as shown in Figure 5.7.

In summary, the experiments show that this framework can handle millions of time points and hundreds of window sizes in several seconds. The average processing time per time point is less than 0.1 millisecond. Therefore, this

framework is suitable for real time processing.

Robustness test

In the static algorithm, the structure of a Shifted Aggregation Tree depends on the input used to train it. We are interested in how sensitive the structure is to whether training on one portion of the data gives good results when tested on another portion, and how the dynamic algorithm performs compared to the static algorithm.

We constructed three training sets for the IBM data. One set is taken from the test data to be detected. The second is taken from the same type of data, but outside the test data. For IBM, this set is taken from trading activities in 2000. The third set is taken from the other type of data, i.e, we use the SDSS data (explained in the next section) to train a Shifted Aggregation Tree, then use it to detect the IBM data. Each training set contains three pieces of training data, each piece contains five days of records. Table 5.2 shows the statistics for the training data. In the table, the first three sets are taken from the data to be detected, the second three sets are taken outside the data to be detected. Table 5.3 shows other parameters used in these tests.

Figure 5.8 shows the CPU times for four different test scenarios on each training set, the CPU times for the dynamic algorithm are shown as a comparison. For clarity, for each setting, only one result is shown for the dynamic algorithm starting with the structures trained with the other type of data.

When testing the structure created based on data from the same data type but distinct from the test data, the performance of the static algorithm on the IBM data is about the same as using a structure based on the test data itself. The reason is that the out-of-sample training set has similar statistics to the

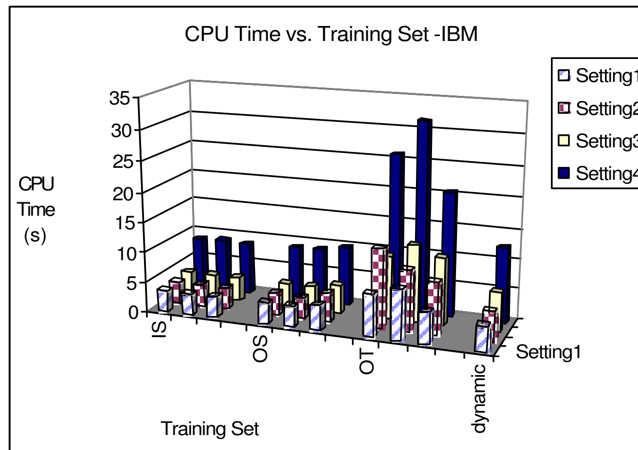

Figure 5.8: Robustness test on the IBM stock data (IS: in-sample, OS: out-of-sample, OT: out-of-type)

in-sample training set. The dynamic algorithm performs better than the static algorithm when the number of window sizes of interest is dense. However, it performs slightly less well than the static algorithm when the number of window sizes is sparse.

A static structure based on a different data type can perform quite poorly. For example, a structure based on SDSS data runs 2 to 3 times slower for IBM data than a structure based on out-of-sample IBM data. The dynamic algorithm achieves much better performance than the static algorithm in this case. The respective times it spent are close to those using the out-of-sample IBM data.

5.3 Click Fraud Detection in Website Traffic Monitoring

As more and more businesses go online, it is critical to make their websites attractive to customers. Website traffic monitoring and analysis plays a greater and greater role in improving the popularity of one's website.

One way to attract website traffic is online advertising on search engines, such as Google or Yahoo. In this scenario, an ad is placed together with the search results. If the visitor clicks the ad, the advertiser has to pay a small amount of money to the search engine. This is called pay-per-click (PPC), which has brought in billions of dollars for Google/Yahoo.

A problem that has arisen with pay-per-click is click fraud. Someone can use an automated script or program to simulate legitimate use of a web browser to click on an ad. This can harm the competitors by forcing them to pay more money without bringing in real profits. Click fraud poses a serious threat to the online advertising business. It's difficult to capture all the frauds because of different click behaviors.

However, one common characteristic behind click fraud is that the number of clicks should be large enough to generate considerable money. Therefore, one feature of click fraud can be a burst of clicks within some limited time period. Because the automated program may generate clicks randomly, the duration will not be known in advance, so multiple window sizes need to be monitored. This is exactly the elastic burst detection task.

Table 5.4: Statistics for the SDSS SkyServer traffic data

	SDSS
Size	31,536,000
Mean	120.95
Standard deviation	64.87
Min	0
Max	576

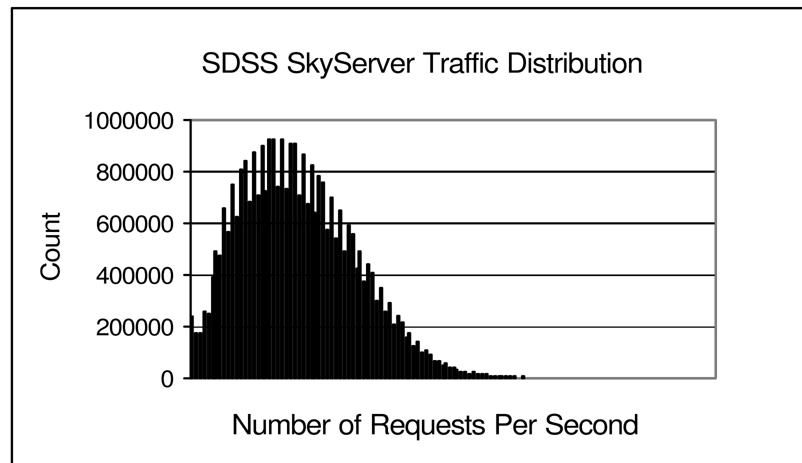

Figure 5.9: The histogram distribution of the Sloan Digital Sky Survey (SDSS) SkyServer traffic data

Data Setup

We use the Sloan Digital Sky Survey (SDSS) SkyServer traffic data in this case study. The Sloan Digital Sky Survey [10] SkyServer is an ambitious website trying to make a map of a large part of the sky. This data set records all the access traffic to the SDSS SkyServer from January 1st, 2003 to December 31st, 2003. Each record includes the request time precisely to the second, the source IP address and the target URL. Thus this data set contains the same information as the click data, which is also generated by browsers. The data set has 17,432,468 records. The preprocessing aggregates all the records for each second and places a zero in the time point entry if there is no activity within that second. The training data consists of seven days of second-by-second data.

The basic statistics are shown in Table 5.4 and the histogram of the SDSS data set is shown in Figure 5.9. The histogram shows that the SDSS SkyServer traffic data follows the Poisson distribution.

Performance Tests

As for to the IBM data, we are interested in comparing the static and dynamic detection algorithms with the Shifted Binary Tree under different settings. The thresholds are dynamically updated based on the observed mean and standard deviation from the previous week.

- Different thresholds

  The thresholds are set to reflect a burst probability ranging from 10^{-2} to 10^{-9}. The maximum window size is set to 300. The task is to detect bursts at every window size.

  Figure 5.10 shows the results. Similar to its performance with the IBM

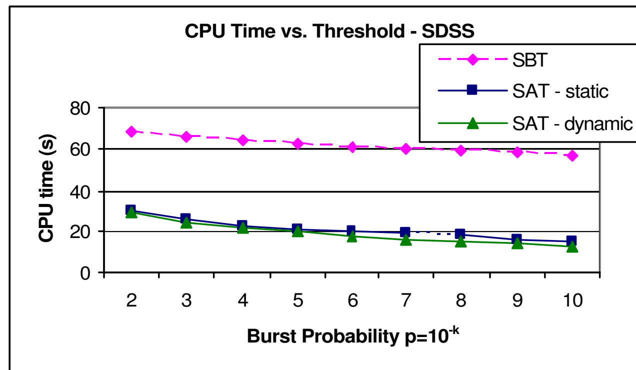

Figure 5.10: The effect of different thresholds in the Sloan Digital Sky Survey (SDSS) data

data, the static algorithm performs two to three times better than the Shifted Binary Tree, and the dynamic algorithm performs slightly (about 1.1 times) better than the static algorithm.

- Different maximum window sizes of interest

  The maximum window sizes are set from 10 seconds up to 1800 seconds. The burst probability is set to 10^{-6}. The task is to detect bursts at every window size.

  Figure 5.11 shows results similar to those achieved with the IBM data set. As the maximum window size increases, the speedup for the Shifted Aggregation Tree over the Shifted Binary Tree increases, as does the speedup for the dynamic algorithm over the static algorithm.

- Different sets of window sizes of interest

  The test is performed to detect bursts for a set of n window sizes exponentially evenly-spaced up to the maximum window size of interest, i.e. $\{N^{\frac{1}{n}}, N^{\frac{2}{n}}, N^{\frac{3}{n}}, \ldots, N\}$, where N is the maximum window size of interest.

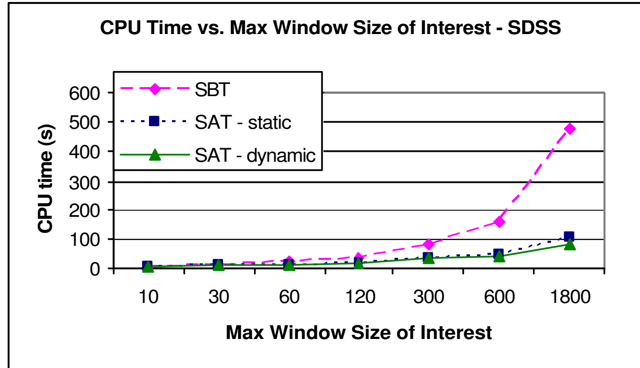

Figure 5.11: The effect of different maximum window size of interest in the Sloan Digital Sky Survey (SDSS) data

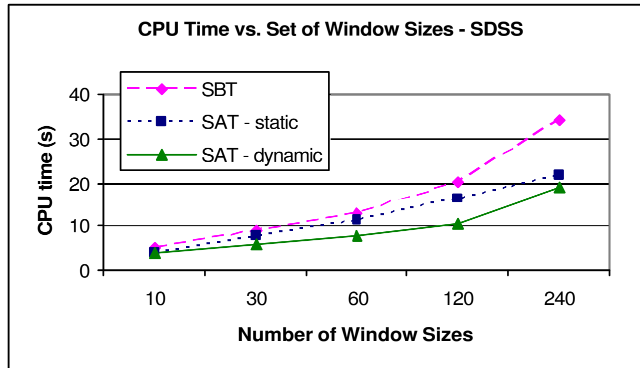

Figure 5.12: The effect of different sets of window sizes of interest in the Sloan Digital Sky Survey (SDSS) data

Table 5.5: Statistics for the test SDSS data for robust test

	Mean	Standard deviation
SDSS_w10	73.92	27.08
SDSS_w18	98.84	33.24
SDSS_w25	121.71	39.17
SDSS_w40	168.85	50.39
SDSS_w45	183.68	55.05
SDSS_w50	197.58	57.57

Table 5.6: Test parameters for robust test - SDSS data

	Max Window Size	Burst Probability	Number of Window Sizes
SDSS_setting1	200	10^{-4}	200
SDSS_setting2	400	10^{-5}	80
SDSS_setting3	600	10^{-6}	60
SDSS_setting4	800	10^{-8}	40

N is set to be 1800 and n is set to be 10, 30, 60, 120, 240 respectively. The burst probability is set to be 10^{-6}.

Figure 5.12 shows the results. As for the IBM data, as the number of window sizes increases, the Shifted Aggregation Tree saves more time compared to the Shifted Binary Tree. The dynamic algorithm performs about 1.5 times better than the static algorithm.

Again, the experiments show that the Shifted Aggregation Tree framework is well suitable for real data stream environment.

Robustness test

We constructed three training sets for the SDSS data similar to those we constructed for the IBM data. One set is taken from the test data to be detected. The second is taken from the same type of data, but from the SkyServer traffic of 2004. The third set is taken from the IBM data. Each training set contains three pieces of training data, each piece contains seven day's records. Table 5.5 shows the statistics for the training data. In the table, the first three sets are taken from the data to be detected, the second three sets are taken outside the data to be detected. Table 5.6 shows other parameters in these tests.

Figure 5.13 shows the CPU times for four different test scenarios on each training set, the CPU times for the dynamic algorithm are shown as a comparison. For clarity, for each set, only one result is shown for the dynamic algorithm.

The in-sample training sets give similar detection times, while the out-of-sample training sets and the out-of-type training sets take 25 percent more time. Again, the dynamic algorithm performs better than the static algorithm when the number of window sizes is dense.

5.4 Burst Correlation in Stock Data

We believe that high-performance burst detection could be a preliminary primitive for further knowledge discovery and data mining processes. As an example, we look at the correlation of bursts in stock data.

We collected the tick-by-tick TAQ stock data in 2003 for the Standard & Poor's 100 stocks. The goal is to discover which stocks share similar volume

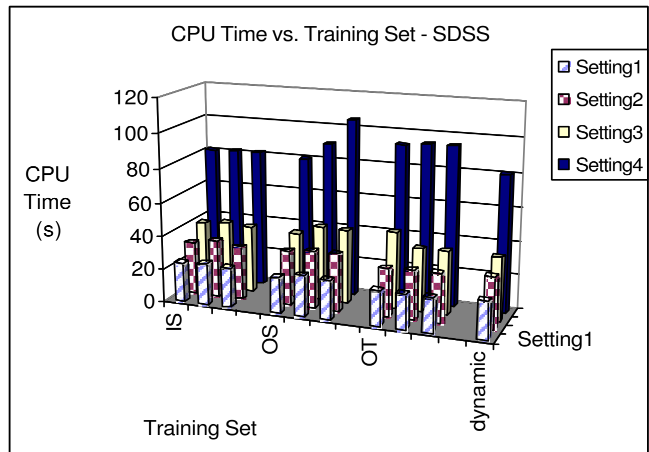

Figure 5.13: Robustness test on the Sloan Digital Survey (SDSS) traffic data (IS: in-sample, OS: out-of-sample, OT: out-of-type)

characteristics, i.e. when there is a burst of trading in one stock, which other stocks also exhibit a burst? Because trading bursts can happen across different time resolutions, we monitored the correlation at multiple time scales and set the window sizes of interest to be 10, 30, 60, and 300 seconds. The burst probability is set to 10^{-9}.

Bursts are detected using a Shifted Aggregation Tree, tuned as described above. The bursts detected are converted to a 0-1 string where 0 means no burst and 1 means a burst. The correlation is computed over these 0-1 strings.

These bursts tell an interesting story. First, stocks within the same sector are correlated strongly e.g. Microsoft (MSFT), Oracle(ORCL) and Cisco(CSCO). Surprisingly strong correlations of bursty behaviors can be found across different industries also however. For example, Pfizer Inc. (PFE, health care, Drugs, major Pharmaceuticals), Pepsico Inc. (PEP, Beverage), Procter & Gamble Co. (PG, Non-Durables Household Products) are highly correlated. Table 5.7 shows

Table 5.7: Some highly-correlated stocks at different durations

Duration	Highly-correlated stocks
10s	C/GE/XOM, CSCO/MSFT/ORCL
30s	C/GE/XOM, CSCO/MSFT/ORCL, PEP/PFE/PG
60s	C/GE/XOM/PEP/PFE/PG/GE, CSCO/MSFT/ORCL
300s	C/GE/XOM/PEP/PFE/PG/GE, CSCO/MSFT/ORCL, WFC/XOM/WMT, KO/USB/VZ

some highly correlated stocks at different window sizes. We are not claiming these still anecdotal observations as a major discovery, but just as a suggestive example of how burst detection can feed into data mining applications.

Chapter 6

Multi-Dimensional Elastic Burst Detection

Real world data often have multiple attributes, for example, a demographic data set often contains information like age, sex, profession, etc.; a geographic information system (GIS) data set often contains latitude, longitude, the measurements mapped on latitude and longitude values, etc. Bursts of events may relate to multiple attributes, for example a disease outbreak in certain age groups and certain professions.

In this chapter, we extend the one-dimensional elastic burst detection to D-dimensional data. We extend the problem definition to the D-dimensional case, then explain the changes in the data structure and the algorithm. We apply it in an epidemiology simulation to detect disease outbreak and spread.

6.1 Algorithm for D-Dimensional Elastic Burst Detection

6.1.1 Problem definition

Let S denote a D-dimensional space defined by D orthogonal axes, each axis denoting an attribute. An event having D attributes can be seen as a point in this D-dimensional space. Assume for attribute k, the minimum and maximum possible values are $x^k_{\min}$ and $x^k_{\max}$ respectively. The whole space of interest is the rectangle region cornered at $[x^1_{\min}, x^2_{\min}, \ldots, x^D_{\min}]$ and $[x^1_{\max}, x^2_{\max}, \ldots, x^D_{\max}]$.

People may be interested in bursts occurring in different regions of different sizes in the space. For example, one may be interested in more than 5 disease cases in a small town but more than 50 disease cases in a large city. The D-dimensional elastic burst detection is to detect bursts of events occurring within multiple regions of different sizes in the D-dimensional space of interest. We use "region" instead of "window" to denote a D-dimensional space of interest.

Generally speaking, a region can be of any shape and any orientation. For simplicity, we divide the whole D-dimensional space into many unit cells. Each cell corresponds to a unit of minimum resolution for each attribute. This is similar to the one-dimensional case: the incoming data are assumed to arrive exactly at the regular time points. We consider only the number of events in these axis-aligned rectangle regions. An axis-aligned rectangle region is defined by its bottom most corner $[x^1, x^2, \ldots, x^D]$ and sizes $[h^1, h^2, \ldots, h^D]$ for each dimension, where $h^i > 0$.

6.1.2 D-dimensional Shifted Aggregation Tree

As in the one-dimensional case, a D-dimensional Shifted Aggregation Tree is composed of several levels. The nodes at level 0 have a one-to-one correspondence to the unit cells in the D-dimensional space of interest. A node at a level above level 0 corresponds to an axis-aligned rectangular region which aggregates all the unit cells inside this region. All nodes at the same level have the same size and the same shifting pattern from the neighboring nodes at this level. Therefore level k is defined by a D-dimensional region/window size $[h_k^1, h_k^2, \ldots, h_k^D]$ and a D-dimensional shift $[s_k^1, s_k^2, \ldots, s_k^D]$.

In the one-dimensional case, for each node at level k, there are two adjacent nodes at the same level: one before this node and another after this node. The overlap is between two adjacent nodes. In the D-dimensional case, there are $3^D - 1$ nodes adjacent to one node. The overlap is among 2^D adjacent nodes. Figure 6.1 shows how four adjacent nodes shift and overlap in the two-dimensional case. The overlap of the adjacent nodes at the same level k is a D-dimensional region denoted by $[h_k^1 - s_k^1, h_k^2 - s_k^2, \ldots, h_k^D - s_k^D]$. Thus, all the regions contained in the region $[h_k^1 - s_k^1 + 1, h_k^2 - s_k^2 + 1, \ldots, h_k^D - s_k^D + 1]$ are contained by a node at level k. Because of the monotonicity, if the aggregate of a node at level k does not exceed the threshold for the size $[h_{k-1}^1 - s_{k-1}^1 + 1, h_{k-1}^2 - s_{k-1}^2 + 1, \ldots, h_{k-1}^D - s_{k-1}^D + 1]$, there is no burst in any region of size containing $[h_{k-1}^1 - s_{k-1}^1 + 1, h_{k-1}^2 - s_{k-1}^2 + 1, \ldots, h_{k-1}^D - s_{k-1}^D + 1]$ but contained by $[h_k^1 - s_k^1 + 1, h_k^2 - s_k^2 + 1, \ldots, h_k^D - s_k^D + 1]$.

The D-dimensional detection algorithm is similar to the algorithm in the one-dimensional case. The structure is updated bottom up. A detailed search is triggered when the aggregate at a node exceeds the minimum threshold of

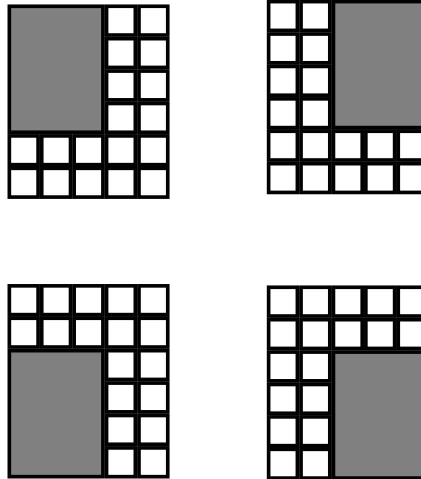

Figure 6.1: The shift and overlap between four adjacent regions (grayed) in a two-dimensional Shifted Aggregation Tree. A grayed area represents a node.

its detailed search region. In contrast to the one-dimensional case, there is no total order between the thresholds for the window sizes within a detailed search region. For example, in the one-dimensional case, suppose that a detailed search region includes window sizes from 8 to 16; due to monotonicity, the threshold for size 8 is less than (or equal to) the threshold for size 9, and so on. In this case a binary search is used to determine the range of the detailed search window sizes, for example, if the aggregate is less than the threshold for size 10, there is no need to search window sizes from 10 to 16. By contrast, in the D-dimensional case, there is no total order between the thresholds for two window sizes, say [9,10] and [10,9], so we cannot use binary search to determine where to start a detailed search. Instead, we have to examine each size of interest contained in a detailed search region for real bursts.

6.1.3 Adaptive D-dimensional Shifted Aggregation Tree

In the above regular D-dimensional Shifted Aggregation Tree, the nodes at each level are over the whole space of interest. For example, in a two-dimensional space of size $[16, 16]$, there are 7×7 nodes at the level of size $[4, 4]$ and shift $[2, 2]$. In other words, the number of levels in different regions are the same. The regular D-dimensional structure does not adapt to different data distributions in different regions. For example, one region may have more bursts and thus require a dense structure while another region may have fewer bursts and thus need only a sparse structure.

An extension of this is to use different numbers of levels in different regions. We may keep more levels in some regions than others. In other words, we can view it as if these extra levels are missing in other regions, i.e. we only keep a subset of the nodes at these extra levels. For example, we can keep just 3×3 nodes — instead of 7×7 in the regular case — at the level of size $[4, 4]$ and shift $[2, 2]$, only covering one of the corners of the whole space of interest. We call these levels *partial* (compared to the *full* levels in the regular structure), and a structure with partial levels an adaptive D-dimensional Shifted Aggregation Tree. Figure 6.2 shows a partial level of two nodes in a two-dimensional space of size $[6, 5]$, compared with the full level of four nodes as shown in Figure 6.1.

In the detection process, each node is still responsible for triggering an alarm for its own detailed search region. In order to detect any possible burst in the whole space of interest without any duplicate, the adaptive D-dimensional Shifted Aggregation Tree should be constructed in such a way that the union of all the detailed search regions partitions the whole space of interest, i.e. the union has to cover the whole space of interest and there is no overlap between

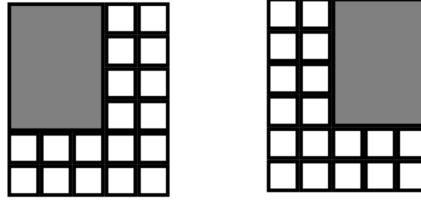

Figure 6.2: A partial level in an adaptive D-dimensional Shifted Aggregation Tree. A grayed area represents a node.

any two detailed search regions.

6.1.4 State Space Search Algorithm

Given sample data and thresholds for different window sizes, the state space search algorithm for the D-dimensional Shifted Aggregation Tree is similar to that for one-dimensional data. Each D-dimensional Shifted Aggregation Tree is viewed as a state, and the growth from one tree to another is viewed as a transformation between states. The algorithm starts with the base level of unit size, and keeps expanding the structure by adding a level on top of the existing structure, until the overlap region of the top level covers the maximum size of interest. Similarly a cost is associated with each state, including the updating cost, the filtering/checking cost and the detailed search cost. The statistics are collected from the sample data to estimate the detailed search cost. The state with the best cost is picked as the next state to be explored.

For the regular D-dimensional Shifted Aggregation Tree, when the structure needs to expand, a full level is simply added to the top of the current structure, e.g. in the above case of size $[16, 16]$, add 7×7 nodes at the level of size $[4, 4]$ and shift $[2, 2]$.

For the adaptive D-dimensional Shifted Aggregation Tree, when the structure needs to expand, a partial level is added to the top of the existing structure. The partial level can be any subset of the full level, and can be added at different possible subregions. For example, add 2×2 nodes at the level of size $[4, 4]$ and shift $[2, 2]$ starting from $[1, 1]$ to $[15, 15]$; or add 3×3 nodes starting from $[1, 1]$ to $[14, 14]$; and so on. Figure 6.3 and Figure 6.4 demonstrate the difference between the state space growth of a regular D-dimensional Shifted Aggregation Tree and that of an adaptive one.

6.1.5 Dynamic Detection Algorithm

In many spatial-temporal applications, spatial data changes over time. For example, the traffic over a metro area changes depending on the working hours.

To detect bursts in a spatial-temporal data set, one can use a static D-dimensional Shifted Aggregation Tree (either regular or adaptive) training with a sample data set at any time point. The dynamic algorithm can be used to adapt to changes in the data distribution in different regions.

The dynamic algorithm is similar to that in the one-dimensional case. The following points show the difference between the D-dimensional dynamic algorithm and the one-dimensional dynamic algorithm.

- The structure to start with may be an adaptive D-dimensional Shifted Aggregation Tree instead of a regular one.
- When adding or deleting a level, a partial level may be added or deleted instead of always a full level as in the one-dimensional case.
- When widening or narrowing a level, there are D shifts which can be

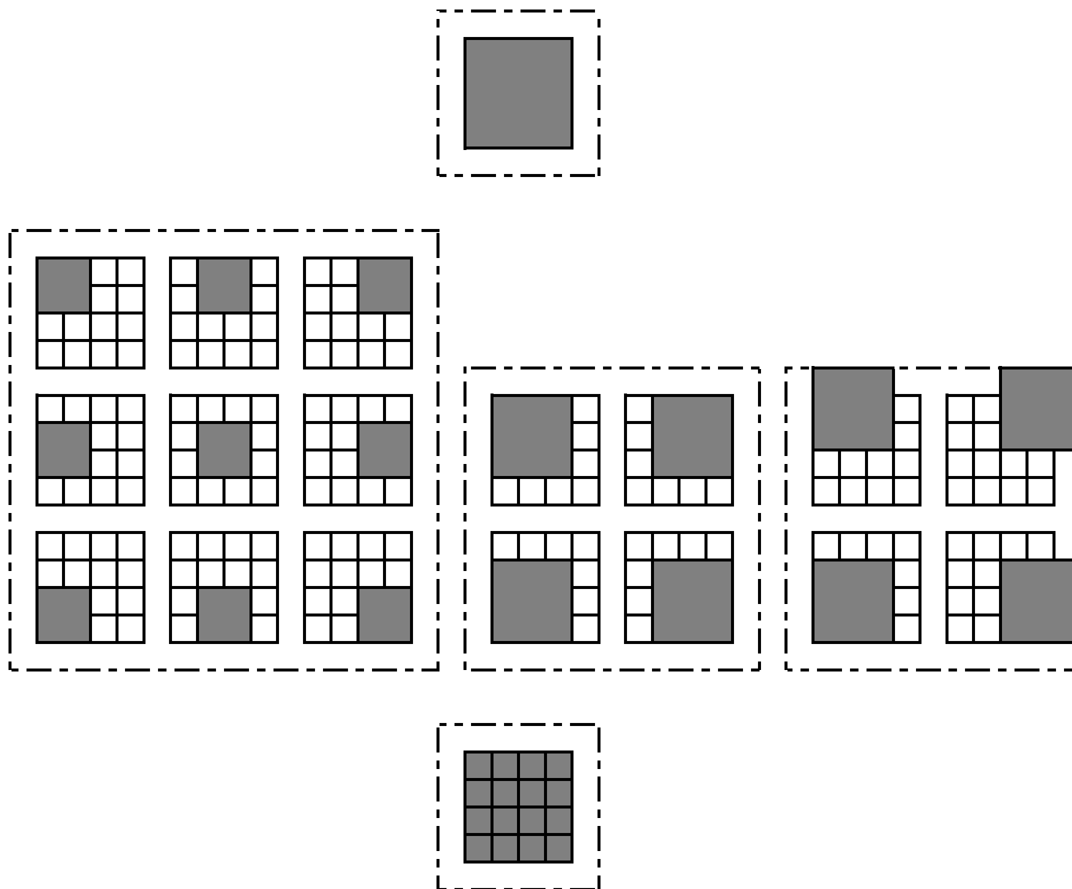

Figure 6.3: State space algorithm for regular D-dimensional Shifted Aggregation Tree in a 4 by 4 two-dimensional space. A grayed area represents a node. Nodes grouped by the dotted lines stand for a full level. The bottom level shows the level of unit size. The top level contains a node covering the whole space. The middle level shows all possible full levels which can be added on top of the bottom level.

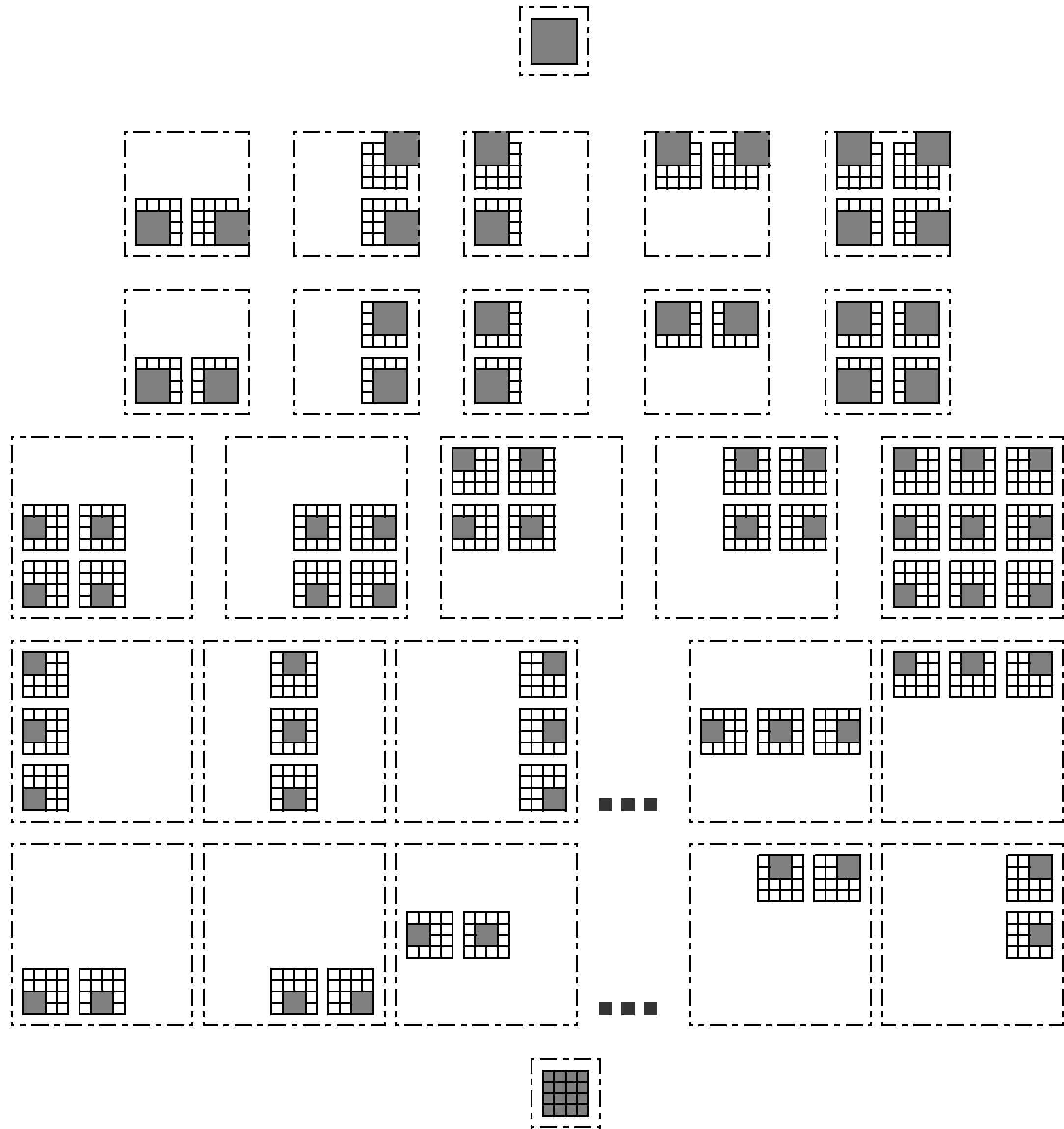

Figure 6.4: State space algorithm for adaptive D-dimensional Shifted Aggregation Tree in a 4 by 4 two-dimensional space. A grayed area represents a node. Nodes grouped by the dotted lines stand for a partial level. The bottom level shows the level of unit size. The top level contains a node covering the whole space. The middle levels show all possible partial levels of different sizes and orientations at different locations, which can be added on top of the bottom level.

changed. There are, in total, D^2 possible shifting actions that will make a level denser or sparser.

- The shape of the alarm region may need to be changed to take into account the spatial-temporal characteristics of the data. Remind that in the one-dimensional case, when an alarm is raised, one may expect more alarms soon after, i.e. alarms occur in clusters. To anticipate these alarms, we do not make the structure sparser in the alarm region. In the multi-dimensional case, for some data sets, the spatial distribution of the events may change quickly from time t to $t+1$, thus there may not be such a cluster phenomenon when an alarm happens. Therefore, we may not need alarm region from time t to $t+1$.

6.2 Fast Detection of Infectious Disease Outbreak and Spread

Epidemics, such as asthma, SARS, influenza, etc., are serious threats to public health. Epidemic outbreak detection, especially infectious disease detection, is of great importance to aid in disease prevention and to control the spread of diseases in their early stages. In Epidemiology, detection of disease occurrence and discovery of the association are two important topics. Burst detection can be a useful tool for detecting disease outbreaks. Bursts can reveal features that suggest association or causal relations [80, 91].

In this section, we simulate the outbreak and spread of an infectious disease and use our multi-dimensional burst detection to detect the outbreak regions.

Figure 6.5: Susceptible-Infectious-Recovered (SIR) model

6.2.1 Mathematical Models in Epidemiology

Epidemiologists have used different mathematical models to model the outcome and spread of infectious diseases [45]. The classic model used in infectious disease modeling is the SIR model as shown in Figure 6.5. In the basic SIR model, the whole population is divided into three classes depending on their experience with respect to the disease. S denotes the susceptible population who have never been infected by the disease and are subject to the infection. Once infected, they change to the I class, denoting the population infected by the disease and will stay in this class for the whole infectious period. When recovered, they change to the R class, denoting the population who recovered from the disease and are assumed to be immune for life. Figure 6.5 demonstrates the relationship between these three groups. β is the contact rate, denoting the contact degree between the susceptible and the infectious. γ is the recovery rate, denoting how fast the infected recover.

The whole progress of the disease infection without birth and death can be modeled by the following ordinary differential equations:

$$\begin{aligned} \frac{dS}{dt} &= -\beta IS \\ \frac{dI}{dt} &= \beta IS - \gamma I \\ \frac{dR}{dt} &= \gamma I \end{aligned}$$

where $S(t)$, $I(t)$ and $R(t)$ are the size of the population in each class respectively, and the constants are positive.

The basic SIR model does not consider the movement of the population. In the real world, people often spread disease when they travel. The epidemic metapopulation model is an extension to the basic SIR model to take population movement into consideration [92].

The metapopulation theory was developed in ecology to study the interaction between populations of the same species distributed in fragmented and isolated locations. The epidemic metapopulation model makes an analogy between the dynamics of ecological metapopulations and the dynamics of infectious diseases. It uses the basic SIR model to compute the sizes of the S, I and R classes for each location. Instead of assuming the population at each location is constant, the spatial movement between different locations is taken into consideration. The population at each location fluctuates based on the movement dynamics between different locations. A simple way to model the movement rate between locations is to use the inverse of the distance between these two locations: the closer two locations, the more movements. A more reasonable method, as described in [92], is to consider the sizes of the populations at these two locations as well: the larger the population of the two locations, the more movements between them.

6.2.2 Simulation

We use the epidemic metapopulation model described above to simulate how an infectious disease would break out and spread in a geographical region after an initial case is detected. We use the tri-state area (New York, New Jersey

and Connecticut) as the spatial region of interest for demonstration in this simulation. The simulation is done over a month-long period to see how a disease would start and spread in the tri-state area. After the number of infectious is computed for each location, two-dimensional burst detection is used to discover the regions with the most serious disease outbreak.

Data Setup

We obtain the population data for the tri-state area from the U.S. Census Bureau [12] and the transportation data from the Bureau of Transportation Statistics [3]. Instead of using the population sizes to compute the movement rate, we use the real transportation data explicitly to quantify the spatial interaction between different locations.

The population data comes from the 2000 census. It contains the summary population at each county-subdivision (i.e. town) level. There are, in total, about 1900 subdivisions in the tri-state area. Figure 6.6 shows the population distribution.

The transportation data includes the passenger travel census data of the tri-state area in 2000. The Census Transportation Planning Package (CTPP) 2000 includes the detailed Journey-To-Work statistics about the commute from home to work. The number of the workers going from the residence to the work place is counted for each possible pair of residence-workplaces. The statistics are per town, i.e. at the same resolution as the population data. We interpret the number of workers as a population movement from the residence to the workplace in the morning and in the opposite direction at night. So the individual population at each location fluctuates, but the overall population stays the same.

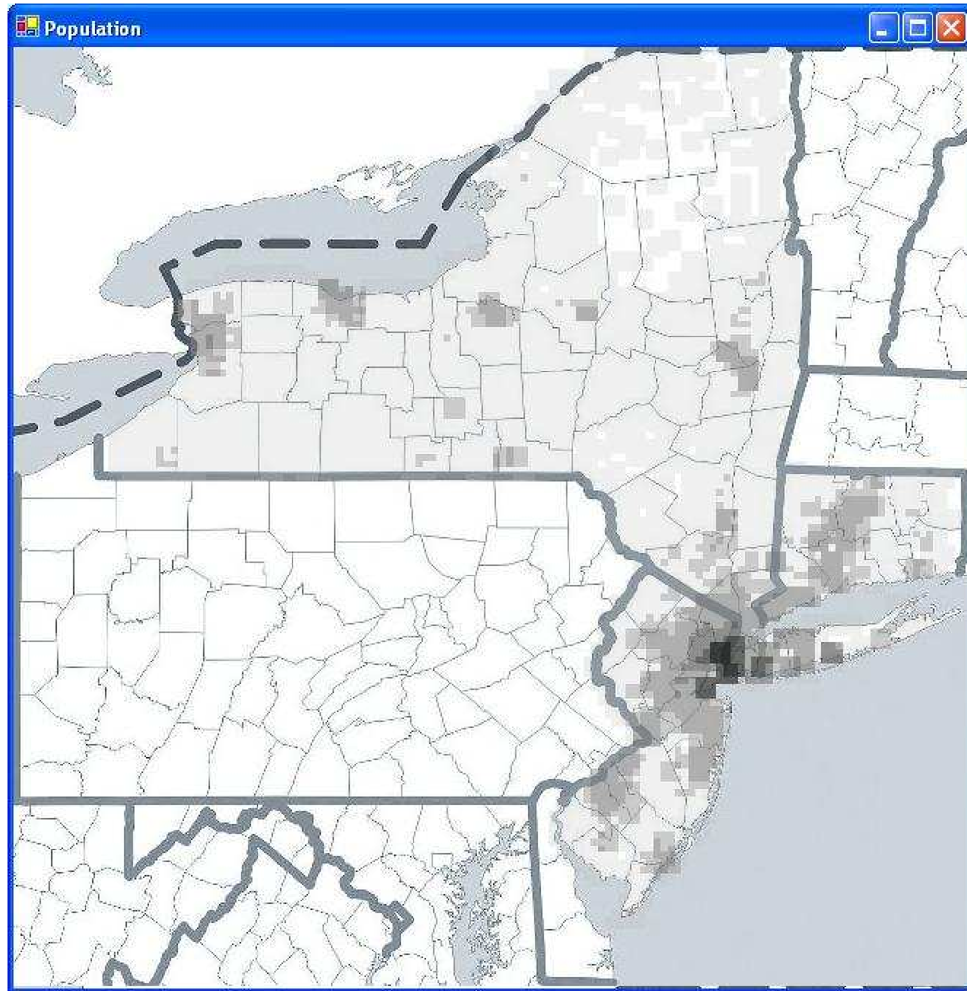

Figure 6.6: Population distribution of the Tri-State area. The darker an area, the denser the population.

Disease outbreak and spread detection

Given the population data and the transportation data, we simulate the outbreak and spread process of an infectious disease in the following steps:

1. A town is picked as the initial place where one disease case is detected, say Queens.

2. For each day, the following revised SIR model is used to compute the number of S, I and R for each town i.

$$\begin{aligned}\frac{dS_i}{dt} &= \sum_j(-\beta I_j S_{ij}) \\ \frac{dI_i}{dt} &= \sum_j(\beta I_j S_{ij}) - \gamma I_i \\ \frac{dR_i}{dt} &= \gamma I_i\end{aligned}$$

   where S_{ij} is the number of susceptible people traveling between town i and town j. The number of newly infected in town i is the sum of the number of newly infected who traveled to other towns and got infected there, plus those newly infected by the infectious in this town. We assume the infectious people do not go to work or travel.

3. After computing the number of the infected in each town, the numbers are mapped to a 128×128 grid which covers the whole region. For simplicity and clarity, the bursts are detected across only 3 window sizes of square regions in this simulation: 1 by 1, 4 by 4 and 8 by 8 respectively. Realistic applications may require a finer-resolution grid and more window sizes of different shapes and different orientations.

In this simulation, the contact ratio β is set to be 0.0001, and the recovery rate γ is set to be 0.33. The thresholds are set to reflect a burst probability of 0.00001. Figures [6.7,6.8, 6.9,6.10,6.11] show a sequence of detected outbreak regions every 6 days. The regions with wave, brick and dot patterns stand for square regions of size 8 by 8, 4 by 4 and 1 by 1 respectively. It shows that starting in Queens, the disease soon spreads to Manhattan. Because there is a large population flow from Manhattan to the tri-state area, the disease spreads along all routes to NJ, upstate NY and CT. Quick burst detection enables us to quickly monitor and respond to the spread of a disease or a bioterror attack.

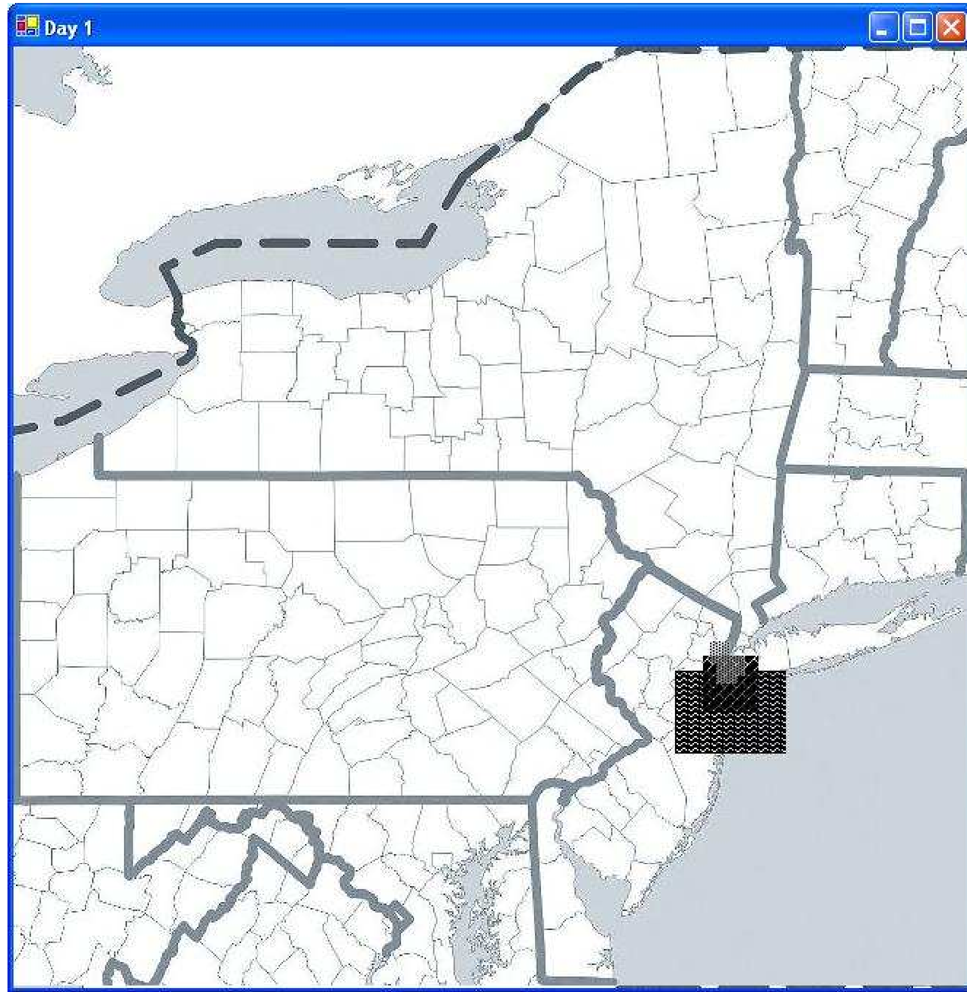

Figure 6.7: Simulation of a disease spread and outbreak detection - Day 1

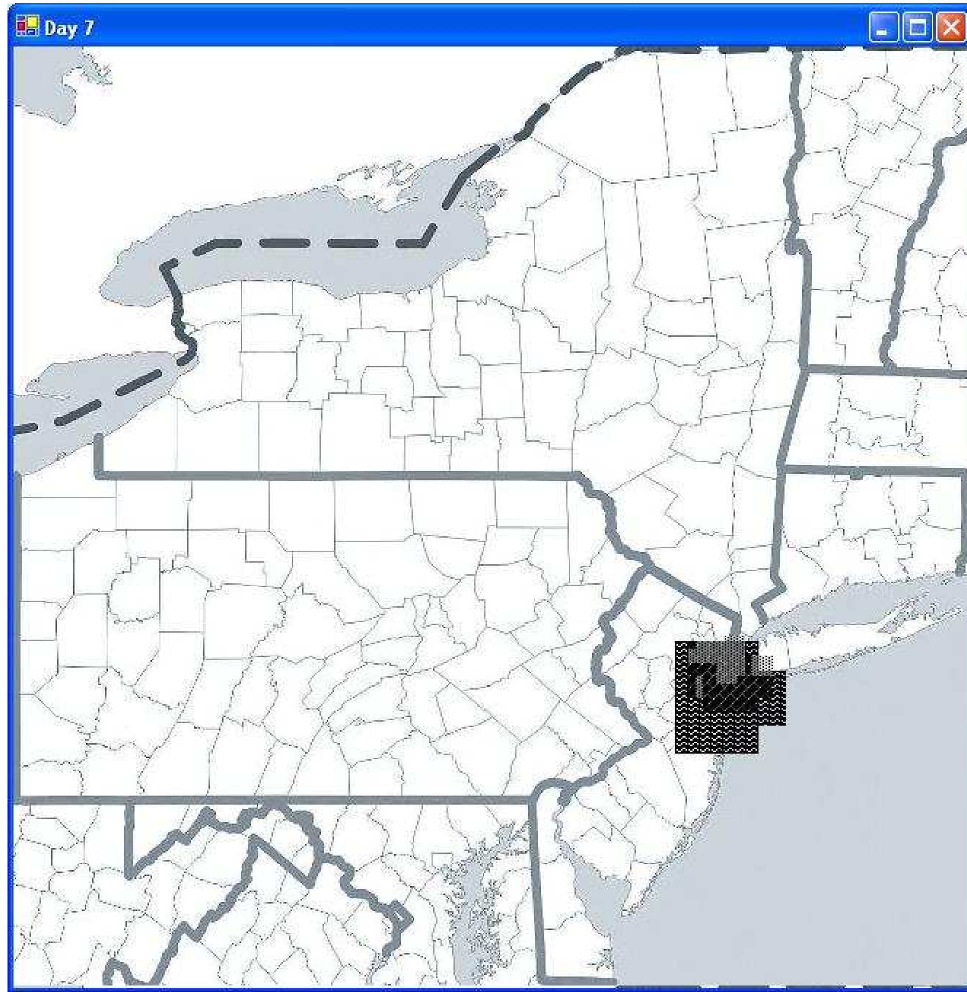

Figure 6.8: Simulation of a disease spread and outbreak detection - Day 7

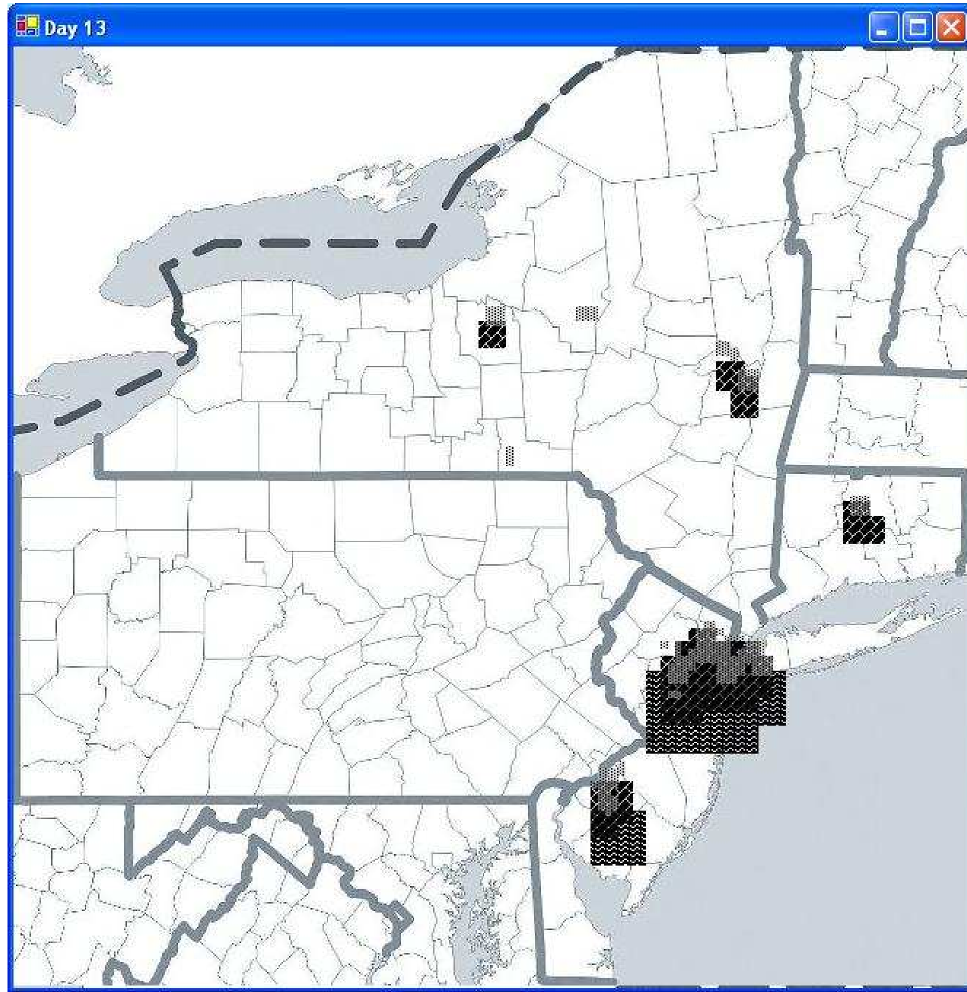

Figure 6.9: Simulation of a disease spread and outbreak detection - Day 13

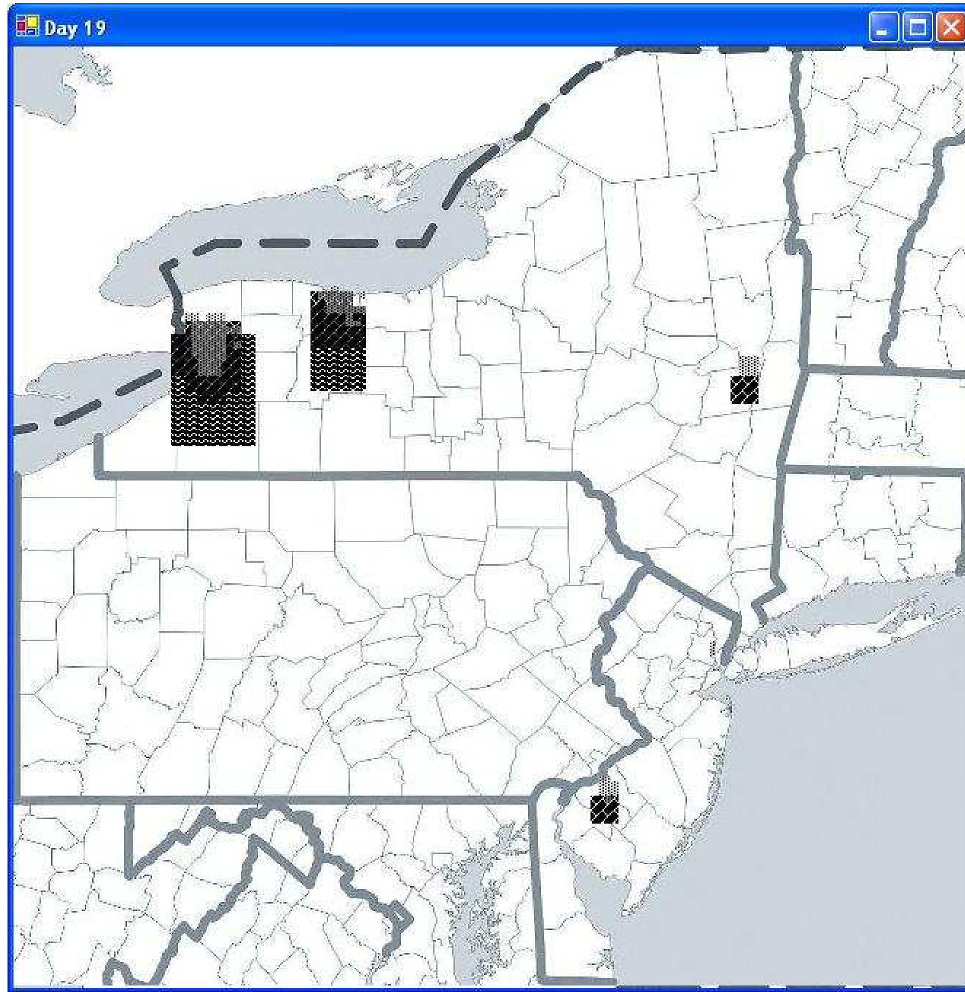

Figure 6.10: Simulation of a disease spread and outbreak detection - Day 19

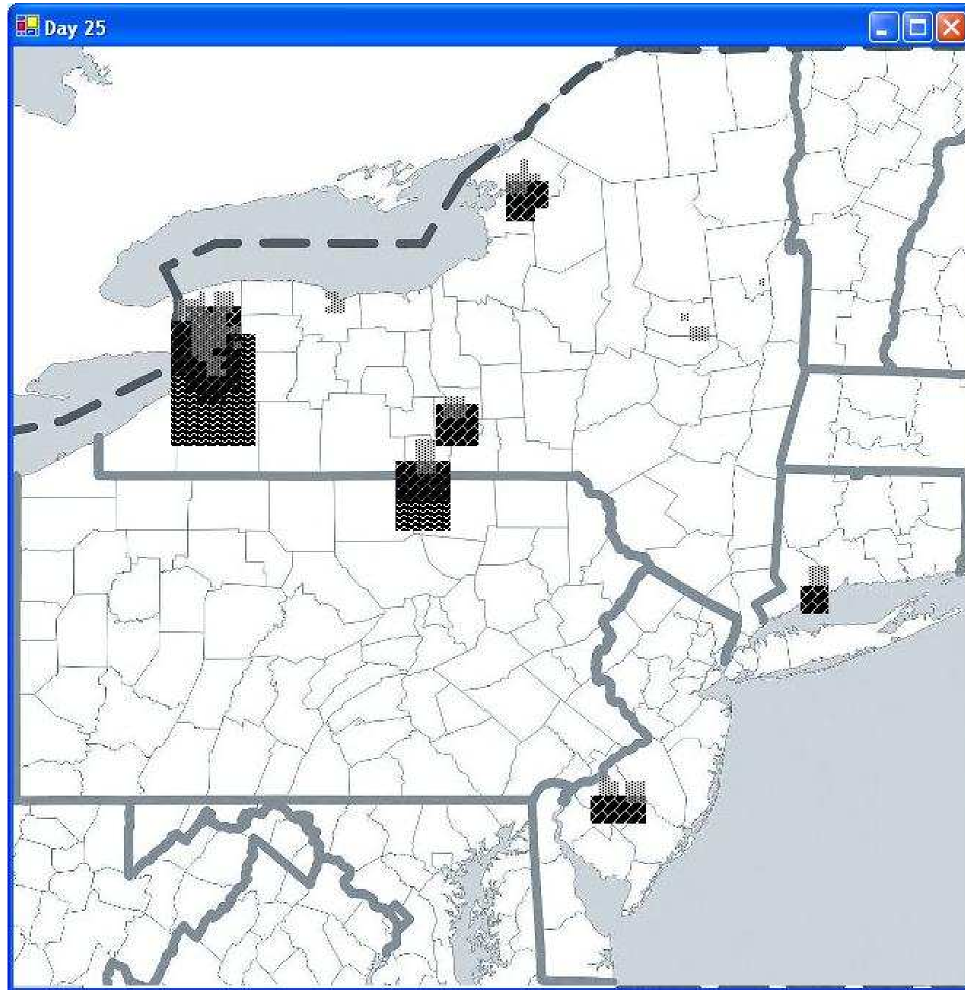

Figure 6.11: Simulation of a disease spread and outbreak detection - Day 25

Chapter 7

Conclusion

In this thesis, we have proposed an efficient algorithmic framework for the elastic burst detection problem. This framework includes a family of data structures and a static algorithm to train an efficient structure given a small sample of input data, and further a greedy dynamic algorithm which dynamically changes the structure to adapt to the incoming data. We tested our framework extensively on different types of data and different parameter settings. The experiments show that our method outperforms the existing method over a variety of inputs. We applied our framework in several real world applications in physics, finance, website/network traffic monitoring, etc. We also extend this work to multi-dimensional data and apply it in an epidemiology simulation to efficiently detect disease outbreak and spread.

Bibliography

[1] Adaptive dataflow for querying streams and deep web and beyond. http://telegraph.cs.berkeley.edu/.

[2] The aurora project. http://www.cs.brown.edu/research/aurora/.

[3] Bureau of transportation statistics. http://www.transtats.bts.gov.

[4] Hubble space telescope website. http://hubblesite.org/.

[5] Maids overview. http://maids.ncsa.uiuc.edu/about/index.html.

[6] Market volume analysis. http://marketvolume.com/.

[7] Milagro gamma-ray observatory. http://www.lanl.gov/milagro/.

[8] New york stock exchange. http://nyse.com/.

[9] Niagara query engine. http://www.cs.wisc.edu/niagara.

[10] Sloan digital sky survey. http://www.sdss.org/.

[11] Stanford stream data manager. http://www-db.stanford.edu/stream/.

[12] U.s. census bureau. http://www.census.gov.

[13] Wharton research data services (wrds). http://wrds.wharton.upenn.edu/.

[14] C. C. Aggarwal, J. Han, J. Wang, and P. S. Yu. A framework for clustering evolving data streams. In *Proceedings of 29th International Conference on Very Large Data Bases*, pages 81–92, 2003.

[15] C. C. Aggarwal, J. Han, J. Wang, and P. S. Yu. A framework for projected clustering of high dimensional data streams. In *Proceedings of 30th International Conference on Very Large Data Bases*, pages 852–863, 2004.

[16] C. C. Aggarwal, J. Han, J. Wang, and P. S. Yu. On demand classification of data streams. In *Proceedings of the 10th ACM SIGKDD International Conference on Knowledge Discovery and Data Mining*, pages 503–508, 2004.

[17] C. C. Aggarwal and P. S. Yu. Outlier detection for high-dimensional data. In *Proceedings of the 2001 ACM SIGMOD International Conference on Management of Data*, pages 37–46, 2001.

[18] B. Babcock, S. Babu, M. Datar, R. Motwani, and J. Widom. Models and issues in data stream systems. In *Proceedings of 21st ACM Symposium on Principles of Database Systems*, pages 1–16, 2002.

[19] B. Babcock, M. Datar, R. Motwani, and L. O'Callaghan. Maintaining variance and k-medians over data stream windows. In *Proceedings of the 22nd Symposium on Principles of Database Systems*, pages 234–243, 2003.

[20] S. Babu and J. Widom. Continuous queries over data streams. In *Proceedings of the 2001 ACM SIGMOD International Conference on Management of Data*, pages 109–120, 2001.

[21] V. Barnett and T. Lewis. *Outliers in Statistical Data*. John Wiley & Sons, 1994.

[22] S. D. Bay and M. Schwabacher. Mining distance-based outliers in near linear time with randomization and a simple pruning rule. In *Proceedings of the 9th ACM SIGKDD International Conference on Knowledge Discovery and Data Mining*, pages 29–38, 2003.

[23] M. Breuing, H.-P. Kriegel, P. Kroger, and J. Sander. Data bubbles: Quality preserving performance boosting for hierarchical clustering. In *Proceedings of the 2001 ACM SIGMOD International Conference on Management of Data*, pages 79–90, 2001.

[24] M. M. Breunig, H.-P. Krigel, R. T. Ng, and J. Sander. Lof: Identifying density-based local outliers. In *Proceedings of the 2000 ACM SIGMOD International Conference on Management of Data*, pages 93–104, 2000.

[25] Y. D. Cai, D. Clutter, G. Pape, J. Han, M. Welge, and L. Auvil. Maids: Mining alarming incidents from data streams. In *Proceedings of the 2004 ACM SIGMOD International Conference on Management of Data*, pages 919–920, 2004.

[26] K. Chakrabarti and S. Mehrotra. Locally dimensionality reduction: A new approach to indexing high dimensional spaces. In *Proceedings of the 6th ACM SIGKDD International Conference on Knowledge Discovery and Data Mining*, pages 89–100, 2000.

[27] Y. Chen, G. Dong, J. Han, B. W. Wah, and J. Wang. Multi-dimensional regression analysis of time series data streams. In *Proceedings of 28th International Conference on Very Large Data Bases*, pages 323–334, 2002.

[28] R. Cole, D. Shasha, and X. Zhao. Fast window correlations over uncooperative time series. In *Proceeding of the eleventh ACM SIGKDD international conference on Knowledge discovery in data mining*, pages 743–749. ACM Press, 2005.

[29] M. Datar, A. Gionis, P. Indyk, and R. Motwani. Maintaining stream statistics over sliding windows: (extended abstract). In *Proceedings of the thirteenth annual ACM-SIAM symposium on Discrete algorithms*, pages 635–644. Society for Industrial and Applied Mathematics, 2002.

[30] V. de Silva and J. B. Tenenbaum. Global versus local methods in nonlinear dimensionality reduction. pages 705–712. Advances in Neural Information Processing Systems, 2002.

[31] C. Ding, X. He, H. Zha, and H. D. Simon. Adaptive dimension reduction for clustering high dimensional data. In *Proceedings of the 2002 IEEE International Conference on Data Mining*, pages 147–154, 2002.

[32] A. Dobra, M. Garofalakis, J. Gehrke, and R. Rastogi. Processing complex aggregate queries over data streams. In *Proceedings of the 2002 ACM SIGMOD International Conference on Management of Data*, pages 61–72, 2002.

[33] P. Domingos and G. Hulten. Mining high-speed data streams. In *Proceedings of the 6th ACM SIGKDD International Conference on Knowledge Discovery and Data Mining*, pages 71–80, 2000.

[34] G. Dong, J. Han, L. V. Lakshmanan, J. Pei, H. Wang, and P. S.Yu. Online mining of changes from data streams: Research problems and preliminary results. In *Proceedings of the 2003 ACM SIGMOD International Conference on Management of Data*, 2003.

[35] W. DuMouchel, C. Volinsky, T. johnson, C. Cortes, and D. Pregibon. Squashing flat files flatter. In *Proceedings of the 5th ACM SIGKDD International Conference on Knowledge Discovery and Data Mining*, pages 6–15, 1999.

[36] C. Faloutsos. Indexing and mining streams. In *Proceedings of the 2004 ACM SIGMOD International Conference on Management of Data*, page 969, 2004.

[37] S. Ganguly, M. Garofalakis, and R. Rastogi. Processing data-stream join aggregates using skimmed sketches. pages 569–586. International Conference on Extending Database Technology (EDBT), 2004.

[38] M. Garofalakis, J. Gehrke, and R. Rastogi. Querying and mining data streams: You only get one look. In *Proceedings of the 2002 ACM SIGMOD International Conference on Management of Data*, page 635, 2002.

[39] V. Geobel and T. Plagemann. Data stream management systems - concepts, prototypes, and applications. Multimedia Interactive Protocols and Systems, 2004.

[40] P. B. Gibbons and S. Tirthapura. Distributed stream algorithms for sliding windows. In *Proceedings of the fourteenth annual ACM symposium on Parallel algorithms and architectures*, pages 63–72, 2002.

[41] L. Golab and M. T. Ozsu. Issues in data stream management. *ACM SIGMOD Record*, 32(2):5–14, 2003.

[42] M. Greenwald and S. Khanna. Space-efficient online computation of quantile summaries. In *Proceedings of the 2001 ACM SIGMOD international conference on Management of data*, pages 58–66. ACM Press, 2001.

[43] D. Gunopulos and G. Das. Time series similarity measures and time series indexing. In *Proceedings of the 2001 ACM SIGMOD International Conference on Management of Data*, page 624, 2001.

[44] S. Heiler. A survey on nonparametric time series analysis. Finance 9904005, EconWPA, Apr. 1999. available at http://ideas.repec.org/p/wpa/wuwpfi/9904005.html.

[45] H. W. Hethcote. The mathematics of infectious diseases. *Society for Industrial and Applied Mathematics Review*, 42:599–653, 2000.

[46] P. Indyk, N. Koudas, and S. Muthukrishnan. Identifying representative trends in massive time series data sets using sketches. In *Proceedings of the 26th International Conference on Very Large Data Bases*, pages 363–372. Morgan Kaufmann Publishers Inc., 2000.

[47] Y. E. Ioannidis and V. Poosala. Histogram-based approximation of set-valued query answers. In *Proceedings of 25th International Conference on Very Large Data Bases*, pages 174–185, 1999.

[48] T. Johnson, I. Kwok, and R. Ng. Fast computation of 2-dimensional depth contour. In *Proceedings of the 4th ACM SIGKDD International Conference on Knowledge Discovery and Data Mining*, 1998.

[49] E. Keogh. A tutorial on indexing and mining time series data. In *Proceedings of the 2001 IEEE International Conference on Data Mining*, 2001.

[50] E. Keogh, K. Chakrabarti, S. Mehrotra, and M. Pazzani. Locally adaptive dimensionality reduction for indexing large time series databases. In *Proceedings of the 2001 ACM SIGMOD International Conference on Management of Data*, pages 151–162, 2001.

[51] E. Keogh, K. Chakrabarti, M. Pazzani, and S. Mehrotra. Dimensionality reduction for fast similarity search in large time series database. pages 263–286. Databases and Knowledge and Information Systems, 2000.

[52] E. Keogh and S. Kasetty. On the need for time series data mining benchmarks: A survey and empirical demonstration. In *Proceedings of the 6th ACM SIGKDD International Conference on Knowledge Discovery and Data Mining*, pages 349–371, 2000.

[53] E. Keogh, S. Lonardi, and W. Chiu. Finding surprising patterns in a time series database in linear time and space. In *Proceedings of the 8th ACM SIGKDD International Conference on Knowledge Discovery and Data Mining*, pages 550–556, 2002.

[54] E. Keogh and M. J. Pazzani. An enhanced representation of time series which allows fast and accurate classification, clustering and relevance feed-

back. In *Proceedings of the 4th ACM SIGKDD International Conference on Knowledge Discovery and Data Mining*, pages 239–243, 1998.

[55] J. Kleinberg. Bursty and hierarchical structure in streams. In *Proceedings of the Eighth ACM SIGKDD International Conference on Knowledge Discovery and Data Mining*, pages 91–101. ACM Press, 2002.

[56] E. M. Knorr, R. T. Ng, , and V. Tucakov. Distance-based outliers: Algorithms and applications. In *Proceedings of 26th International Conference on Very Large Data Bases*, pages 237–253, 2000.

[57] E. M. Knorr and R. T. Ng. Algorithms for mining distance-based outliers in large datasets. In *Proceedings of 24th International Conference on Very Large Data Bases*, pages 392–403, 1998.

[58] E. M. Knorr and R. T. Ng. Finding intensional knowledge of distance-based outliers. In *Proceedings of 25th International Conference on Very Large Data Bases*, pages 211–222, 1999.

[59] A. Lerner, D. Shasha, Z. Wang, X. Zhao, and Y. Zhu. Fast algorithms for time series with applications to finance and physics and music and biology and and other suspects. In *Proceedings of the 2004 ACM SIGMOD International Conference on Management of Data*, pages 965–968, 2004.

[60] X.-B. Li. Data reduction via adaptive sampling. Communication in Information and System, 2002.

[61] J. Lin, E. Keogh, S. Lonardi, and B. Chiu. A symbolic representation of time series, with implications for streaming algorithms. In *Proceedings of*

the 8th ACM SIGMOD workshop on Research issues in data mining and knowledge discovery, pages 2–11. ACM Press, 2003.

[62] J. Ma and S. Perkins. Online novelty detection on temporal sequences. In *Proceedings of the 9th ACM SIGKDD International Conference on Knowledge Discovery and Data Mining*, pages 613–618, 2003.

[63] J. Ma and S. Perkins. Time series novelty detection using one-class support vector machines. International Joint Conference on Neural Networks, 2003.

[64] S. Madden, M. Shah, J. M. Hellerstein, and V. Raman. Continuously adaptive continuous queries over streams. In *Proceedings of the 2002 ACM SIGMOD International Conference on Management of Data*, pages 49–60, 2002.

[65] G. S. Manku and R. Motwani. Approximate frequency counts over data streams. In *Proceedings of 28th International Conference on Very Large Data Bases*, pages 356–357, 2002.

[66] Y. Matias, J. S. Vitter, and M. Wang. Wavelet-based histograms for selectivity estimation. In *Proceedings of the 1998 ACM SIGMOD International Conference on Management of Data*, pages 448–459, 1998.

[67] Y. Matias, J. S. Vitter, and M. Wang. Dynamic maintenance of wavelet-based histograms. In *Proceedings of 26th International Conference on Very Large Data Bases*, pages 101–110, 2000.

[68] D. C. Montgomery and G. C. Runger. *Applied Statistics and Probability for Engineers*. Wiley, 2003.

[69] D. Neill and A. Moore. Rapid detection of significant spatial clusters. In *Proceedings of the 10th ACM SIGKDD International Conference on Knowledge Discovery and Data Mining*, 2004.

[70] D. Neill and A. Moore. Anomalous spatial cluster detection. In *Proceedings of the KDD 2005 Workshop on Data Mining Methods for Anomaly Detection*, August 2005.

[71] D. B. Neill and A. W. Moore. A fast multi-resolution method for detection of significant spatial disease clusters. In S. Thrun, L. Saul, and B. Schölkopf, editors, *Advances in Neural Information Processing Systems 16*. MIT Press, 2004.

[72] D. B. Neill, A. W. Moore, F. Pereira, and T. Mitchell. Detecting significant multidimensional spatial clusters. In L. K. Saul, Y. Weiss, and L. Bottou, editors, *Advances in Neural Information Processing Systems 17*, pages 969–976. MIT Press, 2005.

[73] N. J. Nilsson. *Principles of Artificial Intelligence.* Morgan Kaufmann Publishers, 1980.

[74] S. Papadimitriou and C. Faloutsos. Adaptive and hands-off streaming mining. In *Proceedings of 29th International Conference on Very Large Data Bases*, pages 560–571, 2003.

[75] S. Papadimitriou and C. Faloutsos. Cross-outlier detection. pages 199–213. 8th International Symposium on Spatial and Temporal Databases, 2003.

[76] S. Papadimitriou, H. Kitagawa, P. B. Gibbons, and C. Faloutsos. Loci: Fast outlier detection using the local correlation integral. In *Proceedings of the 19th International Conference on Data Engineering*, page 315, 2003.

[77] C.-S. Perng, H. Wang, S. R. Zhang, and D. S. Parker. Landmarks: a new model for similarity-based pattern querying in time series databases. In *Proceedings of the 16th International Conference on Data Engineering*, pages 33–42, 2000.

[78] L. Qiao, D. Agrawal, and A. E. Abbadi. Rhist: Adaptive summarization over continuous data streams. pages 469–476. Conference on Information and Knowledge Management, 2002.

[79] S. Russell and P. Norvig. *Artificial Intelligence: A Modern Approach*. Prentice Hall, 2002.

[80] R. Sabhnani, D. Neill, and A. Moore. Detecting anomalous patterns in pharmacy retail data. In *Proceedings of the KDD 2005 Workshop on Data Mining Methods for Anomaly Detection*, August 2005.

[81] S. Schaal, S. Vijayakumar, and C. G. Atkeson. Local dimensionality reduction. Advances in Neural Information Processing Systems, 1997.

[82] B. Scholkopf, R. Williamson, A. smola, J. Shawe-Tayleor, and J. Platt. Support vector method for novelty detection. pages 582–588. Advances in Neural Information processing Systems 12, 1999.

[83] C. Shahabi, X. Tian, and W. Zhao. Tsa-tree: A wavelet-based approach to improve the efficiency of multi-level surprise and trend queries on time-

series data. pages 1–14. 12th International Conference on Scientific and Statistical Database Management(SSDBM), 2000.

[84] D. Shasha and Y. Zhu. *High Performance Discovery in Time Series: Techniques and Case Studies*, pages 151–172. Springer, 2004.

[85] L. Shih, J. D. Rennie, Y.-H. Chang, and D. R. Karger. Text bundling: Statistics-based data reduction. pages 696–703. International Conference on Machine Learning, 2003.

[86] R. Typke, F. Wiering, and R. C. Veltkamp. A survey of music information retrieval systems. In *ISMIR 2005, 6th International Conference on Music Information Retrieval*, pages 153–160, 2005.

[87] M. Vlachos, C. Meek, Z. Vagena, and D. Gunopulos. Identifying similarities, periodicities and bursts for online search queries. In *Proceedings of the 2004 ACM SIGMOD international conference on Management of data*, pages 131–142. ACM Press, 2004.

[88] H. Wang, W. Fan, P. S. Yu, and J. Han. Mining concept-drifting data streams using ensemble classifiers. In *Proceedings of the 9th ACM SIGKDD International Conference on Knowledge Discovery and Data Mining*, pages 226–235, 2003.

[89] M. Wang, T. Madhyastha, N. H. Chan, S. Papadimitriou, and C. Faloutos. Data mining meets performance evaluation: Fast algorithms for modeling bursty traffic. In *ICDE '02: Proceedings of the 18th International Conference on Data Engineering (ICDE'02)*, pages 507–516. IEEE Computer Society, 2002.

[90] W. Willinger, M. S. Taqqu, and A. Erramilli. A bibliographical guide to self-similar traffic and performance modeling for modern high-speed networks. 1996.

[91] W.-K. Wong, A. Moore, G. Cooper, and M. Wagner. Bayesian network anomaly pattern detection for disease outbreaks. In *Proceedings of the Twentieth International Conference on Machine Learning*, pages 808–815. AAAI Press, August 2003.

[92] Y. Xia, O. N. Bjrnstad, and B. T. Grenfell. Measles metapopulation dynamics: A gravity model for epidemiological coupling and dynamics. *The American Naturalist*, 164:267–281, 2004.

[93] T. Zhang, R. Ramakrishnan, and M. Linvy. Birch: An efficient data clustering method for very large databases. In *Proceedings of the 1996 ACM SIGMOD International Conference on Management of Data*, pages 103–114, 1996.

[94] X. Zhang and D. Shasha. High performance burst detection. *Technical Report, New York University*, 2005.

[95] X. Zhang and D. Shasha. Better burst detection. In *Proceedings of the 22nd International Conference on Data Engineering (ICDE'06)*, page 146. IEEE Computer Society, 2006.

[96] X. Zhao, X. Zhang, T. Neylon, and D. Shasha. Incremental methods for simple problems in time series: Algorithms and experiments. In *9th International Database Engineering & Application Symposium*, pages 3–14, 2005.

[97] C. Zhu, H. Kitagawa, S. Papadimitri, and C. Faloutsos. Obe: Outlier by example. pages 222–234. Pacific-Asia Conference on Knowledge Discovery and Data Mining, 2004.

[98] Y. Zhu and D. Shasha. Statstream: Statistical monitoring of thousands of data streams in real time. In *Proceedings of 28th International Conference on Very Large Data Bases*, pages 358–369, 2002.